Comparison of feature-based classifiers in Automatic Modulation Classification systems

H.K. Blackie

 orcid.org 0000-0003-4594-1384

Dissertation submitted in fulfilment of the requirements for the degree *Master of Engineering in Computer and Electronic Engineering* at the North-West University

Supervisor: Dr. M. Ferreira

Graduation May 2018

Student number: 23377852

Comparison of feature-based classifiers in Automatic Modulation Classification systems

Dissertation submitted in fulfilment of the requirements for the degree *Master of Engineering* in Computer Engineering at the Potchefstroom campus of the North-West University

H.K. Blackie

23377852

Supervisor: Dr. M. Ferreira

May 2018

Declaration

I, Hermanus Karel Blackie hereby declare that the dissertation entitled "Comparison of feature-based classifiers in Automatic Modulation Classification systems" is my own original work and has not already been submitted to any other university or institution for examination.

H.K. Blackie

Student number: 23377852

Signed on the 15th day of May 2018 at Potchefstroom.

Acknowledgements

1. I would like to acknowledge my God and Saviour, Jesus Christ, for the privilege granted to undertake this study, to travel, to see the world, and countless blessings that He has bestowed on me.

2. I would like to express my gratitude and appreciation for my supervisor, Dr. Melvin Ferreira for his continual guidance, support, encouragement and dedication throughout this journey.

3. My examiners, thank you for the time to appraise the work, and for providing valuable and constructive feedback.

4. I would also like to thank my parents for their support, to my friends and colleagues for their continual support, prayers and insights.

5. The North-West University's Faculty of Electrical, Electronic and Computer Engineering for their financial support throughout the study.

6. And finally, I extend my deepest gratitude to these companies for their involvement during my research:

    - GEW Technologies
    - TeleNet research group (North-West University)
    - Peralex

Abstract

In South Africa, the telecommunications regulator, ICASA, follows a fixed spectrum allocation approach. The radio spectrum is assigned to incumbents (primary users) on a long-term basis. This practice follows a wholesale approach auctioning spectrum to the highest bidder. This approach leads to under-utilised spectrum which causes an artificial spectrum scarcity. Two spectrum allocation processes have been proposed in literature: dynamic spectrum market model, and a spectrum commons model. Cognitive radio (CR) is an enabling technology for either of these models.

Spectrum sensing is a key element and should be performed first before allowing secondary user access. Energy detection, cyclostationary feature detection, matched filtering and cooperative sensing has been proposed as spectrum sensing techniques.

An Automatic Modulation Classification (AMC) system detects the unknown modulation type of a received signal in preparation to demodulate the signal and retrieve its information content. AMC plays an important role in military and civilian applications such as signal confirmation, interference identification, surveillance, monitoring, spectrum management, counter channel jamming and signal intelligence.

Future Software-defined Radio (SDR) and CR systems must be able to sense the spectrum for signals present in the pursuit of enabling Dynamic Spectrum Access (DSA). This interest in increasing spectrum access and improving spectrum efficiency, combined with SDR and new realisations that machine learning can be applied to radios, have created interesting possibilities, such as CR.

The International Telecommunications Union for radio communications (ITU-R) gives guidelines for the technical identification of digital signals. The signal's spectral form, frequency, bandwidth, instantaneous amplitude and phase can be used for this purpose. For any regulator, it is important to monitor signals of interest and to identify them accordingly. Doing this involves traditional software packages which follow a brute-force approach in demodulating the signals. Each demodulation approach gets

tested against the signal of interest until a match is found. Modern digital signals are modulated using a variety of modulation techniques.

In this dissertation, an investigative study is presented towards finding a simple approach to identifying and classifying M-PSK and M-QAM signals in the UHF frequency band. Two approaches can be followed when deciding on a classification approach: Likelihood-based (LB) approach or a Feature-based (FB) approach. A FB (also known as a pattern-recognition) classification approach is followed in the dissertation. A combination of instantaneous time-domain and higher-order statistical features are extracted from the signal's instantaneous amplitude and phase. A Support Vector Machine (SVM) is used to solve the classification problem.

The performance of the AMC is tested in an Additive White Gaussian Noise (AWGN) and multipath fading channel. Two use-cases for evaluating the performance of the classifier is presented: with and without Signal-to-Noise Ratio (SNR) estimation. Introducing SNR estimation as part of the feature set increased the classification accuracy for Quadrature Phase Shift Keying (QPSK) and 8-Phase Shift Keying (PSK) signals at low SNR. A 2% classification accuracy improvement was obtained at 4 dB for QPSK signals, while a 12% classification accuracy improvement for 8-PSK signals was obtained for an SNR of 1 dB.

Furthermore, the performance of the proposed classifier was assessed for two multipath channel conditions: for a stationary transmitter and receiver, and secondly for a moving receiver. Four randomly selected Doppler shifts were chosen and evaluated. An overall classification accuracy of 90% was reported for the stationary case, while the accuracy of the different Doppler shifts were 85%, 86%, 77.5% and 78% respectively.

Finally, the performance of the classifier was evaluated using recorded In-phase and quadrature (I/Q) data of a TETRA signal. The proposed classifier correctly identified the TETRA signal to be part of the PSK modulation group. However, the classifier was not able to determine the modulation order.

The research done in the dissertation showed that following a simple FB classification

approach to classifying digital signals is possible. The work showed that higher-order statistics extracted form the instantaneous amplitude and phase of the received signal can be used as features.

Keywords: Automatic Modulation Classification, Higher-order statistics, Feature-based classification, Support Vector Machine, multipath fading.

Contents

List of Figures

List of Tables

List of Acronyms

ADC analog-to-digital converter

ALRT Average Likelihood Ratio Test

AMC Automatic Modulation Classification

ANN Artificial Neural Network

AoA angle of arrival

ASK Amplitude Shift Keying

AUC area under curve

AWGN Additive White Gaussian Noise

bps bits per second

BPSK Binary Phase Shift Keying

CMA Constant modulus algorithm

CR Cognitive Radio

DFT Discrete Fourier Transform

DNN deep neural network

DSA Dynamic Spectrum Access

DTT Digital Terrestrial Television

FB Feature-based

FCC Federal Communications Commission

FIR finite impulse response

FN false negatives

FP false positives

FPR false positive rate

FSK Frequency Shift Keying

GLRT Generalized Likelihood Ratio Test

GP Genetic Programming

HLRT Hybrid Likelihood Ratio Test

HOS Higher-order Statistics

ICASA Independent Communications Authority of South Africa

i.i.d. independent and identically distributed

I/Q In-phase and quadrature

ISI inter-symbol interference

ITU International Telecommunications Union

ITU-R Radiocommunications sector of the ITU

KNN K-nearest neighbour

LA Link Adaptation

LB Likelihood-based

LMS Least Mean Square

LOS Line-of-Sight

ML Machine learning

MLSE Maximum-Likelihood Sequence Estimation

M-PSK M-ary phase shift keying

M-QAM M-ary quadrature amplitude modulation

NFP National Frequency Plan

NLOS non line-of-sight

Ofcom The Office of Communications

OFDM Orthogonal frequency division multiplexing

OOK On-Off Keying

PDF probability density function

PLL Phase-Locked-Loop

PSK Phase Shift Keying

PU primary user

QAM Quadrature Amplitude Modulation

QPSK Quadrature Phase Shift Keying

RLS Recursive least squares

ROC receiver operating characteristic

SATNAC Southern Africa Telecommunication Networks and Applications Conference

SDR Software-defined Radio

SM spectrum management

SNR Signal-to-Noise Ratio

SU secondary user

SVM Support Vector Machine

TDL Tapped delay line

TN true negatives

TP true positives

TU Typical Urban

UN United Nations

Chapter 1

Introduction

This chapter provides the essential background of the thesis. It presents an introduction to spectrum management, Dynamic Spectrum Access (DSA) and the need for better spectrum usage technologies. It also provides guidelines set out by Radiocommunications sector of the ITU (ITU-R) for identifying digital signals and the need for automatic modulation classification. The research problem, objectives, deliverables and research methodology are also presented.

1.1 Introduction

Since the beginning of time man needed to convey thoughts, feelings, and ideas. Whether verbal, non-verbal or through pictures and carvings. Effective communication is essential. Just as humankind has evolved, our means of communication has also evolved. With what began with paintings in a cave, have changed into a variety of endless ways to express oneself. Through the development of written documentation and books to the revolution of the printing press, telegraph and radio, photography and the internet. Mankind has a tendancy to communicate further, faster and more efficient.

Communicating over long distances were limited to face-to-face encounters. Long-distance communication was first accomplished through the sound of a beating drum, horn blasts, smoke signals and waving flags. A piece of paper extended the distance over which messages could be sent, and long distance communication could be achieved through a runner on horseback, by ship or train. The discovery of electricity in the nineteenth century changed the way we communicate forever [7].

With work done by Faraday and Ampere, they managed to show that a time-varying magnetic field induces an electric field and that a time-varying electric field induces a magnetic field. This phenomenon had the properties of a wave and is referred to as an electromagnetic wave. Maxwell studied electromagnetic waves analytically and developed a set of equations that could describe this interrelationship between an electric and magnetic field. Maxwell proved that these waves propagate at the speed of light through space. Maxwell laid the foundation on which researchers could work to develop methods of converting signals into high-frequency oscillating currents to be transmitted over long distances. In radio communication, radio spectrum is the most valuable resource mankind has. Radio spectrum is a natural resource, but it is not used the same as coal, water, gold, oil, or any other resource, in the sense that radio spectrum cannot be accumulated over time for later usage. Spectrum must be managed.

Around the world, each country has its own regulatory body for managing and assigning spectrum to users, some of which include Independent Communications Authority of South Africa (ICASA) in South-Africa, Federal Communications Commission (FCC) in the United States and The Office of Communications (Ofcom) in the United Kingdom. In South Africa, ICASA follows a fixed spectrum allocation approach. The radio spectrum is assigned to incumbents (primary users) on a long-term basis. This practice follows a quantitative approach auctioning spectrum to the highest bidder. This approach leads to under-utilised spectrum which causes an artificial spectrum scarcity [8], [9]. The geographic nature of the under-utilisation of spectrum results in *spectrum holes* or *white spaces*.

Two alternative spectrum allocation processes have been proposed in the literature: dynamic spectrum market model, and a spectrum commons model. The dynamic spectrum market model allows incumbents to resell unused spectrum. The spectrum commons model employs open sharing of spectrum among peers with an equal right to access. Extensive research has been done towards enabling Cognitive Radio (CR) technologies [8], [10] to help overcome this problem of spectrum scarcity. CR senses the spectrum according to pre-defined criteria before allowing secondary access.

The radio spectrum has different properties at different frequencies, which makes specific frequencies more preferable than others. Each frequency band has different propagation properties which enables the use for different technologies. The radio spectrum, as mentioned in [2], ranges from 3 kHz to 300 GHz . Table 1.1 shows the most commonly used radio frequency bands and their respective applications as adapted from [5] and [6].

As mentioned, CR has been proposed as a prime enabler for spectrum reuse. Spectrum sensing is a crucial element and should be performed first before allowing secondary user (SU) access. Energy detection, cyclostationary feature detection, matched filtering, and cooperative sensing have been proposed as spectrum sensing techniques [10], [11]. A new approach has been proposed in [12] and [13] which includes automatically identifying and classifying digital signals based on their modulation type to determine spectrum availability.

The focus of this dissertation is to find a simple method towards identifying and classifying digital signals based on their modulation type (with the assumption that the digital signals have been separated from the analog signals). The proposed approach must be computationally efficient, with the ultimate aim of being implemented on commodity hardware for future research. The ITU-R made some proposals in [14] which can be used as a point of departure to solve the classification problem.

Table 1.1: Radio frequency bands and applications, adapted from [5] and [6].

Frequency Band	Range	Application
Very low frequency (VLF)	9 kHz - 30 kHz	Radio navigation and maritime mobile
Low frequency (LF)	30 kHz - 300 kHz	Radio navigation and maritime mobile
Medium frequency (MF)	300 kHz - 3 MHz	AM radio broadcasting, aeronautical mobile and maritime mobile
High frequency (HF)	3 MHz - 30 MHz	Broadcasting, aeronautical mobile, maritime mobile and amateur
Very high frequency (VHF)	30 MHz - 300 MHz	FM and TV broadcasting, land and aeronautical mobile, navigation, public trunking, mobile
Ultra high frequency (UHF)	300 MHz - 1 GHz	TV broadcast, mobile, cellular, RFID, trunked radio, satellite, radio astronomy
L-band	1 GHz - 2 GHz	GPS, GLONASS, air traffic control, radar, satellite broadcasting fixed broadband data, mobile-satellite
S-band	2 GHz - 4 GHz	Wireless LAN, Bluetooth PAN, mobile, satellite broadcasting, IMT video surveillance, RFID, space research
Super high frequency (SHF)	3 GHz - 30 GHz	Fixed satellite, Wireless LAN, aircraft radar altimeters, weather and maritime radar, space research

1.2 ITU-R Digital Signal Identification Recommendation

The International Telecommunications Union (ITU) is the United Nations (UN) specialised agency for information and communication technologies. The ITU-R ensures the rational, equitable, efficient and economical use of the radio-frequency spectrum by

all radiocommunications services. The ITU-R has recommendations for spectrum management (SM), which addresses the technical identification of digital signals (SM.1600-2) [14].

This recommendation describes the process, methods, and tools for technical identification of digital signals:

- identification based on signal external characteristics,
- identification based on signal internal characteristics (low or partial apriori knowledge available about the signal),
- identification based on correlation with a known waveform (strong apriori knowledge available about the signal),
- identification is confirmed through signal demodulation, decoding, and comparison with know waveform characteristics.

By preserving the provided or captured In-phase and quadrature (I/Q) signal data, more advanced analysis of the signal internal characteristics can be done. According to SM.1600-2, standard modern digital signals typically include the following modulation schemes and multiple access formats [14]:

- Amplitude-, frequency- and phase shift keyed (ASK, FSK, PSK).
- Quadrature amplitude modulation (QAM).
- Orthogonal frequency division multiplexed (OFDM).
- Time division multiple access (TDMA).
- Code division multiple access (CDMA).
- (Coded) Orthogonal frequency division multiplexed (Access) (C)OFDM(A).
- Single carrier frequency division multiple access (SC-FDMA).
- Single carrier frequency domain equalisation (SC-FDE).

Current signal identification systems and software can provide positive signal identification of modern digital signals. The software correlates the signal's waveform to a library of predefined known patterns (signatures) (pre-amble, mid-amble, guard times, synchronisation words and tones, training sequences, pilot-symbols and codes, and scrambling codes).

If the I/Q signal data is accessible, it allows all of the amplitude, frequency and phase information contained in the signal to be preserved. The I/Q data can then be used to analyse and demodulate the signal accurately and to extract the advanced signal internal characteristics for classification.

Modulation recognition software operates on the raw I/Q data and estimated signal characteristics. These characteristics include center frequency, frequency distance between carriers, signal bandwidth, signal duration, modulation class (single or multiple carriers, linear or non-linear), symbol rate, Signal-to-Noise Ratio (SNR) and signal-specific patterns such as pilot tones, guard times, guard intervals and frame structure.

Furthermore, vector signal analysers, monitoring receivers and error vector magnitude systems are used for advanced time-domain and spectrum-time-domain analysis and are useful for providing the ability to collect the raw I/Q data on the signals of interest.

1.2.1 Identifying Digital Signals

As mentioned earlier, ITU-R recommends that signal identification takes place by evaluating the signal external and internal characteristics, using signal analysis software to gain additional insight, I/Q data processing, and other advanced methods such as correlation, auto-correlation, wavelet transforms [15] or the use of artificial intelligence [16].

1.2.2 Signal External Characteristics

In each country, a spectrum regulator has a prescribed frequency plan and licensed signal database. Evaluating this database and frequency plan is the first approach in evaluating the external characteristics of a digital signal. Each licensed signal must comply with this frequency plan and database which usually include external parameters such as:

- centre frequency and frequency distance between carriers (ensuring the signal is centered on an allocated channel),
- signal bandwidth (checked for compliance with standards of channelisation),
- spectral shape,
- signal duration when impulsive or intermittent,
- frequency shift.

Through visual inspection of the signal of interest, and comparing it to the regulator's database and frequency-plan, is a good point of departure when identifying andclassifying signals.

1.2.3 Signal Internal Characteristics

To evaluate the internal characteristics of a signal, a recording of the signal's I/Q data must be available. The I/Q data will give further insight into the amplitude, frequency, and phase of the signal of interest. The internal parameters according to [14] include:

- modulation format (this includes parameters such as instantaneous amplitude, phase, frequency, and spectrum of the signal).
- baud rate.

Furthermore, SM.1600-2 recommends how to make I/Q recordings using a vector spectrum analyser (VSA) or a monitoring receiver. The process of making I/Q recordings is not relevant at this stage of the discussion.

The I/Q data can be played back through software packages to gain insight into the signal internal characteristics. These software packages must be set-up properly to perform modulation classification. The operator must set the parameters for the software package to analyse the I/Q data. Parameters such as center frequency, sample rate,adjacent channel filtering, burst detection and data block sizes must be set. Mathematical and statistical estimators can be extracted from the recorded I/Q data which includes analysing the signal's statistical moments, power spectral density, linear/nonlinear transforms, instantaneous amplitude, frequency, phase and other parameters.

Other advanced methods used for classifying and identifying the signals include correlation methods such as cross-correlation and auto-correction. Cross-correlation is a way of determining the similarity of two waveforms as a function of a time-lag applied to one of the signals [17]. Also, know as the sliding dot product or the sliding inner-product. Auto-correlation is the cross-correlation of a signal with itself. The auto-correlation is used to find repeating patterns, such as the presence of a periodic signal buried under noise or for missing fundamental frequencies in a signal implied by its harmonic frequencies.

1.3 Automatic Modulation Classification

Automatic Modulation Classification (AMC) was firstly motivated [12] by its application in the military, for electronic warfare, gathering signal intelligence [13], surveillance and threat analysis [18], preparing jamming signals [19] and to recover the intercepted signals [20]. AMC was later implemented in civilian applications which includes spectrum management, interference identification and signal confirmation [20].

With the current increase in spectrum usage, the need arises to use the available spectrum more efficiently. Therefore Link Adaptation (LA), also known as adaptive modulation and coding (AM& C) creates an adaptive modulation scheme, from which a pool of modulations are employed in the same system, to enable the optimisation of the reliability of transmission and data rate through the adaptive selection of modulation schemes depending on the channel conditions. In current communication systems, the receiver must be aware of the transmitted signal's modulation scheme to demodulate the signal for information extraction.

Demodulation is accomplished through including extra information about the modulation type in the transmitted signal frame to let the receiver know of the modulation type and whether any changes occurred. Transmitting this extra information requires more channel bandwidth, which results in the inefficient use of the available spectrum, AMC is a solution for that problem. AMC automatically detects and classifies the receiving signal's modulation type, AMC is the intermediate step between signal detection and demodulation. By automatically identifying the modulation type of the received signal, the receiver does not need to know about the modulation type, and demodulation can be done successfully, and spectrum efficiency is improved.

Furthermore, with recent developments in Software-defined Radio (SDR) and CR, AMC has become an integral part of this intelligent radio environment. The realisations that Machine learning (ML) can be applied to CR and SDR, have created exciting possibilities which AMC is one of.

CR is an emerging technology for dynamic spectrum access. The idea in a cognitive radio is to enable secondary spectrum access to a user to share the underutilised spectrum allocated to the primary user (PU) user. The SU must be fully aware of the spectrum and the signal transmitted by the PU to avoid interference. AMC enhances the performance of a cognitive radio by identifying the modulation type of the signal present as part of spectrum sensing.

1.4 Research Problem

Commercially available software packages used in classifying digital signals' modulations are in the order of a few hundred thousand rands, and these packages use a brute force approach for demodulating digital signals. The problem that needs investigating is to find a simple approach towards automatically identifying and classifying digital modulations as part of spectrum sensing.

1.5 Objectives

The main objectives of this dissertation are to find a simple approach towards classifying digital signal modulations as part of spectrum sensing. The objectives include:

- selecting the type of classification approach (Likelihood-based (LB) or Feature-based (FB)),
- comparing the performance of the classifier in different communication channels,
- and testing the performance of the classifier on recorded I/Q data.

The focus of the study will be on single-carrier signals, with the assumption that digital signals have been separated from analog signals in the frequency band.

The following problems are not addressed in this dissertation, however, the model and simulations include residual baseband effects:

- carrier frequency and bandwidth estimates,
- baud rate estimation,
- and signal equalisation and the use of pulse-shaping filters in the transmitter and receiver chain.

Other constraints include:

- selecting the frequency band,
- and selecting the modulation classes.

1.6 Dissertation Overview

The remainder of the dissertation is organised as follows. In Chapter 2 a literature study is presented. This chapter will introduce basic digital communication concepts such as digital-to-analog conversion, digital modulation, and communication channels. Chapter 3 provides an in-depth study of FB classifiers, feature selection and related work, followed by a general system model and implementation of a FB classifier.

Chapter 4 gives an overview of the verification and validation of the proposed FB classifier. Chapter 5 and 6 presents the implemented AMC in an Additive White Gaussian Noise (AWGN) channel and in a multipath fading channel respectively.

Finally, Chapter 7 concludes the dissertation with revisiting the research goal and giving recommendations for future work.

Chapter 2

Literature Study

This chapter presents an overview of some of the basic concepts of data- and telecommunication. Concepts such as digital-to-analog conversion, digital modulation, signal space models and communication channel models are presented. It is important to understand these concepts before continuing with the literature on AMC, which is presented in chapter 3.

2.1 Digital-to-Analog Conversion

Digital-to-Analog conversion involves the process of changing the characteristics of an analog signal based on information in the digital data. Before the message signal is transmitted through a communication channel or medium (more about communication channels in Section 2.4), a modulation scheme is employed to make the information signal more compatible with the medium [7], [2]. The information signal is also known as a *baseband signal*. Transmitting the original audio, video or data (baseband signal) without modulation is known as baseband transmission. In many instances, baseband signals are incompatible with the medium.

Transmitting a baseband signal directly by radio is theoretically possible, but realistically impractical. The baseband signal is used to modulate a higher-frequency signal, also know as a carrier signal. The higher-frequency carrier signal radiate more efficiently than the baseband signals themselves [7].

The modulated carrier signal is a continuous, non-negative sine wave. This sine wave is characterised by its amplitude, frequency, and phase. By changing either of these three characteristics, a different version of the same analog signal can be constructed. These differences are used to represent the digital data [1].

Changing the amplitude, frequency and phase gives three mechanisms by which to modulate digital data onto an analog signal: Amplitude Shift Keying (ASK), Frequency Shift Keying (FSK), and Phase Shift Keying (PSK). In addition to these three, a fourth mechanism exists that combines both amplitude and phase changes, known as Quadrature Amplitude Modulation (QAM). QAM is the most efficient of the three options when favourable channel conditions (channels with a high SNR) are availble. QAM is the most used mechanism in today's digital communication systems [1].

Before getting into the specifics on digital-to-analog conversion, two issues need to be addressed that make a modulation scheme more preferable than another: data rate (bit rate) and signal rate (baud rate). Data rate (bit rate) is the number of data elements (bits) sent in 1s, measured as bits per second (bps). The signal rate (baud rate) is the number of signal elements sent in 1s, measured as baud. The goal in any communication system is to increase the data rate while decreasing the signal rate. An increase in the data rate increases the speed of data transmission. Decreasing the signal rate, reduces the bandwidth requirement, and increases the spectrum-usage efficiency.

Figure 2.1 shows the relationship between data elements and signal elements. The relationship between data elements and signal elements is defined as the ratio r, which is the number of data elements carried by each signal element. In Figure 2.1 (a) one data element is carried by two signal elements $(r = 1/2)$, In Figure 2.1 (b) two data elements are carried by 1 signal element $(r = 2)$. In Figure 2.1 (c) one data element is

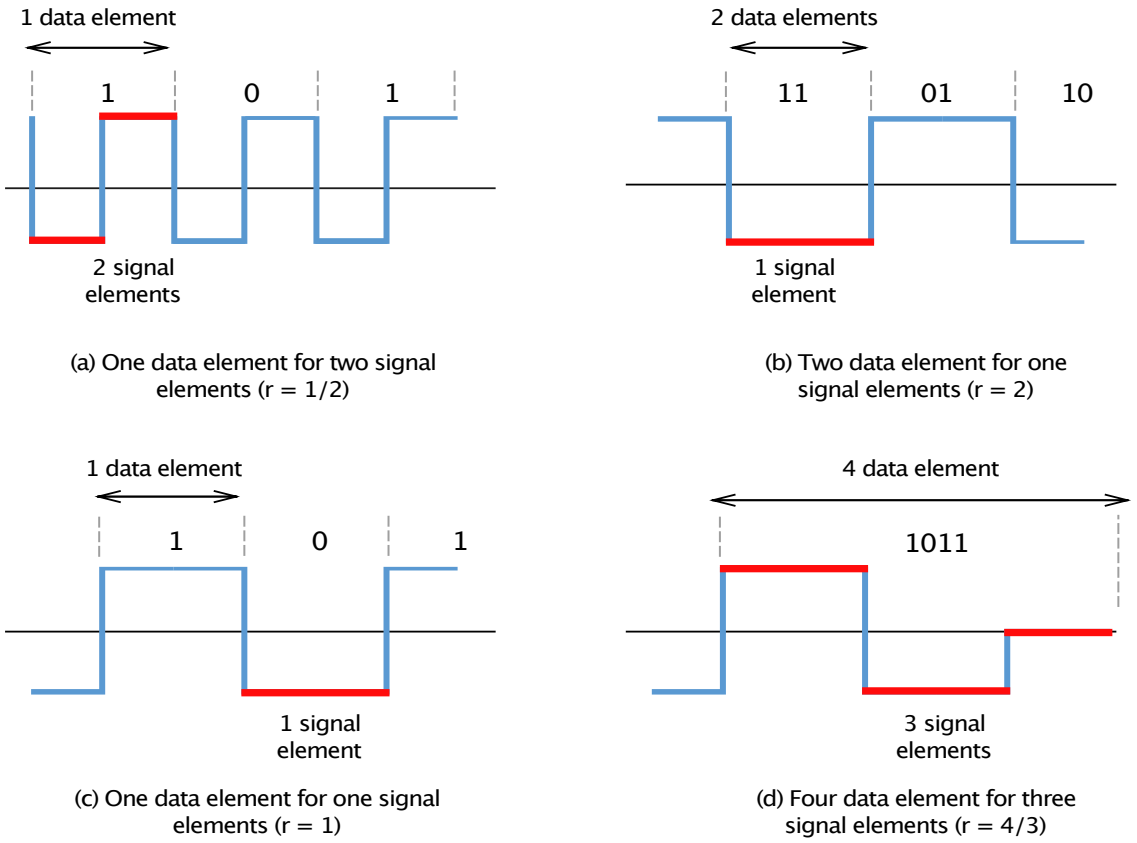

Figure 2.1: Data elements vs signal elements [1]

carried by one signal element $(r = 1)$, and Figure 2.1 (d) four data elements are carried by three signal elements $(r = 4/3)$.

Given the data rate N (bps), the signal rate S is given as,

$$S = N/r, \tag{2.1}$$

where r previously defined as the ratio between data and signal elements. The value of r in analog transmission is $r = log_2 L$ (bits/baud), where L is the number of different signal elements. Either the required bit rate must be specified and rely on the choice of quantisation levels to represent the different amplitude levels, or L is chosen to be large enough to represent the sampled signal accordingly.

The appropriate modulation scheme is chosen according to these specifications. The available bandwidth is another important constraint. The bandwidth (BW) of the digital data is proportional to the signal rate, except for FSK [1].

2.2 Digital Modulation

Advances in hardware and digital signal processing over the past years have made digital transceivers more powerful, faster, power-efficient and cheaper than analog transceivers. As a result digital modulations have also improved resulting in higher data rates, powerful error correction, resistance against channel impairments, more efficient multiplexing techniques, better security and improved privacy [2]. This makes digital modulations more attractive than analog modulations.

Referring to Section 2.1 and [2], the main considerations for choosing a particular digital modulation scheme are:

1. high data rates (N),
2. high spectral efficiency (minimal BW),
3. high power efficiency (low transmit power),
4. robustness to channel impairments,
5. and low cost implementation.

The technique that achieves the best tradeoff between these requirements is selected. Digital modulations are grouped into two main categories: amplitude/phase modulations and frequency modulation. Frequency modulation is generated using non-linear techniques [2]. This type of modulation is also known as a constant envelope modulation. The data is embedded in the frequency information of the transmitted signal. Non-linear modulation leans itself towards spectral broadening, which increases the bandwidth requirement of the signal [2].

Amplitude/phase modulations are known as linear modulations. Linear modulated signals have better spectral properties. Linear modulation embeds the data in the amplitude and phase of the signal. Linear modulations are more susceptible to interference and fading. Linear modulations require the use of linear amplifiers, which makes it a more expensive and less power efficient option. The tradeoff between linear and non-linear modulations are those of high spectral efficiency versus power efficiency versus resistance to channel impairments [2].

After selecting the modulation technique, the next step is to determine the constellation size. The constellation size depends on the data rate required by the application at hand. Modulations with a vast constellation have higher data rates (bps), but they are more susceptible to noise, fading and other system imperfections.

2.2.1 Amplitude Shift Keying

ASK varies the amplitude of the carrier signal to create the signal elements. The frequency and the phase of signal stay constant. ASK is usually implemented using only two signal levels, known as binary ASK or On-Off Keying (OOK). The peak amplitudes are either 0 or the same as the carrier signal.

$$ASK(t) = s(t)sin(2\pi ft) \tag{2.2}$$

Figure 2.2 shows an example of ASK, and how the amplitude changes with a change in data element. For a $bit = 1$ the amplitude of the modulated signal is the same as the amplitude of the carrier signal. For a $bit = 0$, the amplitude of the modulated signal changes to zero.

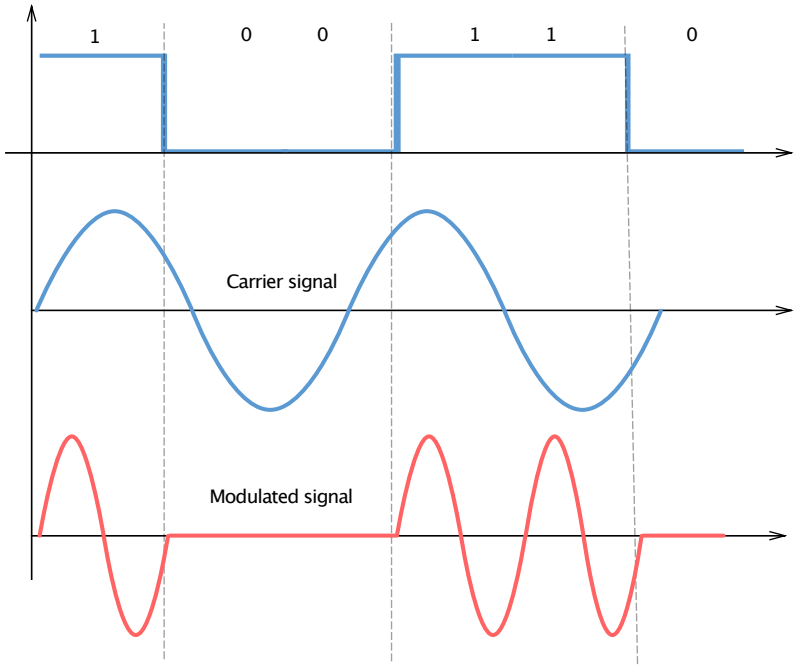

Figure 2.2: ASK modulated signal [1]

2.2.2 Frequency Shift Keying

In FSK the frequency of the carrier signal changes depending on the data elements. Both the amplitude and phase of the carrier signal remain the same. Figure 2.3 gives an example of a binary FSK (2-FSK) modulated signal. For a $bit = 1$ the frequency of the carrier signal is low, and for $bit = 0$ the frequency of the carrier signal is higher, or vice versa.

The frequency of the modulated signal is a combination of these two frequencies resulting in the modulated signal.

$$FSK(t) = \begin{cases} sin(2\pi f_1 t) & \text{for bit 1} \\ sin(2\pi f_2 t) & \text{for bit 0} \end{cases}$$

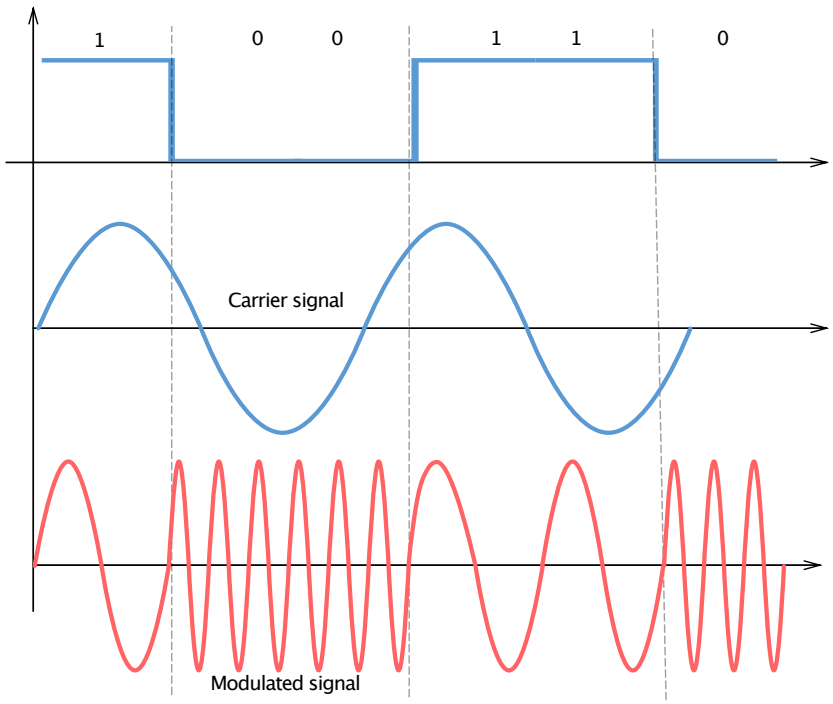

Figure 2.3: FSK modulated signal [1]

2.2.3 Phase Shift Keying

In PSK the phase of the carrier signal in an indication of the data elements. The phase of the carrier signal is measured concerning the starting angle of the sinusoid. Figure 2.4 is an example of a binary PSK (BPSK or 2-PSK) modulated signal. The phase of the carrier signal changes with each data element with π rad ($2\pi/M$ where $M = 2$) or with 180^o.

$$PSK(t) = \begin{cases} sin(2\pi ft) & \text{for bit 1} \\ sin(2\pi ft + \pi) & \text{for bit 0} \end{cases}$$

In PSK, both the amplitude and the frequency of the carrier signal stay constant.

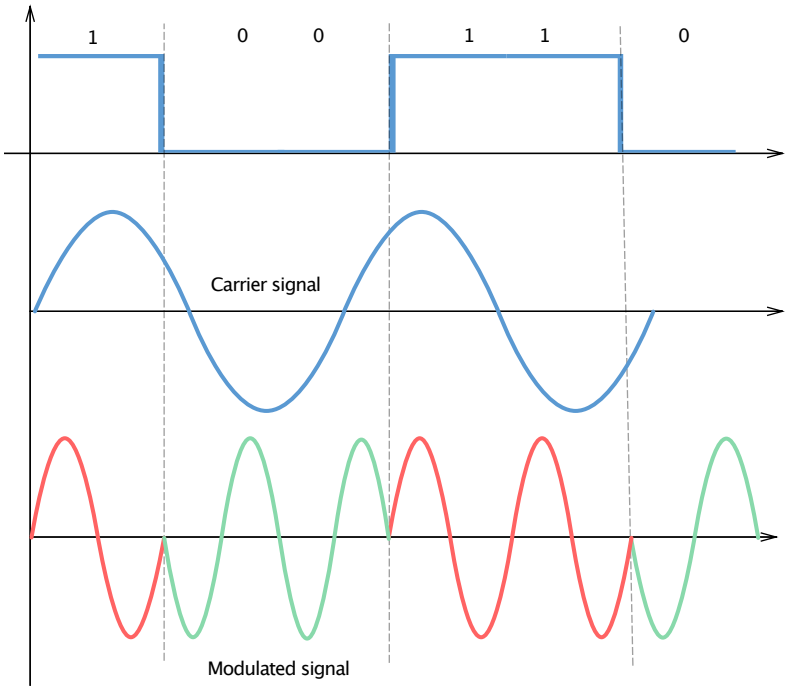

Figure 2.4: PSK modulated signal [1]

2.2.4 Quadrature Amplitude Modulation

QAM is a combination of amplitude and phase shift keying. PSK is limited by the sensitivity of the receiver to distinguish between the phase changes. With an increase in modulation order (constellation size), the phase difference decreases, and it becomes increasingly more difficult to detect the phase changes. Any channel interference or fading may result in total data recovery failure. QAM combines two carrier signals with different amplitudes. This is referred to as the *in-phase* (I) and *quadrature* (Q) signals. The in-phase and quadrature components can be reduced to two sinusoids with a 90^o or $\pi/2$ rad phase offset concerning each other.

2.3 Signal Space

In digital communication and modulation, the receiver must minimise the probability of detection error when decoding the received signal. The received signal symbols are mapped to a set of possible transmitted symbols that are the closest to those symbols transmitted. Therefore a metric to determine the distance between the received and transmitted symbols is required.

The transmitted symbols are mapped to a set of basis functions to obtain a one-to-one correspondence between the set of transmitted symbols and their equivalent vector representations [2]. The symbols are then analysed in vector space instead of function space. A signal is demodulated by analysing the signal in the vector space.

Each modulation scheme is expressed mathematically regarding their vector representation. The following sections show how this can be accomplished and how the vector representation contributes to the detection, and finally to the classification, of different modulations.

2.3.1 Signal Model Syntax

Table 2.1 clarifies the syntax and variables used throughout the section. Let [square brackets] denote the values included and (rounded brackets) be the values excluded from a set.

2.3.2 Signal Model

The signal model and the corresponding vector representation are adapted from [2].

Let us consider Figure 2.5. The transmitter sends $K = log_2 M$ bits of information through the communication channel every T seconds at a data rate of $N = K/T$ bps, where $M = 2^K$ possible sequences of K bits.

Table 2.1: Signal model syntax description

Variable	Description
M	modulation order
K	bits per symbol
m_i	message to be transmitted
$\hat{m}_i$	estimate of message m_i
$\mathcal{M}$	set of all messages
$\mathbf{b}_i$	vector denoting bit sequence of length K for message m_i
$\hat{\mathbf{b}}_i$	vector denoting the estimated bit sequence of length K for message $\hat{m}_i$
$\mathbf{S}$	vector denoting a set of analog signals
s_i	analog signal corresponding to message m_i with bit sequence $\mathbf{b}_i$
$n(t)$	noise signal
$r(t)$	received signal
n_{10}	base 10 or decimal notation
$\Re$	real part of a complex signal
$\Im$	imaginary part of a complex signal

Each possible bit sequence of length K forms a message $m_i = \{\mathbf{b}_1, \mathbf{b}_2, ..., \mathbf{b}_k\} \in \mathcal{M}$, where $\mathcal{M} = \{m_1, m_2, ..., m_M\}$ is the set of all the messages. Each message has equal probability p_i of being transmitted, and $\sum_{i=1}^{\mathcal{M}} p_i = 1$.

Let message signal m_i be transmitted during the time interval $[0, T)$. The channel is analog in nature and the message signal needs to be converted to an analog signal for transmission. Each message $m_i \in \mathcal{M}$ is mapped to an unique analog signal $s_i(t) \in \mathbf{S} = \{s_1(t), s_2(t), ..., s_i(t)\}$, where $s_i(t)$ is defined on time interval $[0, T)$.

Because each message signal represents a bit sequence, each signal $s_i(t) \in \mathbf{S}$ also represents a bit sequence. The detection of the transmitted signal $s_i(t)$ at the receiver is the same as detecting the transmitted bit sequence, as each signal can be traced back to its specific bit sequence representation.

When sent sequentially, the transmitted signal becomes a sequence of the analog signals over the time interval $[kT, (k+1)T) : s(t) = \sum_k s_i(t - kT)$, where $s_i(t)$ are analog signals which corresponds to the message signal m_i designated to be transmitted. Let's view the mathematics in context of the following example.

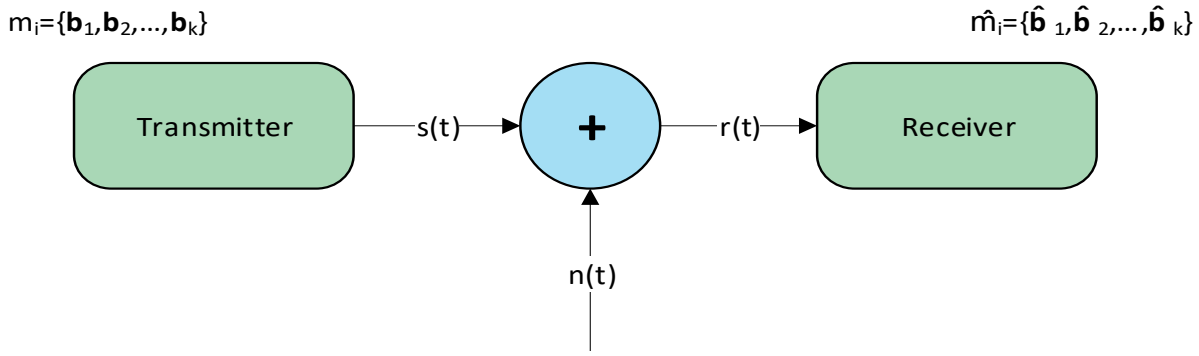

Figure 2.5: Transceiver communication flow [2]

Example 2.1

Consider two messages being transmitted using Quadrature Phase Shift Keying (QPSK) modulation (modulation order $M = 4$). The system transmits $K = log_2(4) = 2$ bits through the channel every $T = 1\mu s$, with a data rate of $N = 2/1\mu s = 2$ Mbps. Four possible sequences of sending two bits per time interval are available. The four possible sequences are [00 01 10 11]. Lets assume that $\mathcal{M} = \{m_1, m_2\}$. Each message $m_i \in \mathcal{M}$ has a bit length which can be divided into smaller bit sequences of length K. Therefore let $m_1 = 180_{10}$, with its equivalent byte of [10110100], $m_2 = 27_{10}$ with its byte of [00011011].

Each message $m_i = \{m_1, m_2\} \in \mathcal{M} \; \forall \; i \in [1,2]$ is divided into $m_1 = \{10, 11, 01, 00\}$, with $\mathbf{b}_1 = 10$, $\mathbf{b}_2, = 11$, ..., etc. Following the same procedure for m_2 will result in $m_2 = \{00, 01, 10, 11\}$.

As a result of QPSK being the chosen modulation, four different analog signals are needed to represent the four different bit sequences. PSK makes use of phase differences between the signals to represent the data. Four phases are required, with $2\pi/M$ phase increments, which results in $\theta_i = \{0, \pi/2, \pi, 3\pi/2\}$.

For m_1 an $s(t) \in \mathbf{S}$ exists with $\mathbf{S} = \{s_1(t), s_2(t), s_3(t), s_4(t)\}$, and $s_i(t) = Acos(2\pi ft + \theta_i)$ and $i = [1,4]$, with A being the constant amplitude of the signal. The transmitted

signal $s(t)$ for m_1 is then $s(t) = \sum_{i=1}^{4} s_i(t), \forall\, i \in [1,4]$. Same applies for m_2.

Figure 2.5 shows the transmitted signal sent through an AWGN channel. The AWGN channel adds noise (see section 2.4) $n(t)$ to the transmitted symbols which corrupts the transmitted signal. Given the received signal $r(t) = s(t) + n(t)$, the receiver must estimate $s_i(t)$, and map the estimated signals to the corresponding message bit sequence $\hat{m}$.

The best possible estimate (based on minimising the probability of message error) for $s_i(t)$ is mapped to the best estimate of the message $m_i \in \mathcal{M}$ and the receiver then needs to output the best estimate $\hat{m} = \{\hat{\mathbf{b}}_1, ..., \hat{\mathbf{b}}_k\} \in \mathcal{M}$ of the transmitted bit sequence. The received message is corrupted by noise. The receiver is tasked with deciding, based on a decision rule, whether the received message falls within a certain decision region. The receiver tries to minimise the probability of error by selecting the appropriate output.

As mentioned before, the basic principle behind a vector representation of the signals is the concept of a basis set. It can be shown [2] that any set M real energy signals $\mathbf{S} = \{s_1(t), ..., s_M(t)\}$ defined on $[0, T)$ can be expressed as a linear combination of $N \leq M$ real orthogonal basis functions $\{\phi_1(t), ...\phi_N(t)\}$. Therefore $s_i(t) \in \mathbf{S}$ can be expressed in terms of their basis function [2] as

$$s_i(t) = \sum_{j=1}^{N} s_{ij}\phi_j(t), 0 \leq t < T, \tag{2.5}$$

where

$$s_{ij} = \int_0^T s_i(t)\phi_j(t)dt \tag{2.6}$$

is a real coefficient representing the projection of $s_i(t)$ onto the basis function $\phi_j(t)$ and

$$\int_0^T \phi_i(t)\phi_j(t)dt = \begin{cases} 1 & i = j \\ 0 & i \neq j \end{cases} \tag{2.7}$$

If the signals $\{s_i(t)\}$ are linearly independent then $N = M$, otherwise $N < M$. For linear passband modulation techniques, the basis set consists of sine and cosine functions:

$$\phi_1(t) = \sqrt{\frac{2}{T}}\cos(2\pi f_c t) \tag{2.8}$$

and

$$\phi_2(t) = \sqrt{\frac{2}{T}}\sin(2\pi f_c t), \tag{2.9}$$

where $\sqrt{2/T}$ is needed for normalisation so that $\int_0^T \phi_i^2(t)dt = 1, i = 1, 2$. These basis functions are only an approximation to equation (2.7), since

$$\int_0^T \phi_1^2(t)dt = \frac{2}{T}\int_0^T 0.5[1 + \cos(4\pi f_c t)]dt = 1 + \frac{\sin(4\pi f_c T)}{4\pi f_c T} \tag{2.10}$$

The numerator in equation (2.10) is bounded by one and for $f_c T >> 1$ the denominator of this term is very large. Thus, this second term can be neglected. And similarly

$$\int_0^T \phi_1(t)\phi_2(t)dt = \frac{2}{T}\int_0^T 0.5[\sin(4\pi f_c t)]dt = \frac{-\cos(4\pi f_c T)}{4\pi f_c T} \approx 0, \tag{2.11}$$

where the approximation is taken as an equality for $f_c T >> 1$. With the basis set $\phi_1(t) = \sqrt{2/T}\cos(2\pi f_c(t))$ and $\phi_2(t) = \sqrt{2/T}\sin(2\pi f_c(t))$ the basis function representation in equation (2.5) corresponds to the complex baseband representation of $s_i(t)$ in terms of its in-phase and quadrature components with an extra factor of $\sqrt{2/T}$:

$$s_i(t) = s_{i1}\sqrt{\frac{2}{T}}\cos(2\pi f_c t) + s_{i2}\sqrt{\frac{2}{T}}\sin(2\pi f_c t) \tag{2.12}$$

2.3.3 Constellation Mapping and I/Q Channels

The coefficients $\{s_{ij}\}$ are denoted as a vector $\mathbf{s}_i = (s_{i1}, ..., s_{iN}) \in \mathcal{R}^N$, which is called the signal constellation point corresponding to the signal $s_i(t)$. The signal constellation consists of all the constellation points $\{\mathbf{s}_1, ..., \mathbf{s}_M\}$. With the given basis functions $\{\phi_1(t), ..., \phi_N(t)\}$ there is a one-to-one correspondence between the transmitted signal $s_i(t)$ and its constellation point $\mathbf{s}_i$. The representation of $s_i(t)$ in terms of its constellation points is called the signal space representation and the vector space containing the constellation is called the signal space.

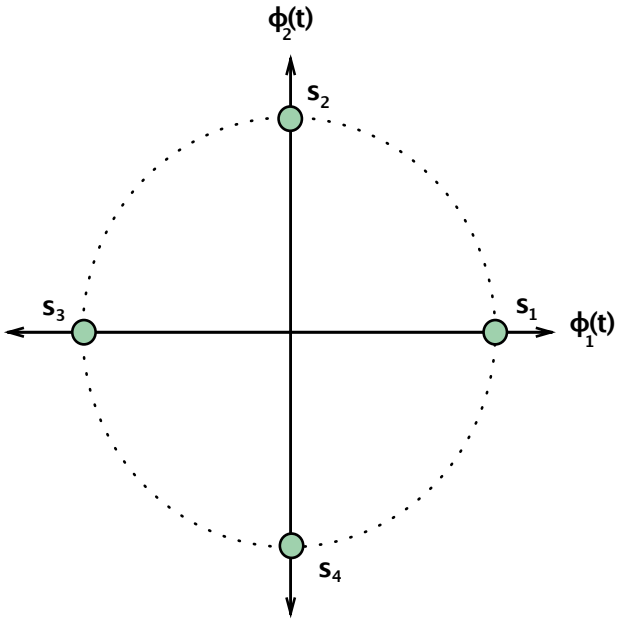

Figure 2.6: Signal space representation [2]

Figure 2.6 illustrates a two-dimensional signal space, which corresponds to the basis functions $\phi_i(t), i = 1, 2$, where $\mathbf{s}_i \in \mathcal{R}^2$ with the ith axis of $\mathcal{R}^2$ corresponding to the basis functions. Common modulation techniques like M-PSK and M-QAM are two-dimensional, with the in-phase and quadrature-phase basis functions on the time axis.

The principle of digital modulation, as mentioned earlier, is to encode information into a carrier signal which is then transmitted over a communication channel. The goal is to send the information at a high data rate while minimising the bandwidth used and

keeping the probability of making an estimation error of the received data low.

The modulated signal can be expressed as

$$s(t) = \alpha(t)\cos[2\pi(f_c + f(t))t + \theta(t) + \phi_0] = \alpha(t)\cos(2\pi f_c t + \phi(t) + \phi_0) \tag{2.13}$$

with information being encoded in the amplitude $\alpha(t)$, frequency $f(t)$ or phase $\theta(t)$ of the carrier signal. In equation (2.13) $\phi(t) = 2\pi f(t) + \theta(t)$ and ϕ_0 is the phase offset of the carrier. This combines the phase and frequency modulation part of the signal into angle modulation. Equation (2.13) can be rewritten in terms of the previously mentioned in-phase and quadrature components (I/Q), using the trigonometric identity that

$$\cos(x \pm y) = \cos x \cos y \mp \sin x \sin y \tag{2.14}$$

and setting the phase offset ϕ_0 of the carrier to zero,

$$\begin{aligned} s(t) &= \alpha(t)\cos\phi(t)\cos(2\pi f_c t) - \alpha(t)\sin\phi(t)\sin(2\pi f_c t) \\ &= s_I(t)\cos(2\pi f_c t) - s_Q(t)\sin(2\pi f_c t), \end{aligned} \tag{2.15}$$

where $s_I(t) = \alpha(t)\cos\phi(t)$ is the in-phase component of $s(t)$ and $s_Q(t) = \alpha(t)\sin\phi(t)$ is the quadrature component. Lets define the complex signal

$$u(t) = s_I(t) + js_Q(t), \tag{2.16}$$

so that $s_I(t) = \Re\{u(t)\}$ and $s_Q(t) = \Im\{u(t)\}$. Then with $u(t)$ in mind, equation (2.15) can be rewritten in its complex baseband form as

$$\begin{aligned} s(t) &= \Re\{u(t)\}\cos(2\pi f_c t) - \Im\{u(t)\}\sin(2\pi f_c t) \\ &= \Re\{u(t)e^{j(2\pi f_c t)}\}, \end{aligned} \tag{2.17}$$

Alternatively, this expression can be written as

$$u(t) = a(t)e^{j\phi(t)} \tag{2.18}$$

with the complex envelope

$$a(t) = \sqrt{s_I^2(t) + s_Q^2(t)} \tag{2.19}$$

and the phase

$$\phi(t) = \tan^{-1}\left(\frac{s_Q(t)}{s_I(t)}\right). \tag{2.20}$$

With this representation equation 2.17 becomes

$$s(t) = \Re\left\{a(t)e^{j\phi(t)}e^{j2\pi f_c t}\right\} = a(t)\cos(2\pi f_c t + \phi(t)), \tag{2.21}$$

the expression $a(t)$ is known as the instantaneous amplitude of the received signal sample and $\phi(t)$ is the instantaneous phase [21].

2.3.4 M-PSK in Terms of I/Q

In Section 2.2 the general formulation for M-ary phase shift keying (M-PSK) modulation has been covered. To recap, M-PSK modulation encodes the information that needs to be transmitted in the phase of the signal.

Each transmitted M-PSK signal element, $s_i(t) \in \mathbf{S}$, is expressed in terms of its respective in-phase and quadrature-phase components, which is given by [2]:

$$\begin{aligned} s_i(t) &= \Re\{Ag(t)e^{j2\pi(i-1)/M}e^{j2\pi f_c t}\}, && 0 \le t \le T_s \\ &= Ag(t)\cos\left[2\pi f_c t + \frac{2\pi(i-1)}{M}\right] \\ &= Ag(t)\cos\left[\frac{2\pi(i-1)}{M}\right]\cos 2\pi f_c t - Ag(t)\sin\left[\frac{2\pi(i-1)}{M}\right]\sin 2\pi f_c t. \end{aligned} \tag{2.22}$$

In a two-dimensional signal space, the signal constellation points $(s_{i1}, s_{i2}) \in \mathbf{s}_i$, are given by $s_{i1} = A\cos[\frac{2\pi(i-1)}{M}]$ and $s_{i2} = A\sin[\frac{2\pi(i-1)}{M}]$ for $i = 1, ..., M$, where M is the modulation order. $g(t)$ forms part of the pulse shaping filter.

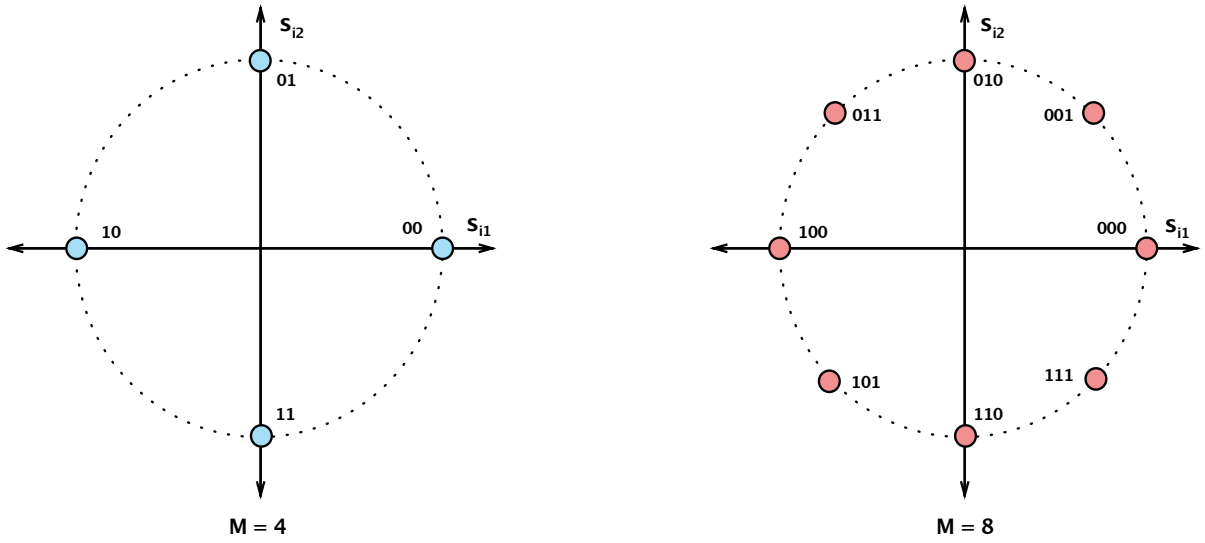

Figure 2.7: A general representation of an M-PSK modulation in the signal space. [2]

The different phases used to convey the information bits for representing the symbols are $\theta_i = \frac{2\pi(i-1)}{M}, i = 1, 2, ..., M = 2^K$. Figure 2.7 shows the general signal space representation for a QPSK modulated signal ($M = 4, K = 2$, with $\theta = [0, \pi/2, \pi, 3\pi/2]$), and for 8-PSK modulated signal ($M = 8, K = 3$, with $\theta = [0, \pi/4, \pi/2, 3\pi/4, \pi, 5\pi/4, 3\pi/2, 7\pi/4]$).

2.3.5 M-QAM in Terms of I/Q

In Section 2.2 the general formulation for an M-ary quadrature amplitude modulation (M-QAM) has been covered. The M-QAM modulated signal conveys the information bits in both the amplitude and the phase of the transmitted signal (two degrees of freedom). As a result, M-QAM is more spectrally-efficient [2], as it can encode more bits per symbol for any given message signal. The expression for an M-QAM modulated signal in terms of its in-phase and quadrature components are

$$\begin{aligned} s_i(t) &= \Re\{A_i e^{j\theta_i} g(t) e^{j2\pi f_c t}\} \\ &= A_i \cos(\theta_i) g(t) \cos(2\pi f_c t) - A_i \sin(\theta_i) g(t) \sin(2\pi f_c t), \quad 0 \leq t \leq T_s. \end{aligned} \tag{2.23}$$

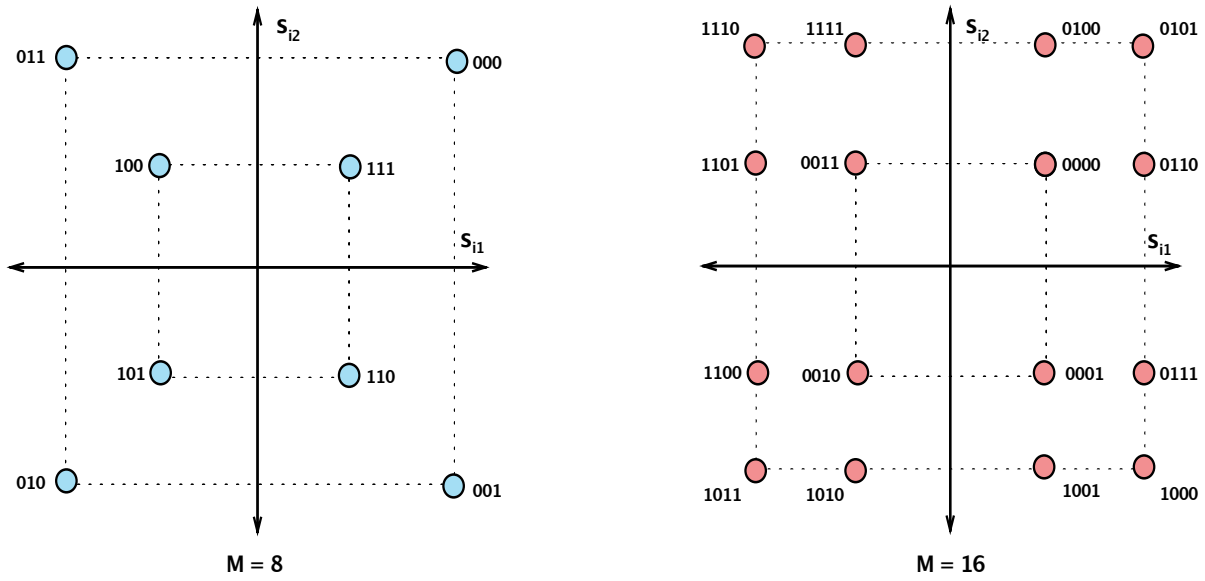

Figure 2.8: A general represenation of an M-QAM modulation in the signal space. [2]

For a squared signal constellation, s_{i1} and s_{i2} take values on $(2i-1-L)d, i = 1, 2, ..., L = 2^l$ where d is the distance between any pair of symbols in the signal constellation given by

$$d_{ij} = ||\mathbf{s}_i - \mathbf{s}_j|| = \sqrt{(s_{i1} - s_{j1})^2 + (s_{i2} - s_{j2})^2}. \tag{2.24}$$

These square constellations have $M = 2^{2l} = L^2$ constellation points, used to transmit $2l$ bits per symbol, or l bits per dimension. Figure 2.8 shows the general signal space representation for an 8-QAM ($M = 8, L = 2\sqrt{2}$) and 16-QAM modulated signal ($M = 16, L = 4$).

2.4 Communication Channel Models

The communication channel is the medium through which electromagnetic signals are sent from one place to another. This is usually accomplished through three mediums

[7]; electrical conductors (twisted-pair cable used for Local Area Networks (LAN)), optical media (fiber-optic cable) and free space, also known as *wireless* or *radio*.

In wireless communication, radio propagation refers to the behaviour of radio waves (3 kHz - 1 GHz range of the electromagnetic spectrum). The propagation of these radio waves are affected by three physical phenomena [3]: *reflections*, *diffractions* and *scattering*.

Reflections occur when the propagating electromagnetic wave impacts a large object. The large object's dimensions are more significant compared to the wavelength of the signal, and reflects back to the source, instead of propagating to the receiver.

Diffractions occur when objects obstruct the path between the transmitter and receiver with irregularities and small openings, which causes the signal to spread or bend around the objects and openings. The waves generated by the diffractions are useful for reaching the receiver when no Line-of-Sight (LOS) path is available.

Scattering is the phenomena that cause the radio wave to deviate from the straight path to the receiver by obstacles smaller in dimension compared to the wavelength of the signal. Scattering occurs from objects such as street lights, signs, lamp posts, and foliage.

Another phenomenon that occurs in radio wave propagation is fading, which is a degradation of the signal, characterised as a non-additive disturbance which causes variations in the signal amplitude over time and frequency. Fading can be classified into two types [3]: large-scale fading and small-scale fading. Large-scale fading is characterised by an average path loss (movement of the receiver over vast distances) and shadowing.

Small-scale fading is described as the rapid variations of signal levels due to constructive and destructive interference of multiple signal paths due to movements over short distances and time variations in the channel as a result of the movement speed of the receiver (characterised by a Doppler spread). Figure 2.9 and 2.10 gives a visual break-

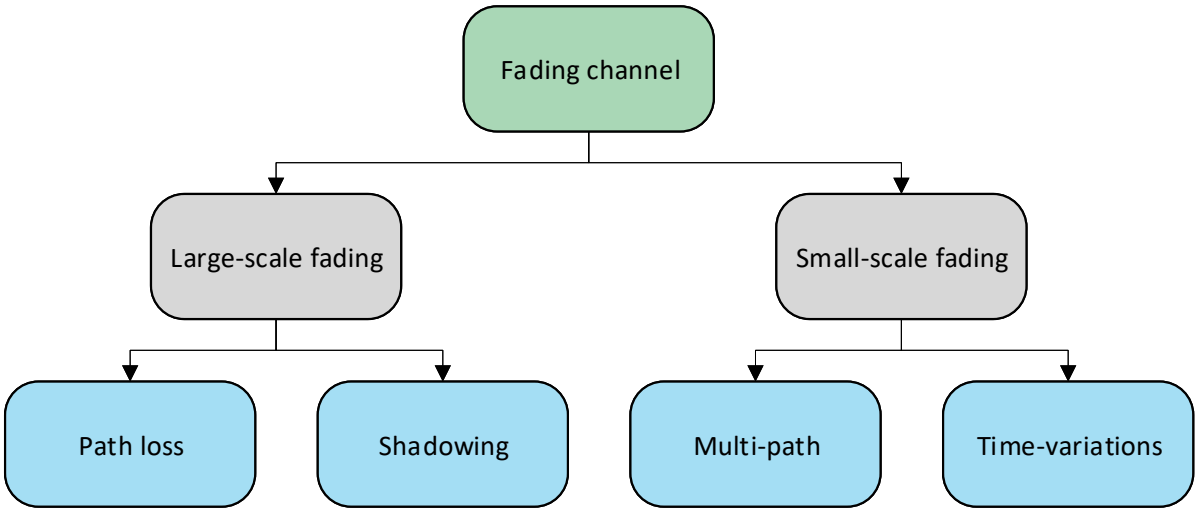

Figure 2.9: Fading channel classification [3]

down of different categories of fading channels.

2.4.1 AWGN Channel

Two of the commonly used communication channel models used to model communication systems in general are the AWGN channel and the Rayleigh- and Rician multipath fading channels. AWGN is added noise that might be intrinsic to the information systems [3], [7]. This type of noise is caused by external sources such as atmospheric conditions, extraterrestrial sources (solar, cosmic), and internal noise at the receiver. Internal noise includes thermal noise, and reflections caused by transmission line impedance mismatching, and quantisation noise introduced by the analog-to-digital converter. The term white refers to the idea that the noise has uniform power across the frequency band (constant spectral density) and a Gaussian distribution of amplitude.

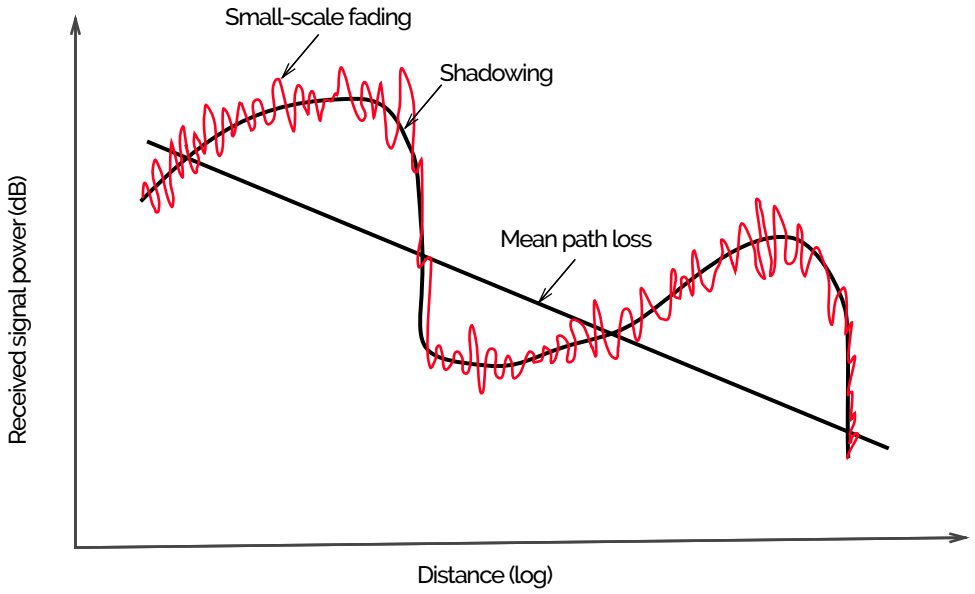

Figure 2.10: Large and small scale fading [3]

2.4.2 Rician and Rayleigh Channel Model

Rayleigh- and Rician channels [3] fall within the class of small-scale fading. Fading in the broad sense causes variations of the signal amplitude over time and frequency. In general, any wireless channel is subject to LOS and non line-of-sight (NLOS) propagation. The probability density function (PDF) of a signal envelope in a LOS environment follows a Rician distribution, while that in a NLOS environment follows a Rayleigh distribution [3].

The strongest scattering component usually corresponds to the LOS component (specular component). All the other components are NLOS components. In equation (2.25) the PDF of a Rician channel is expressed, where $\widetilde{p}(\theta)$ denotes the PDF of angle of arrival (AoA) for the scattering components and θ_0 denotes the AoA for the specular component [3].

$$p(\theta) = \frac{1}{K+1}\widetilde{p}(\theta) + \frac{K}{K+1}\delta(\theta - \theta_0) \tag{2.25}$$

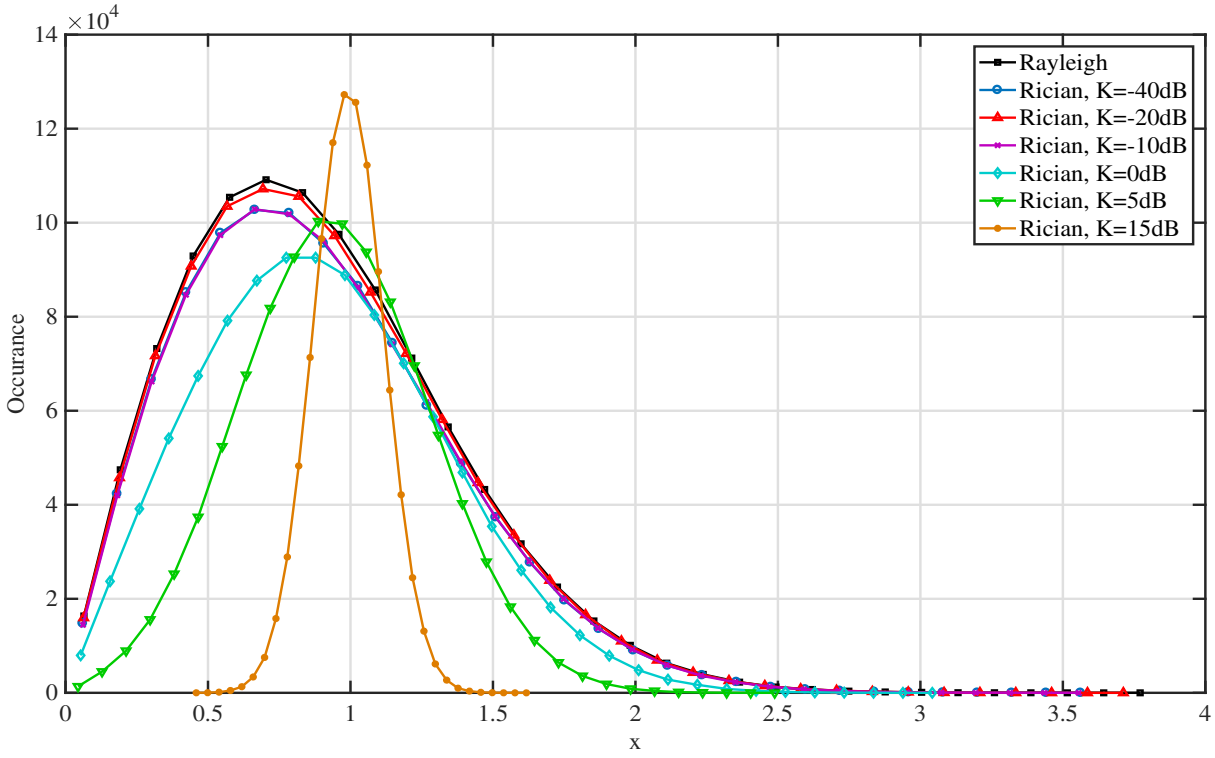

Figure 2.11: Comparison of Rician channel model at different K-factors [3].

K is defined as the Rician factor, which denotes the strength of the LOS component.

$$K = \frac{c^2}{2\sigma^2}, \tag{2.26}$$

where c^2 is the power of the LOS component and $2\sigma^2$ is the power of the scattering component. A Rician channel approaches an AWGN channel as $K >> 0dB$ and a Rayleigh channel as $K < 0dB$. Figure 2.11 shows how the Rician distribution would change when K changes. The value for K is in dB. This can be converted to σ^2 through $10^{(K_{db}/10)}$. From Figure 2.11 can be seen how the LOS component impacts the channel distribution.

2.4.3 Tapped Delay Line Model for Representing Fading Channels

Simulating fading channels fall within one of the following categories [2], [22]:

1. Transfer function models for time-invariant channels. This type of channel is assumed to be static (the channel has a time-invariant impulse response). This provides a particular frequency response due to its fixed delays within the channel. The transfer function is said to be flat when the bandwidth of the message source has a constant gain response. The channel is said to be frequency-selective if the message source has a bandwidth over which the channel has a significant gain variation.
2. Tapped delay line (TDL) for time-varying channels. The channel is said to be fast fading when the time interval over which the signal that is applied changes during the smallest of time intervals. A channel is treated as a slow fading channel when the channel remains static for a large number of consecutive symbols.

Since different paths are of different lengths, a single impulse transmitted will result in multiple copies being received at different times. The maximum delay after which the received signal becomes negligible is called maximum delay spread. A large delay spread indicates a highly dispersive channel [4]. Figure 2.12 is an illustration of the received power delay profile for a multipath channel.

The impulse response of a multipath channel can be represented by a discrete number of impulses:

$$h(t,\tau) = \sum_{i=1}^{N} c_i(t)\delta(\tau - \tau_i), \tag{2.27}$$

where the impulse response changes with time and N is the number of coefficients, and the coefficients $c_i(t)$ vary with time. The power delay profile in Figure 2.12 can be represented by a 4-tap model (TDL model). Any movement between the transmitter and receiver will result in a change of channel characteristics.

The time for which the channel remains constant is called coherence time. The frequency bandwidth for which the channel remains the same is called the coherence bandwidth. The larger the delay spread, the less the coherence bandwidth, and the channel is said to be more frequency selective.

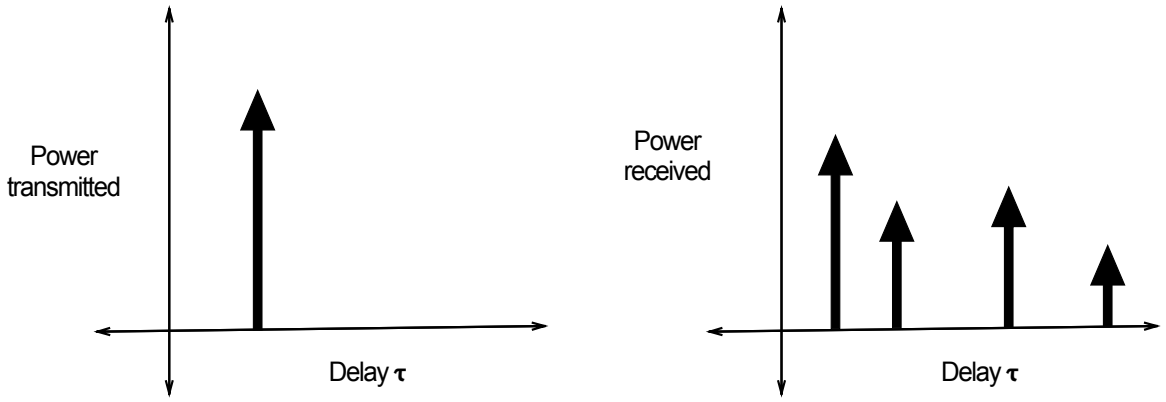

Figure 2.12: Multipath power delay profile [4]

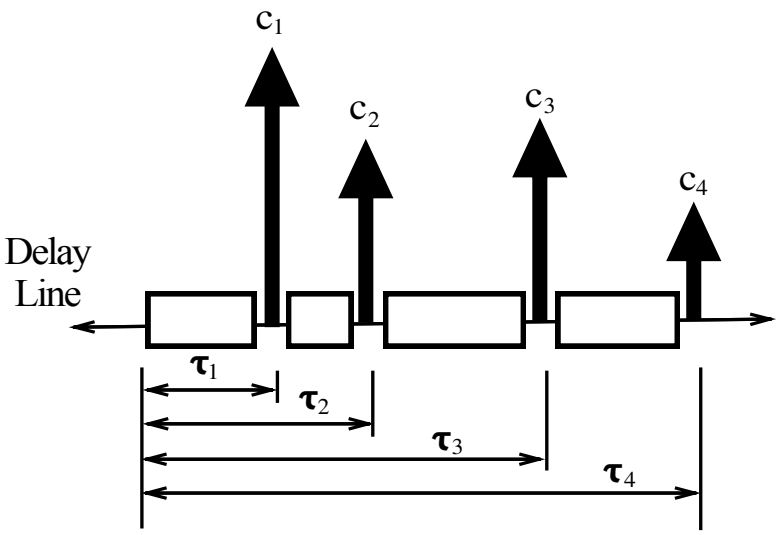

Figure 2.13: Tapped delay line model [4]

The delay profile gives a statistical power distribution (Rayleigh or Rician distribution) of the channel over time for a signal transmitted for just an instant. The Doppler power spectrum gives the statistical power distribution of the channel for a signal transmitted at just one frequency. Therefore, a power delay profile is a result of multipath, while the Doppler spectrum is caused by motion of objects in the channel [4]. When objects move very fast, the Doppler spread is large, and the coherence time is small, and the channel changes fast.

Different fading channel models have been proposed. ITU-R M.1225 [23] proposed three tapped-delay line parameters for different wireless environments: indoor office test environment, outdoor to indoor and pedestrian test environment and a vehicular test environment. For each terrestrial test environment, a channel impulse response model based on a tapped-delay line model is given.

Another well known and widely adopted fading channel model is the COST 207 channel model for multipath fading channels published by the Commission of the European Communities [24]. The COST 207 project channel model is used for GSM and DVB-T [25] standards. Radio propagation in the mobile radio environment is described by highly dispersive multipath caused by reflections and scattering.

Chapter 3 gives a more detailed look at these two fading channel models.

2.5 Conclusion

In this chapter, basic data- and telecommunication concepts such as digital-to-analog conversion, digital modulation, signal space representation of digital modulations and I/Q modulation were presented. Different communication channel models were also discussed. The next chapter proceeds to describe AMC in general with the main focus on FB classification.

Chapter 3

Feature-based Classification Approach

This chapter discusses AMC in general with the main focus on a feature-based classification approach. Feature-based classification consists of three main parts; pre-processing of the signal, feature extraction, and the classification algorithm. Related work regarding FB classification is discussed together with the feature-selection process for classifying digital modulations. The procedure for selecting the classification algorithm is also investigated. The general system model and implementation of a FB classifier is also developed and described.

3.1 Introduction

Chapter 2 introduced the discussion on AMC by mentioning the mechanics behind digital-to-analog conversion and the relationship between going from digital data to an analog signal through modulation. Different modulation techniques like ASK, FSK and PSK have been introduced, and a more advanced signal model concerning complex I/Q modulation has been introduced.

3.2 Automatic Modulation Classification Approaches

Chapter 1 introduced AMC as an alternative approach towards spectrum monitoring and spectrum sensing. Two steps are involved when developing an AMC system [12], [26]: pre-processing of the received signal and the selection of the classification algorithm. Two main classification approaches have been studied in this regard [13], [12], [18], [27], [28]: a decision-theoretic approach and a pattern recognition approach. The decision theoretic approach is also known as a LB classifier [29] and the pattern recognition approach is known as a FB classifier [30].

In an ideal AMC system, a trade-off must be made between:

- classification accuracy [12],
- robustness against unpredictable channel conditions [12],
- computational efficiency [12],
- and versatility in terms of modulation types [12].

LB classifiers are by far the most popular approach, which is motivated by the optimality of its classification accuracy [12] when channel model and parameters are entirely known. The typical approach of a LB classifier consists of two steps. LB classifiers treat the classification problem as a hypothesis testing problem, so firstly the likelihood is evaluated for each modulation hypothesis with observed signal samples. The likelihood function is derived from the selected signal model and can be modified to fulfil the need of reduced computational complexity. Secondly, the likelihood of the different modulation hypothesis is compared to conclude the decision. The decision making is accomplished with a ratio test between the two hypothesis. The requirement of a threshold adds another layer of performance improvement, but more attentive efforts must be made to select the thresholds.

LB classifiers suffer from computational complexity and is difficult to implement as complete knowledge of the received signal's probability density function must be known

to derive the likelihood function of the received signal. Some of the LB classifiers studied in literature [13], [12] include maximum likelihood (ML), Average Likelihood Ratio Test (ALRT), Generalized Likelihood Ratio Test (GLRT), and Hybrid Likelihood Ratio Test (HLRT).

The FB classification approach is easier to implement and is not as computationally sophisticated as the LB approach. The selection of suitable features and classification algorithm is the challenge. FB classifiers are divided into two subsystems: the feature extraction subsystem and the classifier subsystem (shown conceptually in Figure. 3.1). Several features are extracted from the received signal and a decision is made based on the values of those features.

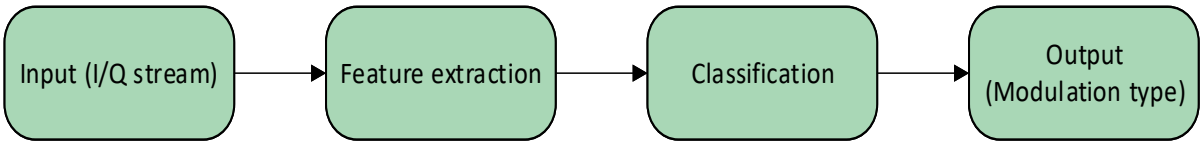

Figure 3.1: Conceptual diagram for a feature-based classification approach

The features extracted must be able to represent the difference between signal classes. The features are either instantaneous amplitude, frequency and phase, Fourier and Wavelet transform based or higher-order statistic (moments and cumulants) based. Similarly, Hazza et al. [18] showed that many combinations of classification algorithms and features had been used to solve the classification problem.

In this chapter, a closer look into the pattern-recognition or FB modulation classification approach will be taken. From this moment onward, the discussion will focus on the FB approach, as this will aid in solving the research problem in finding a simple approach to classify digital modulations.

Figure 3.1 shows a conceptual diagram for a general FB classifier. The two most important components in FB classification are the feature extraction process and the classi-

fication algorithm. The selection of suitable features and an appropriate classification algorithm is the challenge. Various combinations of features and pattern-recognition algorithms are possible, and many have been studied. The features are categorised into five types [18]:

1. instantaneous time-domain features,
2. transform domain features,
3. statistical features,
4. constellation shape,
5. and zero-crossing features.

Similarly, several types of classification algorthms have been employed in AMC. Some methods include Artificial Neural Network (ANN), Support Vector Machine (SVM), decision trees and clustering [12], [18], [27]. Other ML algorithms such as K-nearest neighbour (KNN), Logic regression and Genetic Algorithm has also been employed [12], [20], [26].

It is not easy to compare the performance of these approaches as each approach considers different modulation sets, and is based on different assumptions. Some of the assumptions include the channel model (AWGN or fading), the presence or lack of frequency and carrier offsets, the presence of shaping filters, equalisers and the sample size. The following section proceeds to discuss related work and research trends on FB classifiers which will aid in motivating the design and implementation of a simple FB classification approach.

3.3 Related Work

Numerous modulation recognition methods have been proposed. E.E. Azzouz and A.K. Nandi have made a significant contribution to the field, who have proposed an analog modulation recognition algorithm [31], digital modulation recognition algorithm [31], and a combination thereof [31]. Nandi et al. [31] classified (2, 4)-ASK, (2, 4)-PSK, (2, 4)-FSK and 16-QAM modulations in AWGN, using four instantaneous time domain features extracted from the instantaneous amplitude, phase and frequency of the received signal.

Popoola et al. in [27] and [30] proposed a combined analog and digital classifier in AWGN with an ANN as their classifier. The proposed combined analog and digital AMC system is capable of recognising nine mixed analog and digitally modulated signals. The modulations classified include (2, 4)-ASK, 2-FSK, BPSK, QPSK, AM, DSB, SSB and FM. Their overall result indicated a 99.0% success rate at low SNR ratios (SNR between 0 and 5 dB), using an ANN for classification. The feature set included a total of five features, which is the same set proposed by Nandi and Azzouz in [32]. The features are derived from the instantaneous amplitude, phase and frequency of the received signal. However, a new feature, the signal power key β, is introduced to discriminate between a signal with complex and real signal components. In [27] Popoola et al. demonstrated the effect training algorithms have on the performance of an ANN in the developed AMC system.

Pambudi et al. [33] proposed a classification approach for classifying an Orthogonal frequency division multiplexing (OFDM) signal with QPSK, 16-QAM and 64-QAM as sub-carrier modulation, a cyclic prefix of 1/4, 1/8 and 1/16, in a 6-tap Rayleigh fading channel. They followed a statistical approach using the received signal's magnitude component to extract the mean, variance, skewness and kurtosis. They demonstrated that higher-order moments (10, 14, 18, 20) could be used to distinguish between these sub-carrier modulations.

Prakasam et al. [15] considered using both wavelet transform as well as statistical

moments to classify (2, 4, 8, 16)-PSK, (2, 4, 8, 16)-QAM, GMSK and MFSK modulation schemes under low SNR in an AWGN channel. They achieved a classification accuracy of 96.8% under noisy channel conditions using a decision tree approach. Features such as higher-order moments and the mean are calculated from the normalised histogram generated from the wavelet transform coefficients.

In [34] Gang et al. proposed a new SVM classification algorithm based on higher-order cumulant features (fourth- and sixth-order cumulant) extracted from the received signal in AWGN channel. They reported a classification accuracy of 96% at an SNR of 6 dB with 200 samples, and 98% at an SNR of 4 dB with 500 samples. They proposed classifying (2, 4)-ASK, (2, 4, 8)-PSK and 16-QAM modulations schemes. Gang et al. transmitted the signal through a raised-cosine filter with a roll-off factor of $\alpha = 0.5$. Gang et al. reported that the longer the data length and the higher the SNR, the closer the cumulants are to the theoretical value, and thus the better the classification performance.

Ebrahimzadeh et al. [35] proposed classifying (2, 4)-ASK, (2, 4, 8)-PSK, (8, 16, 32, 64, 128)-QAM, and V29, V32 modulation schemes using the second, fourth, sixth and eigth order moment and cumulant as features. They achieved a classification accuracy of 83.23%, 88.23%, 93.62%, 96.14%, and 97.82% at -3, 0, 3, 6 and 9 dB SNR respectively in an AWGN channel, through a particle swarm optimisation algorithm, to enhance the classification performance of a radial-basis function neural network.

In [28] Shih et al. used a decision tree classification approach to classify BPSK, QPSK, 8-PSK, 16-QAM and 64-QAM modulations using fourth-order cumulants, which achieved a classification accuracy of 95% for a SNR lower than 10 dB, and 100% for a SNR over 15 dB.

Aslam et al. [26] introduced a Genetic Programming (GP) and KNN classification approach to classify Binary Phase Shift Keying (BPSK), QPSK, 16-QAM and 64-QAM. A classification accuracy of 81% at a SNR of 5 dB with a sample size of 1024 using a KNN classifier was advised. Combining KNN with GP a performance increase of 7% was

achieved. At a SNR of 15 dB, an accuracy of 97% with 1024 samples was achieved.

Additionally [28], [36], [37], and [38] proposed an AMC technique using higher-order cumulants to classify M-PSK and M-QAM signals for multipath fading channel. The authors estimated the cumulants through taking the channel effect into consideration.

In [13] and [18] an extensive survey is done on FB classifiers, in which Fourier transform based and more wavelet transform based features are discussed. The authors also used these features to classify ASK, PSK, FSK, QAM and AM/FM modulation. Transform domain feature, especially Fourier transform based features are used to distinguish between FSK/PSK and ASK/QAM modulations.

In [39] Muller et al. proposed a new method for AMC based on discriminative learning. The features are the ordered magnitude and phase of the received symbols at the output of a matched filter. Muller et al. used a discriminative learning approach instead of using features obtained from higher-order cumulants or cyclostationary analysis to classify modulations. They used a SVM with the new concatenated sorted symbols approach. Muller mentioned that SVMs are used due to their ability to deal with relatively large feature vectors.

Table 3.1 gives a summary of related feature-based classifiers with their respective features, modulation schemes and communication channel implemented. From the literature, it is clear that the authors proposed many combinations of features, classification algorithms, communication channel models and modulation types. Each author reported good classification accuracy under different channel models. In the end, choosing the best approach for a specific problem comes down to selecting the best trade-off between classification accuracy, robustness against channel conditions, computational efficiency and versatility regarding modulation types.

The related work highlighted the fact that a FB classification approach using statistical features extracted from the time-domain signal is a good approach. When the AMC system needs to be simple and computationally efficient without the need for domain transforms, it can be achieved. From the literature review, none of the authors

Table 3.1: A Summary of related FB classfiers

Author(s)	**Features**	**Modulations**	**Channel**
Nandi [31] et al.	Variance of instantaneous signal parameters	[2, 4]-ASK, [2, 4]-PSK, [2, 4]-FSK, 16-QAM	AWGN
Popoola [27], [30] et al.	Variance of instantaneous signal parameters, signal power key	[2, 4]-ASK, [2, 4]-PSK, 2-FSK, FM AM, DSB, SSB	AWGN
Pambudi et al. [33]	Mean, variance, skewness, kurtosis, HOM	QPSK, [16, 64] -QAM, OFDM	Rayleigh
Prakasam et al. [15]	Wavelet transform, mean, variance	M-PSK, M-QAM, GMSK, M-ary FSK	AWGN
Gang et al. [34]	Wavelet transform, mean, variance	[2, 4]-ASK, [2, 4, 8]-PSK, 16-QAM	AWGN
Ebrahimzadeh [35] et al.	HOS (moments, cumulants up to order eight)	[2, 4]-ASK, [2, 4, 8]-PSK [8, 16, 32, 64, 128]-QAM	AWGN
Shih et al. [28]	Fourth-order cumulants	BPSK, QPSK, 8PSK, 16QAM, 64-QAM	AWGN, Rayleigh
Aslam et al. [26]	Fourth- and sixth order cumulants	BPSK, QPSK, 16QAM, 64QAM	AWGN

mentioned that they tested the performance of the classifier with recorded I/Q. The authors only tested the performance of their respective classifiers through intensive simulations.

From the problem identified in Chapter 1, a simple approach for classifying digital modulation in an a AWGN and fading channel is needed. From evaluating the clas-

sifiers proposed in the literature and related work, a need to test the performance on recorded I/Q exists. Using recorded I/Q will give further insight into how much work still needs to be done to make the classifier more robust against channel impairments.

Chapter 1 mentioned that the proposed solution needs to be computationally efficient, simple to implement and should be able to classify digital modulations. The next section will give an overview of the most used features in AMC.

3.4 Feature Discussion

Many features have been proposed throughout literature. Feature extraction tries to describe the modulation classes using a minimum number of features or attributes [30] in discriminating amongst modulation classes. This section will build on the related work in Section 3.3 and on the five classes of features identified in Section 3.1, which will motivate the choice of features for this work.

Instantaneous time-domain features are related to the instantaneous amplitude, phase and frequency of the received signal [13], [12], [18], [27], [30], [40], [41]. Transform domain features are extracted from the Fourier, wavelet and cosine transforms of the signal [13], [15], [18]. Statistical features are derived from higher-order statistics (higher-order moments and cumulants, and cyclo-stationary) [13], [12], [19], [35], [36], [42], [43], [44]. Signal constellation features include comparing the received signal's constellation points to reference points. Zero-crossing features involve counting the number of zero-crossings of an intercepted signal. These features are used in likelihood tests for decision making. The rate of zero-crossings for a PSK signal is fixed for all signal symbols, while it varies in FSK.

3.4.1 Instantaneous Time-Domain Features

The following features have been proposed which exploits the instantaneous amplitude and phase of the received signal:

1. The standard deviation of the absolute value of the normalised-centred instantaneous amplitude of the signal [13], [12], [18], [32], [41].

$$\sigma_{aa} = \sqrt{\frac{1}{N}\left(\sum_{i=1}^{N} a_{cn}^2(i)\right) - \left(\frac{1}{N}\sum_{i=1}^{N} |a_{cn}(i)|\right)^2}, \tag{3.1}$$

   where $a_{cn}(i) = a(i)/m_a - 1$, and m_a is the sample mean of $a(i)$. The feature σ_{aa} is dimensionless and measures the amount of information in the signal's instantaneous amplitude.

2. The standard deviation of the centred non-linear component of the absolute instantaneous phase (in radians) [13], [12], [18], [32], [41].

$$\sigma_{ap} = \sqrt{\frac{1}{C}\left(\sum_{a_n(i)>a_t} \phi_{NL}^2(i)\right) - \left(\frac{1}{C}\sum_{a_n(i)>a_t} |\phi_{NL}(i)|\right)^2}, \tag{3.2}$$

   where $\phi_{NL}(i)$ is the value of the non-linear component of the instantaneous phase at time instant $t = i/f_s$, C is the number of samples in $\phi_{NL}(i)$, and a_t is the threshold. The feature measures the variance in the absolute instantaneous phase in modulations with information in their phase. Modulations with order $M \leq 2$ does not have information in their absolute instantaneous phase because there are only two states, and therefore their values will be the same.

3. The standard deviation of the non-linear component of the direct instantaneous phase [13], [12], [18], [32], [41].

$$\sigma_{dp} = \sqrt{\frac{1}{C}\left(\sum_{a_n(i)>a_t} \phi_{NL}^2(i)\right) - \left(\frac{1}{C}\sum_{a_n(i)>a_t} \phi_{NL}(i)\right)^2} \tag{3.3}$$

This feature is similar to σ_{ap}, in the sense that σ_{dp} measures the variance in the absolute instantaneous phase which provides the ability to distinguish BPSK from other modulations.

4. The maximum value of the power spectal density for the normalised centre instantaneous amplitude [13], [12], [18], [32], [41].

$$\gamma_{max} = \frac{max|DFT(a_{cn})|^2}{N}, \tag{3.4}$$

where Discrete Fourier Transform (DFT) is the discrete Fourier transform, N is the number of samples, $a_{cn}(i)$ is the value of the normalised-centred instantaneous amplitude defined as

$$a_{cn}(i) = a_n(i) - 1; a_n(i) = \frac{a(i)}{\mu_a}, \tag{3.5}$$

where μ_a is the mean of the instantaneous amplitude

$$\mu_a = \frac{1}{N}\sum_{n=1}^{N} a(i). \tag{3.6}$$

The normalisation of the signal amplitude is to compensate the unknown channel conditions. The feature would generally be classified under the transformation domain feature group, however, it makes use of the instantaneous amplitude. This feature measures the variance in the signal's instantaneous amplitude. For modulations where information is conveyed in the amplitude, this value should be non-zero. For modulations with constant amplitude, this value should be zero.

5. Another unique feature proposed is the signal power key denoted by β [27]. This feature was used to discriminate between signals with complex and real signal components.

$$\beta = \frac{\int_{\infty}^{\infty} r_Q^2(t)dt}{\int_{\infty}^{\infty} r_I^2(t)dt}, \tag{3.7}$$

where $r_Q(t)$ and $r_I(t)$ are the in-phase quadrature components respectively. Equation (3.7) can be rewritten for the discrete case as,

$$\beta = \frac{\sum_{n=0}^{N} r_Q[n]^2}{\sum_{n=0}^{N} r_I[n]^2}, \tag{3.8}$$

where $r_Q[n]$ and $r_I[n]$ are the quadrature and in-phase components of the signal respectively [27].

Instantaneous features are easy to extract [18], but they are sensitive to noise and have estimation errors. These features are often used with pattern recognition techniques to improve classification rates at low SNR. These features are also combined with statistical and transformation based features.

3.4.2 Transformation Based Features

There are mostly two transformation based approaches followed in literature: Fourier transform based or Wavelet transform based features.

1. γ_{max} is an example of the DFT based feature. This feature is used to discriminate between both analog and digital amplitude modulations. γ_{max} is also employed with various ANNs and SVMs [18].

2. The maximum value of DFT magnitude of the k^{th} power of the analytic form of the received signal,

$$\Gamma_k = \frac{max|\text{DFT}(a(i)^k)|^2}{N}, \tag{3.9}$$

with $k = 2$, and $k = 4$ is used to classification of PSK signals. This feature is robust against both carrier frequency offset and time offset.

3. The signal spectrogram shows the spectral density variation with time. Two features have been extracted from the spectrogram: moments-like features and principle component analysis (PCA) for classification of PSK/QAM, (2, 4)-FSK, ASK

and OFDM. Spectrogram feature classification has shown to be robust against carrier frequency offset [18].

4. Wavelet transform is another technique used for feature extraction. The features extracted from wavelet transforms contain time and frequency domain information about the signal. Wavelet transform has the advantage of being able to reduce the effect of noise [18]. Using continuous wavelet transform (CWT) features require more intensive pre and post-processing steps to extract features, such as median filtering to remove any outliers. The mean, variance, and kurtosis of the coefficient are then used as features. Digital wavelet transform (DWT) divides the signal into different decompositions before extracting features.

3.4.3 Statistical Features

Higher-order statistical features are found throughout literature, especially when modelling an AMC system in a fading channel. Higher-order statistics are divided into higher-order moments and higher-order cumulants. These features have three advantages [12], [18]:

1. suppression of the effect of noise,
2. robustness against phase rotation,
3. reflects the higher-order statistical characteristics of the signal.

A signal's amplitude and phase distribution can be characterised by its respective PDF. Without knowing beforehand the type of distribution, using order-statistics help to characterise the amplitude and phase distributions. When the signal shows Gaussian characteristics, it can be fully described using the first and second order moments (mean and variance). A non-Gaussian signal needs higher-order statistics to characterise it fully.

The first feature is mean of the received signal components, also know as the first order

moment, denoted as

$$\mu(x) = \frac{1}{N}\sum_{i=0}^{N-1} x_i \tag{3.10}$$

where N is the total number of samples and x_i is the sample value at i. The second feature is the variance of the received signal components, which is the second order moment.

$$\sigma^2(x) = \frac{1}{N-1}\sum_{i=0}^{N-1} (x_i - \mu)^2 \tag{3.11}$$

The third feature is the called the skewness, which is the third order moment, and expressed mathematically as

$$s(x) = \frac{1}{\sigma^3}\frac{\sum_{i=0}^{N-1}(x_i - \mu)^3}{N}. \tag{3.12}$$

The skewness gives a measure of asymmetry of the data around the sample mean. A skewness < 0 is an indication that the data is spread out more to the left of the mean, and a skewness > 0 indicates that the data is spread out more to the right. For a normal distribution, with perfect symmetry, the skewness is zero.

The fourth feature is the kurtosis or the fourth-order moment of the received signal's components,

$$\kappa(x) = \frac{1}{\sigma^4}\frac{\sum_{i=0}^{N-1}(x_i - \mu)^4}{N}. \tag{3.13}$$

The kurtosis is a measure of how outlier-prone a distribution is. A normal distribution has a kurtosis of 3. Some algorithms calculate the excess kurtosis. Kurtosis measures the "fatness" of the tails of the distribution. Positive excess kurtosis means that the distribution has fatter tails than a normal distribution. Fatter tails mean there is a higher normal probability of significant positive and negative returns realisations. A kurtosis of +3 indicates the absence of kurtosis. Some algorithms adjust the result to zero (kurtosis minus 3), and then any reading other than zero is referred to as excess kurtosis [45].

The fifth feature extracted is the higher order-moment

$$\sigma^m(x) = \frac{1}{N}\sum_{i=0}^{N-1} (x_i - \mu)^m \tag{3.14}$$

where m is the moment order.

Moments

Higher-order modulations have higher moment values, which makes then useful for classifying different order PSK signals for example. Calculating the kth order moment of the signal's phase $\phi^k(n)$ [12] is defined as

$$\mu_k(\mathbf{r}) = \frac{1}{N}\sum_{n=1}^{N}\phi^k(n). \tag{3.15}$$

Higher-order moments of a complex valued signal $\mathbf{r} = r[1], r[2], ..., r[N]$ is defined as

$$\mu_{xy}(\mathbf{r}) = \frac{1}{N}\sum_{n=1}^{N} r^x[n]r^{*y}[n], \tag{3.16}$$

where $x + y = k$ and $r^*[n]$ is the complex conjugate of $r[n]$. Equation (3.16) is also written as

$$M_{pq} = E[r^{p-q}(r^*)^q], \tag{3.17}$$

where p is the moment order and r^* is the complex conjugate of r, and $r = a + jb$ with a zero-mean discrete signal sequence, M_{pq} is the moment of a complex random variable, and E is the expected value, or the long run average. Equation (3.16) is also know as the joint moment-to-cumulant generating function. Moments are used to describe the PDF for a distribution [17]. A Gaussian PDF can be completely characterised by its first two moments (mean and variance). When signals are non-Gaussian, higher-order statistics (order greater than two) are needed to define their PDF, which are then able to reveal other information about the distribution.

Normally, a random variable's distribution is not known, but the PDF may be characterised by its moments. Not all distributions have a finite set of moments of all orders. In [17] is mentioned that, even when moments exist for all orders, they do not necessarily determine the PDF completely.

Cumulants

Another useful feature is the cumulant of a random variable. The advantage of cumulants over moments is its benefit to recognise Gaussian and non-gaussian signals [17]. When signals are non-gaussian, the first two moments do not define their PDF, and therefore higher-order statistics (order higher than two) can reveal other information about the signal that second-order statistics cannot. Ideally, the entire PDF is needed to characterise a non-Gaussian signal.

According to [17], the cumulative distribution function (CDF) of a random variable x, is denoted by $F(x)$. The central moment about the mean of order v of x is

$$\mu_v = \int_{-\infty}^{\infty} (x - m)^v dF, \tag{3.18}$$

where $v = 1, 2, 3, 4, ...$ and m is the mean of x. In the following it is assumed that distributions are zero-mean. One can introduce the characteristic function for real values of t,

$$\phi(t) = \int_{-\infty}^{\infty} exp(jtx) dF = \sum_{v=0}^{\infty} \mu_v (jt)^v / v!, \ \forall \mathbb{R} \in t \tag{3.19}$$

where $j = \sqrt{-1}$, $exp(x)$ is the exponential function, and μ_v is the moment of order v about the origin. The coefficients of $(jt)^v/v!$ is the power series Taylor expansion of the characteristic function $\phi(t)$, which is the moments of a random variable. Equation (3.19) is one of many other descriptive constants for a distribution [17]. Moments are not always capable to completely determine a distribution, even when the moment of all orders exist. Cumulants make up another set of constants used to describe a distribution. In [17] cumulants are expressed as,

$$\phi(t) = \int_{-\infty}^{\infty} exp(jtx) dF = exp\left\{ \sum_{v=1}^{\infty} C_v (jt)^v / v! \right\} \tag{3.20}$$

where C_v is the cumulants of x. C_v is the coefficients of $(jt)^v/v!$ in the power series Tay-

lor expansion of the natural logarithm of the characteristic function $\phi(t)$, or $\ln(\phi(t))$. According to [17], cumulants (except for C_1) are invariant under the shift of the origin. This property is not shared by moments. It is not possible to estimate cumulants through summation or integrative processes. Cumulants must be derived from the characteristic function or the moments.

The cumulants of a distribution are expressed in the general form as

$$Cum[s_1, ..., s_n] = \sum_{\forall v} (-1)^{q-1}!E\left\{\prod_{j\in v_1} s_j\right\}..!E\left\{\prod_{j\in v_q} s_j\right\} \tag{3.21}$$

According to [26], and from equation (3.17) and (3.20) the fourth-order cumulants of a received signal $y(n)$ can be expressed in one of three possible ways,

$$\begin{aligned} C_{40} &= cum(y(n), y(n), y(n), y(n)) \\ &= M_{40} - 3M_{20}^2 \\ C_{41} &= cum(y(n), y(n), y(n), y(n)^*) \\ &= M_{40} - 3M_{20}M_{21} \\ C_{42} &= cum(y(n), y(n), y(n)^*, y(n)^*) \\ &= M_{42} - |M_{20}|^2 - 2M_{21}^2 \end{aligned} \tag{3.22}$$

In [42], [44], [46], [26], [19] cumulants are used as features. Cumulants have also been used to successfully classify modulations in fading channels [37], [36], [38], [34].

3.4.4 Constellation Shape and Zero-crossing Features

Throughout the related work, studies which motivates using constellation shape and zero-crossing features are minimal [13], [18]. However, this section will have a quick discussion on these two feature types.

Constellation shape features make use of Euclidean distances between the received signal points and comparing them to a reference constellation. Zero-crossing consists

of counting the number of zero-crossings of the signal symbols. For PSK modulations the zero-crossing intervals is constant, but it changes for FSK modulations.

3.5 Feature Selection

Section 3.3 and 3.4 introduced many features which have been studied in regards to FB classification. From Section 3.4 it is clear that following a combined instantaneous time-domain feature extraction and statistical feature extraction approach would aid in answering the research question.

Instantaneous time-domain features are easy to extract, combined with the computational efficiency of calculating higher-order statistical properties from the instantaneous amplitude and phase of a signal makes for efficient feature selection. From Section 3.3 it is clear that these features are able to distinguish digital modulations (M-PSK and M-QAM) from each other.

Transformation-based features are more computationally intensive (Fourier and wavelets transform) compared to statistical parameters. FSK modulations are not included in the modulation set established in Section 3.6. Extracting frequency domain information from a signal with information encoded in the phase and amplitude is unnecessary.

Extracting the first up to the fourth-order moment of the instantaneous amplitude and phase, the fourth-order cumulant, the high-order moment (moment greater that 10), and the signal power key will be investigated to determine an appropriate feature set for classifying M-PSK and M-QAM modulations in an AWGN channel and multipath fading channel.

3.6 Modulation Selection

In the South-African context most of the digital wireless technologies are implemented in the UHF frequency band. In Chapter 1 Table 1.1 showed that the UHF band range from 300 MHz - 1 GHz, which can also include technologies in the L- and S-band (1 GHz - 4 GHz).

The technologies found in these bands range from digital television (DVB-T), cellular (GSM, EDGE, UMTS and LTE), navigation (GPS, GLONASS, TETRA), traffic control, wireless LAN, Bluetooth, and satellite broadcasting as mentioned in ICASA National Frequency Plan (NFP) [5]. The mostly used modulations for these technologies include M-PSK and M-QAM modulations.

According to [47] the DVB-T standard for digital television makes use of QPSK, 16-QAM and 64-QAM, while DVB-T2 includes 256-QAM for the sub-carrier modulations in the OFDM signal.

According to 3GPP TS 45.005 [48], GSM and EDGE use a Gaussian Minimum Shift Keying (GMSK) and 8-PSK modulation respectively. LTE and LTE-A make use of link adaptation technology, which implements higher-order modulations up to 64-QAM. [49]. GPS, GLONASS and TETRA signals make use of modulation schemes BPSK, and QPSK [50]. Based on the details mentioned above, the proposed classifier will include (2, 4, 8)-PSK and (16, 32, 64)-QAM.

The modulation class for the proposed classifier will include M-PSK and M-QAM. The modulation order is selected based on the modulation orders used for modulating the digital signal in each of the technologies. Classifying (2, 4, 8)-PSK and (16, 32, 64)-QAM would include most of the technologies found in the UHF band.

3.7 Classification Algorithms

A CR is defined in [51] to be an intelligent wireless communication system that is aware of its environment and uses a methodology to understand-by-building to learn from the environment and to adapt to statistical variations in the input stimuli.

According to [51], there are three conditions for intelligence:

1. perception (the ability to sense the surrounding environment and internal states to acquire information),
2. learning (the ability to transform information to knowledge through classification and generalisation of hypotheses),
3. and reasoning (the ability to achieve goals through using the knowledge).

Learning is at the core of any CR, to gather knowledge from observed data. The learning outcomes are used to update the sensing and channel access policies in DSA applications. According to [51], three characteristics need to be considered when an efficient learning algorithm for CR is designed:

1. learning in partially observable environments,
2. multi-agent learning in distributed CR networks,
3. and autonomous learning in unknown RF environments.

Any CR that makes use of these characteristics will be able to work effectively in any RF environment. There are two learning paradigms when it comes to ML: supervised and unsupervised learning [51]. Unsupervised learning is suitable for alien RF environments. Autonomous unsupervised learning explores the environment and makes use of self-adapting actions without any prior information about the radio environment.

Supervised learning makes use of available information, such as signal waveforms characteristics that are known to the CR, and training algorithms may help the CR to detect signals with those characteristics better.

Different learning algorithms are used for different CR problems. Two main CR problems identified include [51]: decision-making and classification. Decision-making problems deal with spectrum sensing policy, power control or adaptive modulation, while classification deals with spectrum sensing. AMC forms part of spectrum sensing and adaptive modulation applications.

3.7.1 Artificial Neural Networks

The classification algorithms fall into the categories of supervised and unsupervised learning. Supervised algorithms require training with labeled data. ANN and SVM algorithms fall into the category of supervised learning [51]. ANN is based on empirical risk minimisation and require prior knowledge of the observed process distribution, as opposed to structural models. ANN are a computational approach which tries to mimic the way a biological brain solves problems. Neural networks are characterised by its pattern of connections between neurons [52].

ANN is an entirely different approach compared to conventional methods. A neural network is a massively parallel distributed processor made up of smaller simple processing units, which has a natural ability to store experiential knowledge and making that information available for use [51].

An ANN mimics the brain in two ways: knowledge is acquired through learning, and adjusting inter-neuron connection strengths (synaptic weights) to store the acquired knowledge. ANNs have the beneficial property of being able to adapt to minor changes in surroundings and to provide information about the confidence of the decision made [51]. However, they do have the disadvantage of requiring training under many different environmental conditions, and their training outcomes may depend crucially on the choice of initial parameters.

3.7.2 Support Vector Machine

A SVM is based on a structural risk minimisation algorithm and has shown to have superior performance, particularly for small training samples. SVM avoid the problem of overfitting [51]. SVM has been used for many pattern recognition and object classification tasks [51].

A SVM is characterised by the absence of local minima, the sparseness of the solution and the capacity control obtained by acting on the margin or other dimension independent quantities. According to [51], SVM based techniques have achieved superior performances in a wide variety of real-world problems compared to ANN, due to their generalisation ability and their robustness against noise and outliers.

A SVM maps input vectors into a higher-dimensional feature space. This higher-dimensional feature space ensures that the features are linearly separable. This process of mapping the input vector is non-linear, which is achieved by kernel functions.

Classification in a SVM is achieved through a hyperplane which allows for the largest generalisation in the higher-dimensional space to be found, also known as a maximal margin classifier [51]. The margin is defined as the distance from a separating hyperplane to the closest data points. The corresponding closest data points are named support vectors, and the hyperplane allowing for maximum margin is the optimal separating hyperplane.

3.7.3 Performance Metrics

A classifier is evaluated based on performance metrics computed after the model-training stage. There is no general consensus regarding which performance metrics to use for evaluating a classifier's performance [53]. It is not uncommon that a classifier performs well when a certain performance metric is evaluated while the same classifier performs poorly compared to another metric. It depends on what the user needs to know from the model.

For every sample in a testing process, the sample has two labels: the real label and the predicted label. The real label is an indication of the class the testing samples belongs to, and the predicated label is the output of the predictor [54]. A classifier should be evaluated with respect to a set of performance metrics that can capture the unique aspect of the classifier performance space. Most performance metrics are based on the four values of the confusion matrix: true positives (TP), number of true negatives (TN), number of false positives (FP), and number of false negatives (FN) [53].

According to these definitions, if both the real and predicted labels are positive, the sample is a TP. If both the real and predicted label is negative, the sample is TN. If the real label is positive while the predicated label is negative, the sample is FN. So finally if the real label is negative while the predicted label is positive, the sample is FP. The matrix which contains TP, TN, FP and FN can be called a confusion matrix.

The following relationships exist [54]

$$TP + FP = PP, \tag{3.23}$$

$$TP + FN = RP, \tag{3.24}$$

$$TN + FN = PN, \tag{3.25}$$

$$TN + FP = RN, \tag{3.26}$$

where PP is the predictive positives, RP the real positives, PN the predictive negatives and RN the real negatives. Because of these relationships, the performance measures are not always represented by these commonly used four counts: TP, TN, FP and FN.

According to [54], three basic performance measures, which are the sensitivity (*Sen*), specificity (*Spe*) and accuracy (*Acc*) can be defined as:

$$Sen = \frac{TP}{TP + FN} = \frac{TP}{RP}, \tag{3.27}$$

where sensitivity is the frequency of correctly predicting positive samples among all real positive samples.

$$Spe = \frac{TN}{TN + FP} = \frac{TN}{RN}, \tag{3.28}$$

where specificity measures the ability of a predictor in identifying negative samples.

$$Acc = \frac{TN + TP}{TN + FN + TP + FP} = \frac{1}{n}\left(TN + TP\right). \tag{3.29}$$

where accuracy measures the ability of a predictor in correctly identifying all the samples, no matter whether it is positive or negative, and n is the number of samples.

Another performance measure includes the receiver operating characteristic (ROC) curve, which describes the relationship between sensitivity and false positive rate (FPR). The FPR can be defined as

$$FPR = 1 - Spe = \frac{FP}{FP + TN}. \tag{3.30}$$

From the plotted ROC curve, the area under curve (AUC) is used to measure the performance of the predictor. The AUC of a ROC curve equals to the probability a randomly selected positive sample gets higher scores than a randomly selected negative sample. However, the shape of an ROC curve may be misleading [54] when the dataset is highly imbalanced.

Finally, the accuracy reflects the average rate of correctly predicted labels among labels that are either the real label or prediction results.

3.8 General System Model

From Section 3.3 and 3.4 it is clear that the authors followed the same general system model. Choosing initial parameters, transmitting the signal through a communication channel, processing the received signal, extracting the feature set, and finally choosing the classification algorithm which best suits their feature set. Figure 3.2 shows the

general system model. The system model describes the flow of data from initialising starting parameters to finally giving the modulation type as output.

Each block is numbered in a hierarchy of levels, with level 1 denoted by {x.0}, level 2 {x.x}, level 3 {x.x.x} and so forth. References to the logical blocks in the text are indicated with curly brackets.

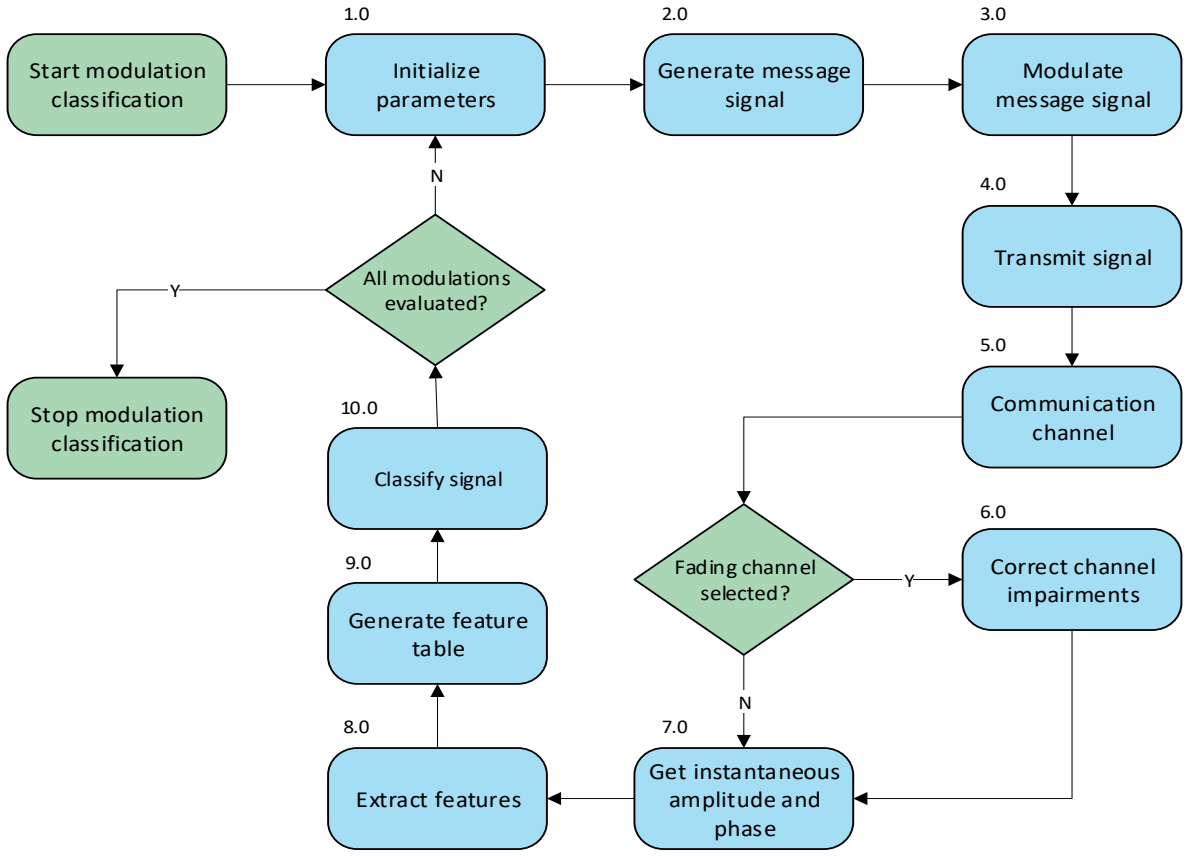

Figure 3.2: General system model

From block {1.0} initial parameters are set. These parameters include the selection of modulation classes, modulation order, signal length, number of frames to view the signal and selecting the channel model(s). Selecting the channel model depends on whether an AWGN channel or a fading channel classification problem are considered. Another essential block is the feature extraction block {8.0}. Many features have been proposed and implemented. Feature extraction tries to describe the modulation classes

employing a minimum number of features or attributes [30] that are effective in discriminating amongst modulation classes. Therefore, selecting the minimum number of features are key.

The classification block {10.0} consist out of selecting the classification algorithm. In Section 3.7 a brief overview of the three mostly adopted algorithms are mentioned. During the training stage, selecting the training and testing set size is essential to avoid over-fitting of the data points [27].

3.9 System Model Breakdown

In Figure 3.2 a flow diagram for the general system model are shown. From the literature is established that following a combined instantaneous time-domain and statistical feature FB classification approach would aid in solving the research problem of finding a simple approach towards classifying digital modulations.

Table 3.2: Level 2 logical flow: Initialize parameters

Block	Description	Values
{1.1}	Set modulation class	M-PSK, M-QAM
{1.2}	Set modulation order	(2, 4, 8)-PSK, (16, 32, 64)-QAM
{1.3}	Set message length	See Chapter 5
{1.4}	Set frame length	See Chapter 5
{1.5}	Set channel model	AWGN, Fading channel

A message signal is generated (Figure 3.3), which is modulated before transmission. Each message signal is randomly generated to ensure that the classifier is message independent. For a given modulation technique, two ways to simulate the modulation technique exist: baseband and passband modulation. Baseband modulation, also known as the lowpass equivalent, requires less computation. Baseband modulation produces a complex envelope of the signal by excluding the carrier frequency component of the signal. Passband modulation tends to be more computationally intensive because the carrier signal typically needs to be sampled at a higher rate. Baseband modulation produces the complex envelope $y[n]$ of the message signal $x[n]$, and $y[n]$ is

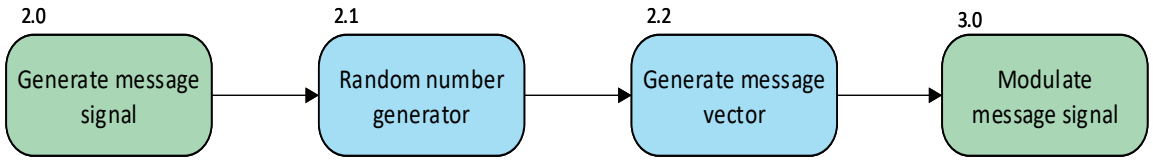

Figure 3.3: Logical flow: Generate message signal

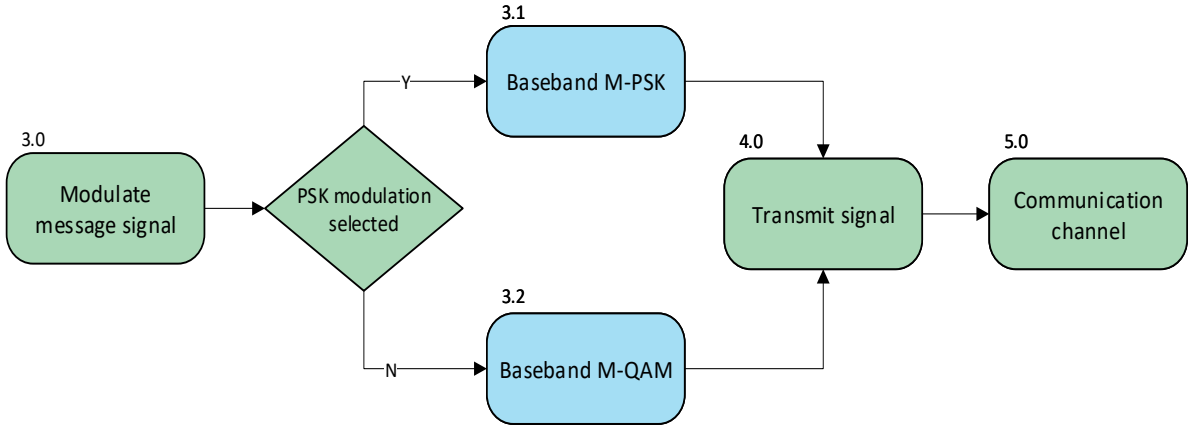

Figure 3.4: Logical flow: Modulate message signal

a complex-valued signal that is related to the output of a passband modulator,

$$Y_1(t)cos(2\pi f_c t + \theta) - Y_2(t)sin(2\pi f_c t + \theta), \tag{3.31}$$

where f_c is the carrier frequency, θ is the carrier signal's initial phase. The baseband signal is equal to the real part of

$$[(Y_1(t) + jY_2(t))e^{j\theta}]exp(j2\pi f_c t) \tag{3.32}$$

which is

$$[(Y_1(t) + jY_2(t))e^{j\theta}], \tag{3.33}$$

and the complex vector $y[n]$ is a sampling vector of the complex signal.

Figure 3.4 shows the logical flow for constructing the modulation block of the system model. Firstly the message signal is modulated using M-PSK, after that M-QAM

modulated signal is generated. The modulated signal is referred to as the transmitted signal. The transmitted signal is sent through the communication channel that corrupts the transmitted signal to produce the noisy received signal.

Communication channel modelling consists of two parts: an AWGN model and a fading channel model. The AWGN channel is the mostly adopted channel model used to introduce random noise into the system. To make the classifier more robust, especially when using recorded I/Q data, a fading channel model will also be included in the analysis. Chapter 6 will expand on fading channel models and implementation (Figure 3.5 and 3.6).

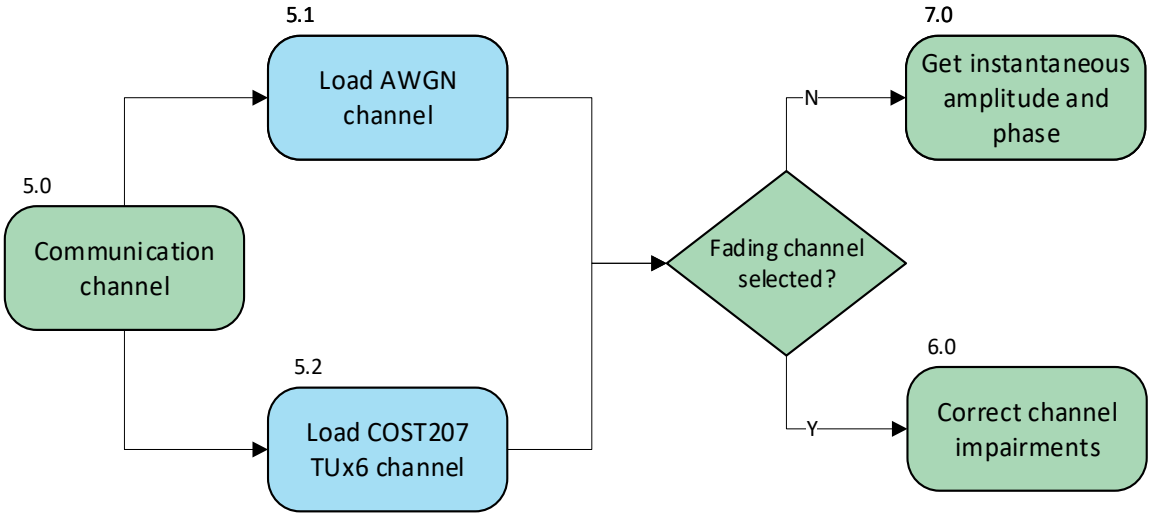

Figure 3.5: Logical flow: Communication channel modelling

Instantaneous time-domain features combined with a Higher-order Statistics (HOS) based approach are followed. The instantaneous amplitude and phase are extracted from the received signal symbols, after which the HOS features are extracted. Chapter 5 will elaborate on the feature selection, extraction and finalising the feature set.

Figure 3.6 shows the process followed to set up the COST 207 channel model for simulating a multipath channel. The multipath channel requires a Doppler object, a path gain and path delay vector, followed by a Rayleigh channel object. Figure 3.7 shows

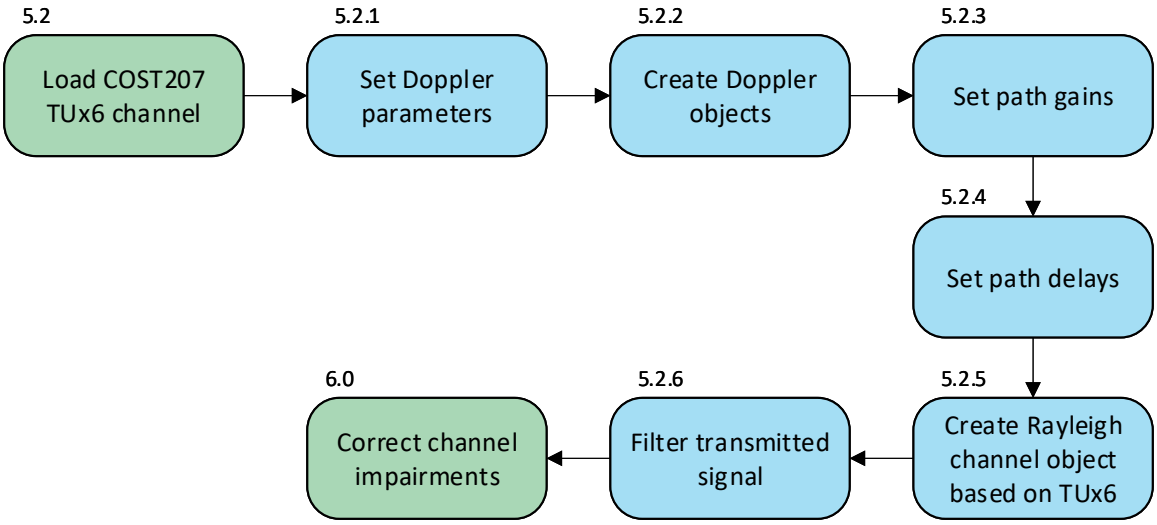

Figure 3.6: Logical flow: Fading channel model

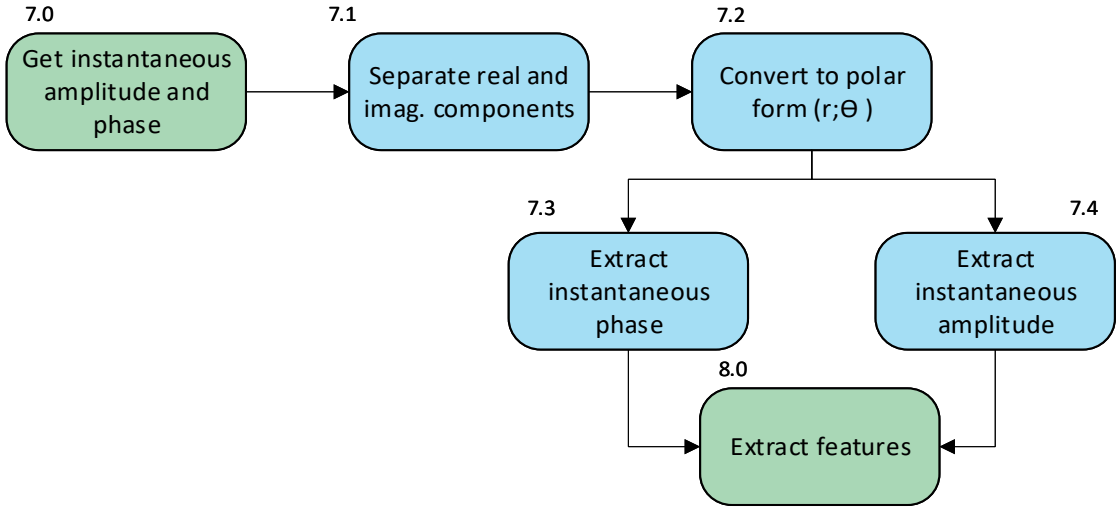

Figure 3.7: Logical flow: Prepare for feature extraction

the process of converting from complex signal samples to the instantaneous amplitude and phase of the received signal components.

3.10 System Implementation

The system model is implemented in the MATLAB simulation package. The functional blocks that deal with decision making, which are self-explanatory, are not included in the implementation discussion.

3.10.1 Generating The Message Signal $\{2.0\}$

The message signal is generated using a random-number generator. The random-number generator draws a vector of size N from a uniformly distributed pseudorandom set of integers with a predefined seed value. The pseudorandom number generation is based on the Mersenne Twister algorithm [55]. The message signal is generated for a number of frames. Each frame is different from one another to ensure that the classifier is message independent, but that the experiment is repeatable.

The message vector is stored in an $m \times n$ size matrix, where $m = N$ and n is the frame-size. Each column in the message vector is modulated, and transmitted on a frame-by-frame base. The random integers are between 0 and $M - 1$, where M represents the M-ary number for the modulation order. Each integer value corresponds to a bit sequence which is a direct signal space representation of the signal symbols being transmitted.

3.10.2 Baseband Modulation $\{3.0\}$

The message vector is passed to the modulator block. The modulator block takes each frame from the message signal and applies either the PSK or QAM modulation to the message signal. A complex-valued vector (of size $m \times n$) is output. The complex vector in the form of $a + jb$ corresponds to the in-phase and quadrature component of the signal, which is mapped to the constellation diagram. Equation (3.33) mentioned in Section 3.9 for block $\{3.0\}$ is used.

3.10.3 Communication Channel {5.1} and {5.2}

The communication block consists of two channel models: an AWGN channel and the fading channel model. The AWGN channel is implemented by adding white Gaussian noise to the signal vector. The added noise is drawn from a zero-mean Gaussian (normal) distribution with variance of σ^2.

The variance of the added noise can also be changed by setting an appropriate SNR for the signal. The variance of the noise signal can also be derived from the SNR value through

$$\sigma^2 = 10^{-SNR/10} \tag{3.34}$$

Different fading channel models have been proposed. ITU-R M.1225 [23] proposed three tapped-delay line parameters for different wireless environments: indoor office test environment, outdoor to indoor and pedestrian test environment and a vehicular test environment. For each terrestrial test environment, a channel impulse response model based on a tapped-delay line model is given.

The model is characterised by the number of taps, time delay relative to the first tap, average power relative to the strongest tap, and the Doppler spectrum for each tap. The channels are modelled more accurately through variable delay spreads, therefore up to two multipath channels are usually defined. Channels A is a low delay spread case, and channel B is the median delay spread. The channel conditions are constant for a certain amount of time, and thereafter changes from channel A parameters to channel B parameters.

Table 3.3 shows the outdoor to indoor and pedestrian test environment as an example to illustrate how the channel is modelled.

Another well known and widely adopted fading channel model is the COST 207 channel model for multipath fading channels published by the Commission of the European Communities [24]. The COST 207 project channel model is used for GSM and DVB-T [25] standards. Radio propagation in the mobile radio environment is described

Table 3.3: Outdoor to indoor and pedestrain tapped-delay-line parameters

	Channel A		**Channel B**		
Tap	Relative delay (ns)	Average power (dB)	Relative delay (ns)	Average power (dB)	Doppler
1	0	0	0	0	Classic
2	110	-9.7	200	-0.9	Classic
3	190	-19.2	800	-4.9	Classic
4	410	-22.8	1200	-8.0	Classic
5	-	-	2300	-7.8	Classic
6	-	-	3700	-23.9	Classic

by highly dispersive multipath caused by reflections and scattering. The path between the transmitter and receiver is considered to consist of large reflections and scattering some distance to the receiver. This gives rise to a number of electromagnetic waves that arrive at the receiver with random amplitudes at different delays.

Four Doppler spectrum types are used for modelling the channels. Some of which include the Jakes or the classic Doppler spectrum, Gaussian 1 for delays in the range of 500 ns to 2 μs, Gaussian 2 for delays greater than 2 μs, and the Rice which is the sum of a classical Doppler spectrum and one direct LOS path to the receiver.

The COST 207 project [24] proposed a typical fading case for

1. rural (non-hilly) area (RA),
2. urban (non-hilly) area (TU) with a 12 and 6-tap model,
3. bad case for hilly urban area (BU) with a 12 and 6-tap model,
4. hilly terrain (HT) with a 12 and 6-tap model.

Table 3.4 shows an example of the 6-tap TU delay profile.

For practical simulation, the propagation models are implemented in terms of a discrete number of taps, each determined by their respective time delays and powers, and the Rayleigh distributed amplitudes of each tap, which are varied according to a Doppler spectrum [48].

Table 3.4: 6-tap TU area tapped-delay profile

Tap	**Delay (μs)**	**Power (dB)**	**Doppler**
1	0	-3	Classic
2	0.2	0	Classic
3	0.6	-2	Gauss1
4	1.6	-6	Gauss1
5	2.4	-8	Gauss2
6	5.0	-10	Gauss2

When evaluating the performance of the modulation classifier in a fading channel, the maximum Doppler shift plays an important role. The maximum Doppler shift is an indication of how static or dynamic a channel is (whether the channel is slow or fast fading in nature). The maximum Doppler shift is a function of the carrier frequency of the signal and the speed at which either the transmitter, receiver or both move relative to each other.

The GSM standard prefers to specify Doppler shifts concerning the speed of the mobile:

$$f_d = \frac{v f_c}{c}, \tag{3.35}$$

where v is the speed of the mobile, and f_c is the carrier frequency of the transmission, and c is the speed of light. For a pedestrian walking might experience a maximum Doppler shift of about 4 Hz at a frequency of 900 MHz. A maximum Doppler shift of 0 corresponds to a static channel that comes from a Rayleigh or Rician distribution. Equation (3.35) can be expanded to include an angular component (direction of movement of the receiver):

$$f_d = \frac{v f_c}{c} \cos(\phi), \tag{3.36}$$

where ϕ is the angle between the direction of motion and line of sight to the transmitter. For simulation purposes equation (3.35) will be implemented when determining the maximum Doppler shift. The angle of movement will be neglected.

3.10.4 Extracting Instantaneous Time-Domain Features {8.0}

The output signal, received from the communication channel block, is a complex vector of the same size as the message signals. Each received value in the form of $a + jb$. The complex values are separated into their respective real and imaginary components, which are then converted into a magnitude and phase component.

The magnitude component corresponds to the signals instantaneous amplitude and the phase to the instantaneous phase of the signal. After separating the received signal into these components, HOS are extracted from the instantaneous amplitude and phase to use as features.

The theoretical noise-free cumulant values for some M-PSK and M-QAM modulation are presented in Table 3.5. In [12] and [19] the cumulant values for (2, 4, 8)-PSK and (4, 16, 64)-QAM are shown. These theoretical values help to verify the implementation of equation (3.21).

Table 3.5: Theoretical second and fourth-order cumulant values

	C_{20}	C_{21}	C_{40}	C_{41}	C_{42}
BPSK	1.0	1.0	-2.0	-2.0	-2.0
QPSK	0.0	1.0	1.0	0.0	-1.0
8-PSK	0.0	1.0	0.0	0.0	-1.0
4-QAM	0.0	1.0	1.0	0.0	-1.0
16-QAM	0.0	1.0	-0.68	0.0	-0.68
64-QAM	0.0	1.0	-0.6191	0.0	-0.6191

3.10.5 Classification Algorithm {11.0}

In Section 3.7 a quick overview of some of the more popular classification algorithms used in AMC are presented. Each of these algorithms have their respective advantages and disadvantages. AMC forms part of spectrum sensing and therefore part of a classification problem in CR. The classification algorithm for the disseration will follow a supervised classification approach. For the reasons mentioned in Section 3.7, a linear SVM is adopted in this work [39].

In [12] Zhu et al. stated that a SVM only needs the training data when establishing the separating hyperplane. The training signal is not involved in any further calculation after training. Therefore the testing stage is relatively inexpensive with regards to computations.

The SVM is verified and tested using a five-fold cross-validation approach. This process contains five steps [54]:

- The dataset is obtained.
- The whole dataset is randomly partitioned into five parts.
- Collectively five training and testing rounds are carried out. 20% of the dataset is used for testing, while the remaining 80% are used for training.
- The testing results are collected from the five rounds of training and testing.
- The testing results are pooled together to estimate the predictive performances.

3.11 Conclusion

In this chapter, AMC and FB classification were discussed in detail. The selection of appropriate features were presented, together with a discussion on different feature categories. Related work regarding FB classification was investigated to determine a good approach to solving the research problem. The reason for following a combined instantaneous time-domain and statistical feature extraction process was presented.

The selection of using (2, 4, 8)-PSK and (16, 32, 64)-QAM modulation classes were also motivated. A quick discussion on machine learning algorithms for CR was presented with a section on supervised and unsupervised learning algorithms. A general system model representing FB classification was described together with a guide to implementing the system model. The next chapter proceeds with the verification and validation of the proposed system model.

Chapter 4

Verification and Validation

In this chapter, the verification and validation of the proposed AMC system model are discussed. The methodology followed to verify the integral elements of the system model is discussed. The overall operational validation of the system model is also discussed.

4.1 Verification Methodology

According to [56], model verification is defined as ensuring that the computer program of the system model, described in Chapter 3, and its implementation are correct. Computerised model verification ensures that the computer programming and implementation of the conceptual model are correct. Two significant factors which influence verification is whether a simulation language (MATLAB) or a higher level programming language (C, C++) is used [56]. According to [56], using a special-purpose simulation language will result in fewer errors than a general purpose simulation language, and using a general purpose simulation language will result in fewer errors than a general purpose higher level programming language.

In [56] Sargent describes the methodology and techniques used for verification and validation of a simulation model. In [56] two basic approaches for testing simulation software are proposed: a static testing and a dynamic testing approach. Static testing involves:

- structured walkthroughs,
- correctness proofs,
- and examining the structural properties of the program.

The dynamic testing approach involves:

- traces,
- investigation of the input-output relations,
- internal consistency checks,
- and reprogramming critical components to determine if the same results are obtained.

The methodology and techniques described for verification and validation are also advocated by [57].

4.2 System Model Verification

4.2.1 General Verification Methodology

A combination of the static and dynamic testing approaches was followed. The general guidelines for good programming practice have been observed [58]. Chapter 3 described the logical flow for each functional block in detail. The functional blocks were verified per block. Each functional block takes a series of input parameters, and each input parameter is chosen to verify the flow through each functional block.

The output from each functional block is compared to the respective theoretical determined results. After verifying that all the essential functional blocks are implemented correctly, the output of a full system implementation is validated based on a black-box approach.

A more detailed verification procedure for blocks {2.x}, {3.x}, {5.x}, and {8.0} are presented in section 4.2.2.

4.2.2 Verification of Blocks 2.x, 3.x, 5.x, and 8.0

The verification for blocks {2.0}, {3.0}, {5.1}, {5.2}, and {8.0} are now described in more detail.

Block {2.1} - Message signal generation

The procedure described for generating the message signal in Chapter 3 is followed. The random integers generated must be between 0 and $M-1$, where M represents the modulation order. Each integer corresponds to a bit sequence which maps directly to the transmitted signal symbols. The integers are drawn from independent and identically distributed (i.i.d.) subset with an equal probability of being drawn. Through visual inspection, the message signal is verified. The *rand* function within MATLAB is used for the generation, which is verified by MATLAB's internal verification process.

Block {3.x} - Modulation of the message signal

In Chapter 2 different digital modulations are discussed. Each modulation is expressed regarding its basis function representation in the vector space, also known as the constellation diagram. Each modulation has a unique constellation diagram representation. The implementation for modulating the message signals is verified through visual inspection. By taking the modulated output from the message signal block {2.1},

and plotting the constellation diagram, the generated constellation diagram is compared to the expected constellation diagram for that specific modulation.

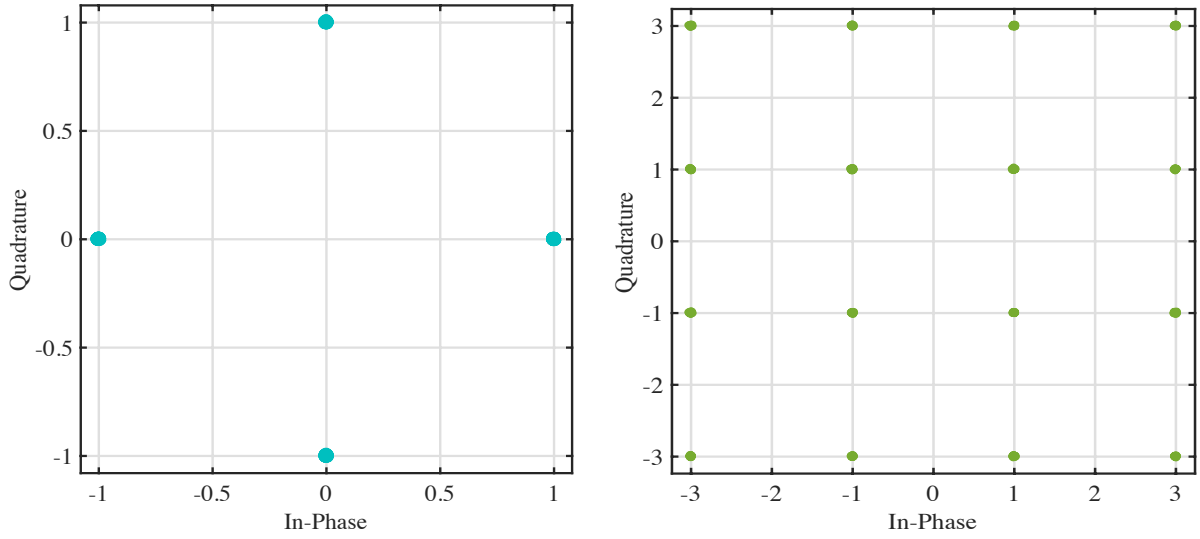

(a) QPSK (b) 16-QAM

Figure 4.1: Constellation diagram for a QPSK and 16-QAM signal.

In Chapter 3, two ways are mentioned to simulated the modulation techniques: baseband and passband modulation. A baseband modulation implementation is followed. Figure 2.7 and 2.8 in Chapter 2 show the expected constellation diagram for a QPSK and 16-QAM modulated signal. Figure 4.1(a) and (b) show the implemented modulation block's output for a QPSK and 16-QAM modulated signal. Figure 4.1(a) and (b) show the same output as that presented in Figure 2.7 and 2.8.

Block {5.x} Implementation of the communication channels

Block {5.0} is divided into two individual functional blocks: {5.1} and {5.2}. Functional block {5.1} is the implementation of an AWGN channel. The AWGN channel is modelled by a Gaussian distribution with a mean μ and variance σ^2. The variance is determined by the SNR. By adding the range of values from the Gaussian distribution to the transmitted signal will result in the amplitude of the signal being distributed in

the same manner. So it can be expected that when plotting the histogram of the received signal magnitude component (also know as the instantaneous amplitude) will resemble a Gaussian distribution. Figure 4.2 shows the histogram for the magnitude component of an 8-PSK signal transmitted through an AWGN channel with a noise variance of 0.1, which corresponds to an SNR of 10 dB.

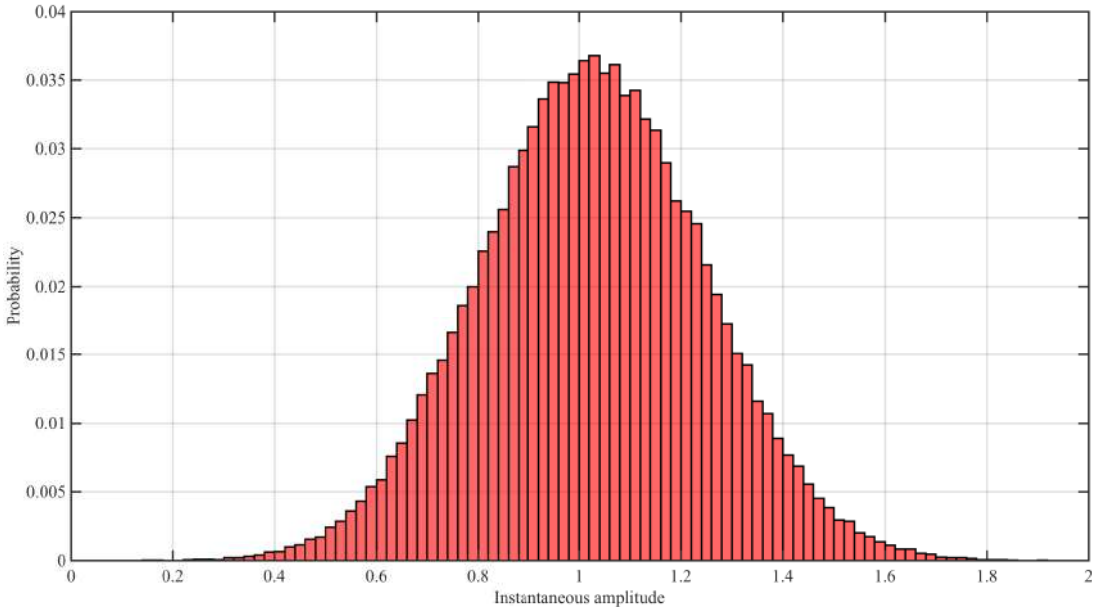

Figure 4.2: Histogram of a received 8-PSK signal's instantaneous amplitude in AWGN.

Functional block {5.2} is the implementation of a multipath fading channel. The channel model is constructed according to Table 3.4, with the relative delay and power for each path, with their respective Doppler spectrum. A special-purpose simulation language results in fewer errors, therefore, MATLAB has a built-in function for constructing a COST 207 Typical Urban (TU) 6-tap model. The Communication Toolbox includes a step-wise guide to implementing the COST 207 channel model. The Communication Toolbox's implementation is compared to the 3GPP standard in [49] to ensure correct implementation.

Firstly the Doppler spectrum objects relevant to the given COST 207 model are constructed. Then a Rayleigh or Rician multipath fading channel object is constructed, and the properties are initialised accordingly to produce the desired channel model, such as TU.

Block {8.0} Feature Extraction

The verification of block {8.0} is done in two steps. Firstly the noise-free normalised fourth-order cumulant values for different modulation are shown in Table 3.5, which acts as our reference values, while the output of the functional block will be regarded as the estimated values.

The results obtained from estimating the noise-free normalised fourth-order cumulants are summarised in Table 4.1. The predicted results compare well with the ideal fourth-order cumulants in Table 3.5. From the literature reviewed in Chapter 3, no theoretical normalised fourth-order cumulant value for 32-QAM could be found. However, in [59] Mathis provides a way to determine the theoretical normalised fourth-order cumulant for a 32-QAM digitally modulated signal. According to [59] this is also called the kurtosis of the signal calculated in the closed form when sampled at the ideal sampling time (once per symbol interval). In [59] the theoretical normalised fourth-order cumulant for a 32-QAM signal is:

$$\kappa'_4 = -\frac{12}{5}.\frac{259M^2 - 64}{(31M - 32)^2}. \tag{4.1}$$

When evaluating equation (4.1), the theoretical normalised fourth-order cumulant amounts to -0.6905. Comparing the estimated results from Table 4.1, we find that the estimated normalised fourth-order cumulant for a 32-QAM signal has a 0.04% error compared to the theoretical value.

Table 4.1: % Error between estimated normalised fourth-order cumulants and their respective theoretical values.

Modulation	Estimated	Theoretical	% Error
BPSK	-2.0	-2.0	0%
QPSK	-1.0008	-1.0	0.08%
8-PSK	-1.0010	-1.0	0.1%
16-QAM	-0.6799	-0.68	0.014%
32-QAM	-0.6902	-0.6905	0.04%
64-QAM	-0.6189	-0.6191	0.032%

Secondly, the extraction of the third and fourth-order moments are verified. We only need to verify this for a modulation's instantaneous amplitude to determine correct implementation. So for verification purposes, the received signal's instantaneous amplitude is extracted. When the signal is transmitted through an AWGN channel, the received signal's instantaneous amplitude will resemble a Gaussian distribution.

For any Gaussian distribution, the skewness (third order moment) has a theoretical value of zero, and a kurtosis (fourth-order moment) of three. When evaluating the excess kurtosis the value should be zero. The output from two independent implementations (Excel and MATLAB) are compared. The output from Excel is regarded as our reference values, while the output from MATLAB is the estimated values. A sample size of 5000 is selected.

Excel defines kurtosis mathematically as:

$$\kappa = \left\{ \frac{n(n+1)}{(n-1)(n-2)(n-3)} \sum \left(\frac{x_i - \mu}{s} \right) \right\}^4 - \frac{3(n-1)^2}{(n-2)(n-3)}, \tag{4.2}$$

where s is the sample standard deviation and μ is the sample average.

MATLAB defines kurtosis mathematically as:

$$\kappa_1 = \frac{\frac{1}{n}\sum_{i=1}^{n}(x_i - \mu)^4}{\left(\frac{1}{n}\sum_{i=1}^{n}(x_i - \bar{x})^2\right)^2}, \tag{4.3}$$

and

$$\kappa_0 = \frac{n-1}{(n-2)(n-3)}((n+1)\kappa_1 - 3(n-1)) + 3 \tag{4.4}$$

Table 4.2: Verification of the skewness and kurtosis for a BPSK signal's instantaneous amplitude.

Statistical moment	**Reference**	**Estimated**
Skewness	-0.0430	-0.0431
Kurtosis	-0.0200	-0.0212

The results obtained from verifying the third and fourth-order moment of the received signal's instantaneous amplitude at 30 dB is shown in Table 4.2. For a Gaussian distribution a skewness of zero, and an excess kurtosis of zero is expected. MATLAB and

Excel have its implementation for calculating the skewness and kurtosis, and the difference between the reference and estimated values can be ascribed to this. However, the results obtained compare well, and the skewness and kurtosis are as expected. As the sample size increase, the kurtosis and skewness will approach zero as expected.

4.3 Validation Methodology

According to [56], model validation is defined as confirming that the computerised model, within its domain of applicability, presents a satisfactory range of accuracy consistent with the intended application of the model, and to develop the confidence in potential users they require to use the model and the information derived from the model.

In [56] Sargent describes a list of validation techniques and tests commonly used in model validation. Sargent proposed a method of *comparison to other models* as a validation approach. The various results (outputs) of the simulation model being validated are compared to the results for other valid models. This includes an approach to compare the simulation model to known results from analytical models, and the simulation model is compared to other simulation models that have been validated.

From [56] a subjective non-observable system validation approach is followed. Non-observable is defined as not being able to collect data on the operational behaviour of the problem entity. However, when vector signal generators and analysers are available, test data can be generated to use for validation. In this chapter, a non-observable approach is assumed.

A subjective non-observable approach includes exploring model behaviour and comparing to other models. Usually, several different experiments are conducted with different conditions to obtain a high degree of confidence in a simulation model and the results obtained. For a non-observable system, which is the case, it is not possible to obtain a high degree of confidence. Therefore the model output behaviours should

be explored as thoroughly as possible, and comparison should be made to other valid models. Other validation tests include a *face validity* test [56]. Individuals knowledgeable about the system are asked whether the model and its behaviour are reasonable. Take for example whether the logic in the conceptual model is correct and whether the model's input-output relationships are reasonable.

4.3.1 System Model Validation

The validation for the proposed statistical FB AMC system in an AWGN channel is validated in this section. Most of the related work presented in Chapter 3.3 for an AMC system in an AWGN channel has been validated. For the purpose of validation, a step wise combination between following the *comparison to other models* and *face validity* is followed.

From the related work reviewed it is clear that several methods are implemented for identifying modulation schemes and signal parameters, and the focus on extracting signal characteristics under different conditions vary. This makes it difficult to compare the performance of AMC with each other.

A study presented by Kim et al. [60] is used as the reference study for validation. They presented a deep neural network (DNN)-based AMC technique for classifying BPSK, QPSK, 8-PSK, 16-QAM and 64-QAM modulated signals. They extracted a total of 21 features from the received signal samples. The feature set is generated by simulation under both an AWGN channel and Rician fading channel. Table 4.3 summarises the reference study parameters used for classification.

DNN is a supervised learning approach used for classification purposes. The SVM used in the proposed classifier is also a supervised learning classifier. Both the DNN and the SVM fall within the same category. The proposed classifier is set-up using the following parameters to validate the system model. A set of six features are selected. Table 4.4 summarises the proposed classifier input parameters for validation purposes. The output is compared to the reference study.

Table 4.3: Reference classifier input parameters

Parameter	**Description**
Modulations	(2, 4, 8)-PSK, (16, 64)-QAM
Classifier	DNN with 3 hidden layers
Number of samples	200 000
Training set size	25 000 samples
SNR	-5:15 dB (5 dB increments)
Fading channel	Rician
Rician factor	0.5
Doppler shift	100, 300 Hz
Features	β, σ_{dp}, σ_{ap}, σ_{aa}, σ_{af}, σ_{v}, v_{20} X, X_2, γ_{max}, C_{20}, C_{21}, C_{40}, C_{41}, C_{42}, C_{63}, C_{80}, κ, s, PR, PA

Table 4.4: Proposed classifier input parameters

Parameter	**Description**
Modulations	(2, 4, 8)-PSK, (16, 64)-QAM
Classifier	Linear SVM
Number of samples	1000 sample per frame
Number of frames	1000 frames per modulation
Training set size	25 000 samples
SNR	-5:15 dB (5 dB increments)
Channel	AWGN only
Features	σ_{θ}^2, β, C_{42}, κ, s, σ^{12}

σ_{θ}^2 is the variance of the instantaneous phase of the received signal, β is the signal power key, C_{42} is the normalised fourth-order cumulant, κ is the kurtosis, s is the skewness, and σ^{12} is the moment-order 12. Table 4.5 shows the verification results from the reference study compared to the proposed implementation.

From the validation results, the proposed classifier performs overall well compared to the reference classifier. The reference classifier makes use of a DNN with 21 features, while the proposed classifier used a SVM with only five features. Both classifiers performed well at an SNR of 5 dB and above.

The reference classifier outperforms the proposed classifier for SNR under 5 dB. The difference in using different machine learning algorithms is acceptable when follow-

ing a black box approach for validation. Both DNN, which is an extension of ANN and SVM lies within the same category of supervised learning algorithms for pattern recognition and classification.

Table 4.5: Overall classification accuracy.

Study	**-5 dB**	**0 dB**	**5 dB**	**10 dB**	**15 dB**
Reference [60]	99.95 %	99.99%	100%	100%	100%
Proposed	80 %	86.40%	97.60%	100%	100%

4.4 Conclusion

In this chapter the verification and validation methodology followed was presented. Specific system model blocks were verified and proven to be correctly implemented. The system validation was confirmed through following a *compare to other models* approach. The output produced by the validation is shown to be acceptable. The next chapter presents an implemented FB automatic modulation classifier in an AWGN channel.

Chapter 5

Feature-based AMC in an AWGN Channel

This chapter presents the methodology followed to evaluate and to select the feature set to classify M-PSK and M-QAM modulated signals in an AWGN channel. Different statistical features are extracted from the instantaneous amplitude and phase of the received signal. These features are then compared to each other to determine which of them have any significance in classifying the modulations. The cumulants of an i.i.d. set of random values are calculated by evaluating the moment generating function. Determining the cumulants are based on a long run average or the expected value parameters, therefore selecting an appropriate sample size will influence the estimated cumulant values.

5.1 Introduction

Chapter 1 began the discussion on the importance of AMC as part of CR, in enabling DSA. ITU-R recommended an approach to use a signal's internal and external char-

acteristics for classifying digital signals. Chapter 2 continued with the discussion on the analysis of a signal's internal characteristics by examining the physical layer of the communication chain (data elements versus signals elements). The discussion continued by showing how to map signal elements to a signal space, also known as the vector space.

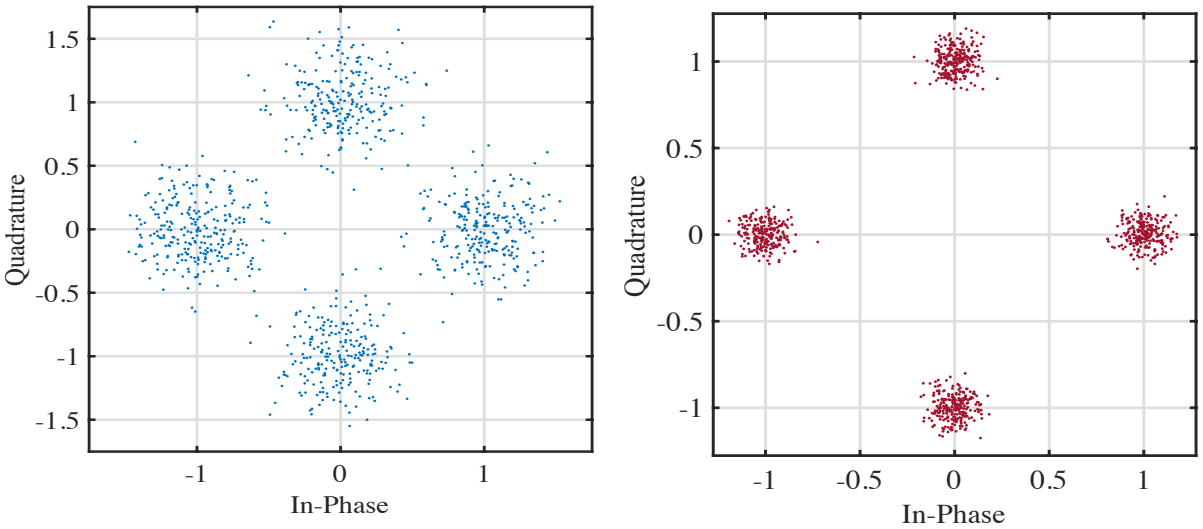

(a) 10 dB (b) 20 dB

Figure 5.1: QPSK signal at different SNR

Chapter 3 introduced FB classification through an in-depth look at related work on the topic of FB classification, and different features and classification algorithms proposed to solve this problem. A general system model was presented from literature, and a complete system model breakdown is shown. The decision to classify M-PSK and M-QAM modulated signals were motivated together with a discussion on the different classification algorithms.

This chapter will focus on extracting the feature set and to evaluate the performance of the statistical features to determine their ability to distinguish between these modulations in the presence of AWGN.

Figure 5.1(a) and (b) shows the effect of AWGN on a QPSK signal for an SNR of 10

dB and 20 dB respectively. In an ideal transmission, the signal symbols should be grouped as closely as possible. More errors are introduced during the demodulation phase when the decision regions cannot estimate the transmitted symbols from the received signal symbols during demodulation. Keeping the received symbols between the appropriate decision regions is important for demodulation, and it enhances the classification accuracy.

5.2 Determining Sample Size

Cumulants are useful features to help determine a proper sample size. Calculating the cumulant requires the use of equation (3.17). Equation (3.17) makes use of the long run average or the expected value of a set. Therefore, with a sample size of adequate length, the cumulant will converge towards the theoretical values.

Table 5.1 gives a summary of the experimental parameters for determining a suitable sample size. Four tests were carried out. For each test, the modulations, SNR, and number of frames were the same. Four different sample sizes were used to estimate the normalised fourth-order cumulant. Normalisation of the signal symbols are needed to eliminate the effect of high signal energy. The results obtained from the tests were recorded in Table 5.2 - 5.5.

Table 5.1: Determining sample size experimental parameters

Parameter	**Value**
Modulations	BPSK, QPSK, 8PSK, 16QAM, 32QAM, 64QAM
Number of runs	4
Number of signal symbols	1000, $10e^3$, $100e^3$, $1e^6$ symbols
SNR	0:50 dB in 1 dB increments
Cumulant	Normalised C_{42}

Figures 5.2(a) - (d) show the results obtained from calculating the cumulant at the different sample sizes at a range of SNR values. From the plots, the effect of SNR on the cumulant value is seen clearly. However it may be, at low SNR, the different modula-

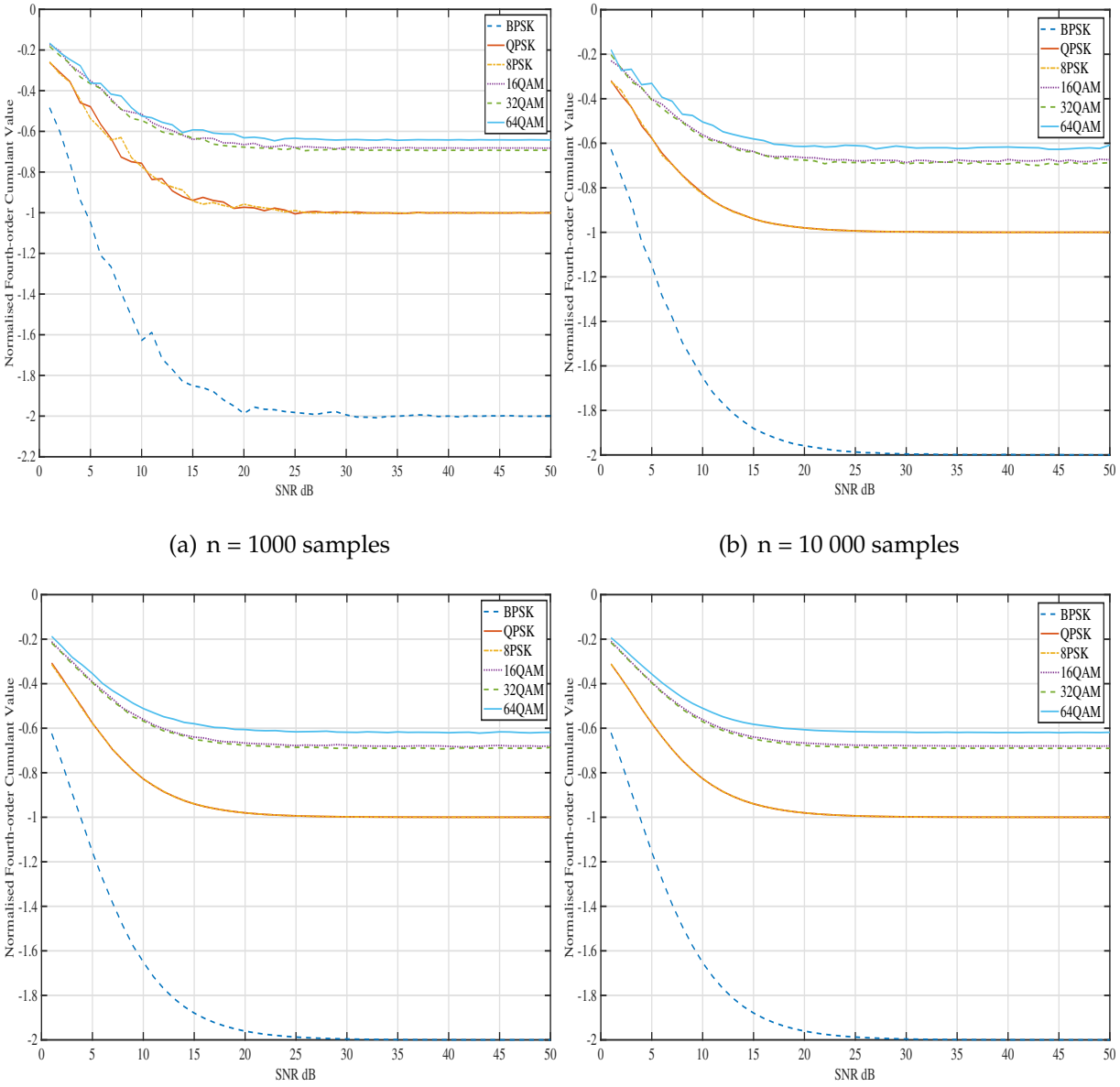

(a) n = 1000 samples

(b) n = 10 000 samples

(c) n = 100 000 samples)

(d) n = 1 000 000 samples

Figure 5.2: Normalised fourth-order cumulant values at different SNR for different sample sizes

tions can still be distinguished. The estimated cumulant value starts to converge to the theoretical value from around 20 dB. In Chapter 3.3 Gang et al. [34] also reported that the longer the data length and the higher the SNR, the closer the cumulants are to the theoretical value, and thus the better the classification performance. The maximum, minimum, mean, and variance were recorded for each modulation's corresponding normalised fourth-order cumulant from 20 dB onwards.

Table 5.2: Normalised fourth-order cumulants for n = 1000

Parameter	**BPSK**	**QPSK**	**8-PSK**	**16-QAM**	**32-QAM**	**64-QAM**
Min	-2.0083	-1.0056	-1.0048	-0.6861	-0.6950	-0.6464
Max	-0.4837	-0.2609	-0.2581	-0.1721	-0.1821	-0.1662
Mean	-1.7839	-0.8906	-0.8901	-0.6071	-0.6189	-0.5735
Variance	0.1556	0.0401	0.0398	0.0180	0.0180	0.0157

Table 5.3: n = 10 000

Parameter	**BPSK**	**QPSK**	**8-PSK**	**16-QAM**	**32-QAM**	**64-QAM**
Min	-1.9999	-1.001	-1.0002	-0.6869	-0.6996	-0.6273
Max	-1.9587	-0.9803	-0.9803	-0.6648	-0.6756	-0.6082
Mean	-1.9932	-0.9967	-0.9969	-0.6771	-0.6885	-0.6186
Variance	1.1155e-04	2.5500e-05	2.4997e-05	2.6631e-05	2.6474e-05	2.5295e-05

Table 5.4: n = 100 000

Parameter	**BPSK**	**QPSK**	**8-PSK**	**16-QAM**	**32-QAM**	**64-QAM**
Min	-1.9999	-1.0000	-1.0000	-0.6834	-0.6928	-06221
Max	-1.9608	-0.9803	-0.9803	-0.6668	-0.6776	-0.6059
Mean	-1.9938	-0.9969	-0.9969	-0.6780	0.6877	-0.6168
Variance	1.0088e-04	2.5618e-05	2.5217e-05	1.5313e-05	1.3341e-05	1.2274e-05

Table 5.5: n = 1 000 000

Parameter	**BPSK**	**QPSK**	**8-PSK**	**16-QAM**	**32-QAM**	**64-QAM**
Min	-2.0000	-1.0000	-1.0000	-0.6807	-0.6906	-0.6202
Max	-1.9606	-0.9803	-0.9803	-0.6665	-0.6766	-0.6067
Mean	-1.9938	-0.9969	-0.9969	-0.6779	-0.6879	-0.6173
Variance	1.0145e-04	2.5353e-05	2.5380e-05	1.2468e-05	1.1866e-05	9.7262e-06

Table 5.6 summarises the effect of the sample size on the estimated cumulant value. For a sample size of $n = 1000$, the difference between the calculated and theoretical value differ by an estimate of 10%. From $n = 10000$ onward, the error is less than 1%. Therefore a sample size of $(1000 < n \leq 10000)$ is effective for estimating the cumulants. Anything greater then $n > 10000$ is redundant.

Table 5.6: Error between mean calculated fourth-order cumulant and the theoretical value

Sample Size	Modulation	Estimated	Theoretical	% Error
n = 1000	BPSK	-1.7839	-2.0	10.81%
	QPSK	-0.8906	-1.0	10.94%
	8-PSK	-0.8901	-1.0	10.99%
	16-QAM	-0.6071	-0.68	10.72%
	32-QAM	-0.6189	-0.6905	10.37%
	64-QAM	-0.5735	-0.6191	7.35%
n = 10 000	BPSK	-1.9932	-2.0	0.315%
	QPSK	-0.9967	-1.0	0.33%
	8-PSK	-0.9969	-1.0	0.31%
	16-QAM	-0.6771	-0.68	0.42%
	32-QAM	-0.6885	-0.6905	0.29%
	64-QAM	-0.6186	-0.6191	0.064%
n = 100 000	BPSK	-1.9938	-2.0	0.31%
	QPSK	-0.9969	-1.0	0.31%
	8-PSK	-0.9969	-1.0	0.31%
	16-QAM	-0.6780	-0.68	0.29%
	32-QAM	-0.6877	-0.6905	0.26%
	64-QAM	-0.6168	-0.6191	0.35%
n = 1 000 000	BPSK	-1.9938	-2.0	0.31%
	QPSK	-0.9969	-1.0	0.31%
	8-PSK	-0.9969	-1.0	0.31%
	16-QAM	-0.6779	-0.68	0.30%
	32-QAM	-0.6879	-0.6905	0.38%
	64-QAM	-0.6173	-0.6191	0.27%

5.3 Determining Frame size

For any received signal of length n samples, there exists a message matrix **rxSig** = $[l \times m]$, where l is the number of rows in the message matrix and m is the number of columns in the message matrix. We can divide the received signal of length n samples into m columns of length $l = n/m$. In the message matrix, m is called the frame size.

When recording a signal, the sample rate of the analog-to-digital converter (ADC) determines the number of samples the radio front-end can capture and process per second. The received signal symbols are split into frames, which simplifies the feature extraction process. For a 1 s recording of a signal of interest, a frame size of 100 will result in a 100 ms resolution to view and process the signal, and then extracting the

features on a frame-by-frame basis, and averaging over the frames. The number of samples per frame, l is dependant on the sample rate of the front-end device.

For a front-end device with a sample rate of 2 MHz, it will capture 2 M samples per second. Selecting an arbitrary frame size of 100, each frame will have 20 000 samples for feature extraction. Therefore, selecting an appropriate frame size is another important factor which influences the computational efficiency of the classifier.

A time analysis is done to determine how long it would take to extract the feature set for a given sample size n and a frame size m. Each received signal is analysed on a frame-by-frame basis. The elapsed time from extracting the feature set for frame one to frame m is recorded.

The complexity of an algorithm is a function describing the efficiency of the algorithm in terms of the data that the algorithm must process. Time complexity is a function the describes the time an algorithm takes regarding the amount of input to the algorithm. The time can be an indication of the number of comparisons between integers, the number of times an inner loop is executed, or the time related to the amount of real-time the algorithm takes. Many factors unrelated to the algorithm itself can affect the real-time measurement. Factors such as the programming language, computer hardware and optimisation of the compiler. However, extracting the features are not so much an analysis of the efficiency of the features extraction algorithms themselves, rather a hardware architectural test.

Table 5.7 shows the test parameters for the time analysis. The time analysis is only an estimate to indicate the expected duration of the operation. Table 5.8 summarises the hardware specifications for the test computer.

Table 5.7: Test parameters

Parameter	**Value**
Frames	1, 10, 100
Number of samples	[1:100 000]

Figure 5.3 shows the results obtained from the time analysis. For a sample size $n = 10000$, and a frame size of $1 \geq m \leq 10$, (total message length of 10 000 $\times m$) the time it takes to extract the features are less than 0.05 seconds. For a frame size of 100, extracting the features for the same sample size $n = 10000$ per frame (total of 1 M samples) is 0.2 seconds. The time it takes increase linearly for each frame size tested as the sample size increases. Selecting more frames will result in better statistical feature estimates, therefore a frame size of 100 is selected for further evaluations.

A frame size of $m = 100$ and $l = 10000$, will allow us to analyse and extract our feature set of a recorded signal with 1 M samples within 0.2 seconds.

Table 5.8: Testing computer hardware specifications

Hardware Component	
CPU	Intel i7-6700
CPU Clock	3.6 GHz
CPU Cores	4
Memory	8 GB
Storage	500 GB HDD 7200 RPM

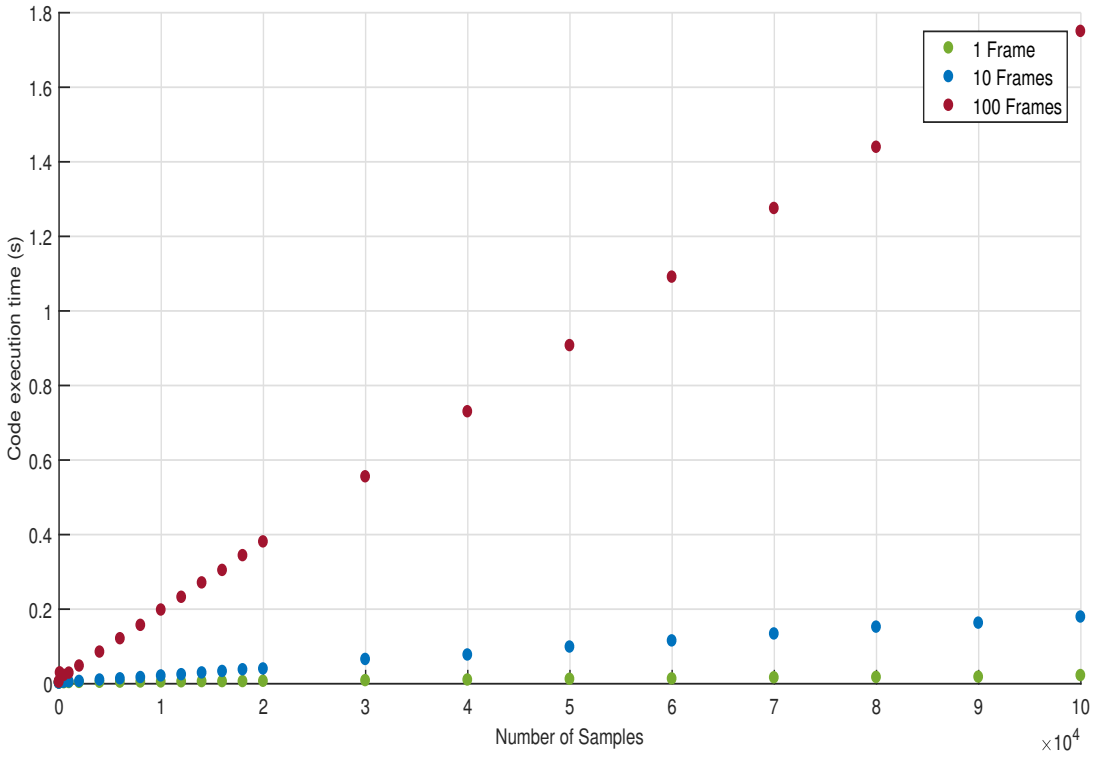

Figure 5.3: Time complexity analysis for running the feature extraction block.

5.4 Feature Evaluation

Refer to Figure 3.2. The output signal from the communication block {5.0} is a complex signal in the form of $a + jb$. The complex samples are processed and from the complex samples its respective magnitude and phase components are derived (block {7.0}) according to equation (2.19) and (2.20). The magnitude and phase component is also known as the instantaneous amplitude and phase of the signal. From the instantaneous amplitude and phase, the mean (μ), variance (σ^2), skewness (s), kurtosis (κ), higher order-moments (σ^m), and cumulants (C_{pq}) are evaluated. The signal power key β is also evaluated.

5.5 Simulation Results

5.5.1 Methodology

Two simulation experiments are conducted in this section. The first experiment evaluates the statistical features to determine the core features needed to distinguish the modulation from each other. The second experiment evaluates the performance of a SVM in an AWGN channel. The feature extraction and classification is implemented in MATLAB. The implementation procedure explained in Chapter 3 and the verification steps described in Chapter 4 are followed to ensure that the correct outputs are obtained.

For the first experiment, the mean, variance, skewness, kurtosis, 12^{th}-order moment of the instantaneous amplitude and phase are extracted and compared to each other at SNR levels of 0 dB to 20 dB. The normalised fourth-order cumulant of the received signal and the signal power key is also evaluated.

Figure 5.4 - 5.5 present the results obtained. The modulations considered include BPSK, QPSK, 8-PSK, 16-QAM, 32-QAM, and 64-QAM (from Chapter 3.6). A total of

100 frames are evaluated, with a sample size of 1000 samples per frame. The experimental parameters are summarised in Table 5.9.

Table 5.9: Experimental Parameters

Parameter	**Value**
Modulations	BPSK, QPSK, 8-PSK, 16-QAM, 32-QAM, 64-QAM
Phase-offset	0 rad
Number of signal symbols	1000 symbols
Number of frames	100
Training dataset size	12 000 entries (2000 per modulation)
SNR	0:20 dB

For the second experiment, a SVM is the chosen classifier (from Chapter 3.10.5) to evaluate the performance of these features in AWGN noise. The SVM can separate the modulations from each other through a higher-dimensional hyperplane.

Five input features and six possible outputs, a total of 12 000 data elements were used to train the classifiers. The training data were randomly sorted and loaded. Fifty percent of the generated data were used for training, 25% were used for validation and the last 25% for testing.

5.5.2 Feature Evaluation

From the results obtained, it is clear that the mean of the normalised instantaneous amplitude and phase in Figure 5.4(a) and 5.4(b) do not contribute to discriminating the modulations. Even at higher SNR, the mean values cannot be used to discriminate between any modulations. The variance of the normalised instantaneous amplitude in Figure 5.4(c) makes a clear distinction between M-PSK and M-QAM signals. The variance of the instantaneous phase in Figure 5.4(d) shows that it is able to discriminate BPSK, QPSK and 8-PSK from the QAM modulations.

From Figure 5.4(e) the skewness of the normalised instantaneous amplitude is again able to separate M-PSK and M-QAM modulation from each other.

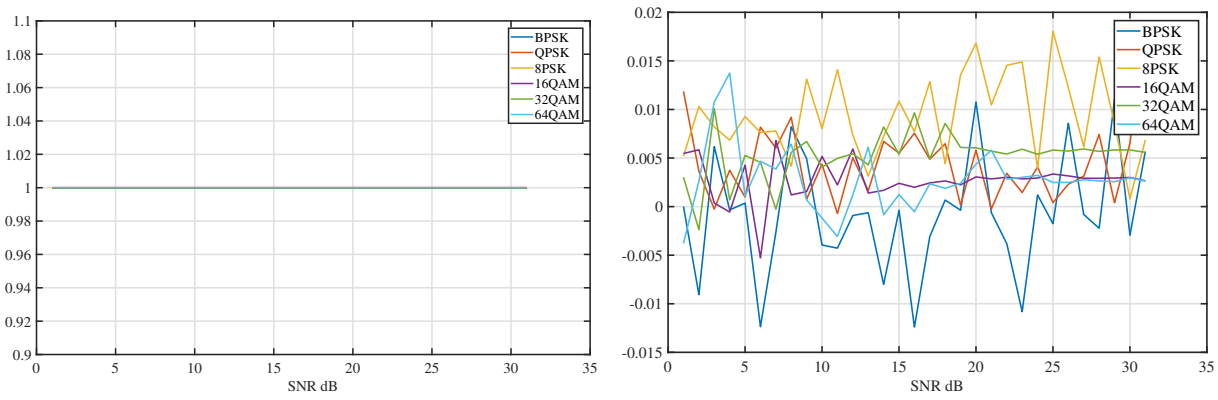

(a) Mean A_n (b) Mean $\theta(t)$

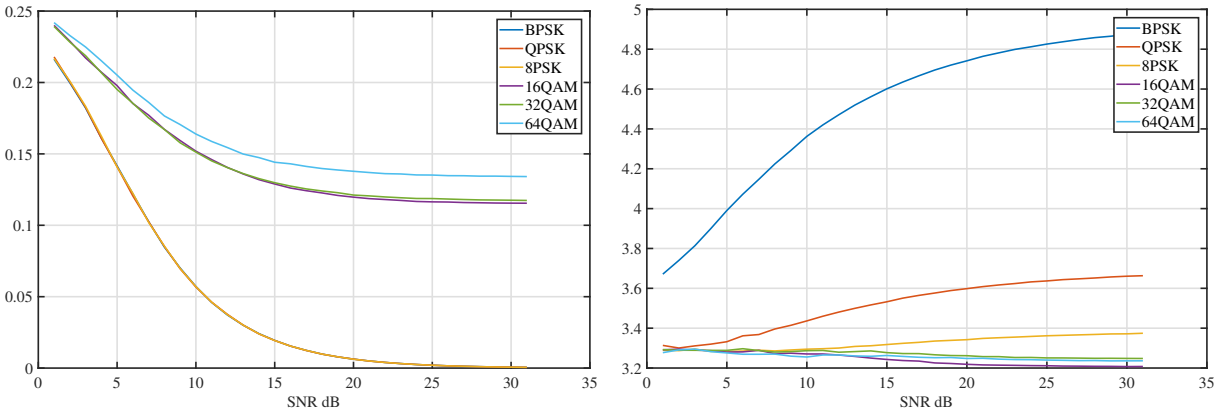

(c) Variance A_n (d) Variance $\theta(t)$

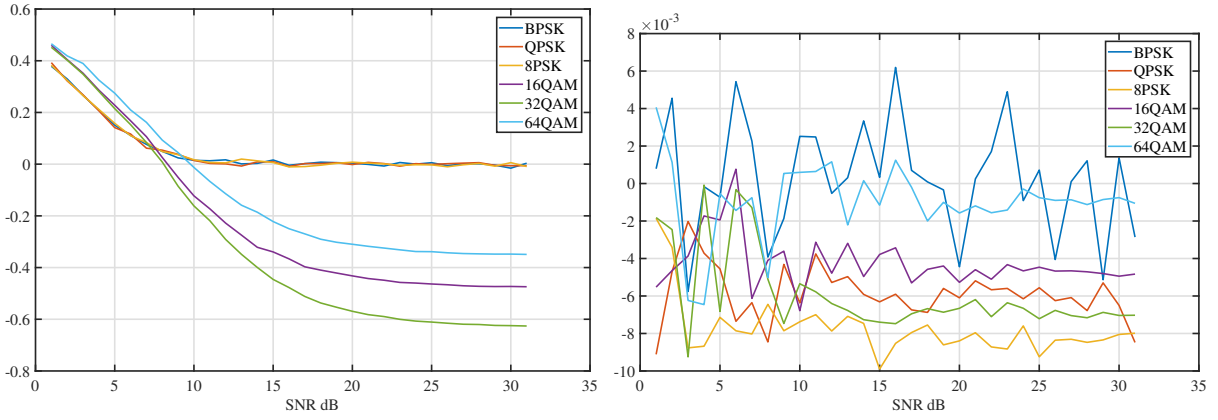

(e) Skewness A_n (f) Skewness $\theta(t)$

Figure 5.4: HOS features vs SNR

From Figure 5.4(f) can be seen that the skewness of the instantaneous phase does not make any contribution to distinguish between the modulations.

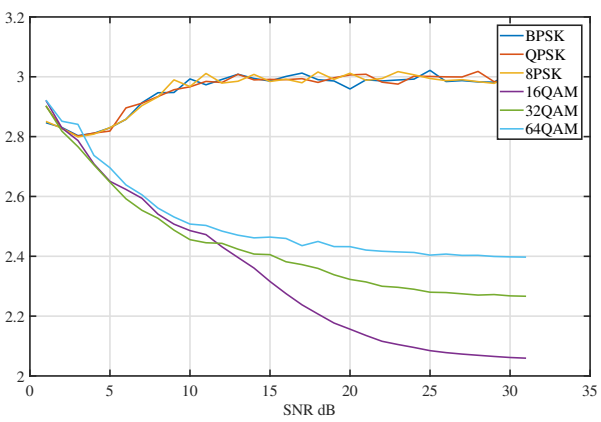

(a) Kurtosis A_n

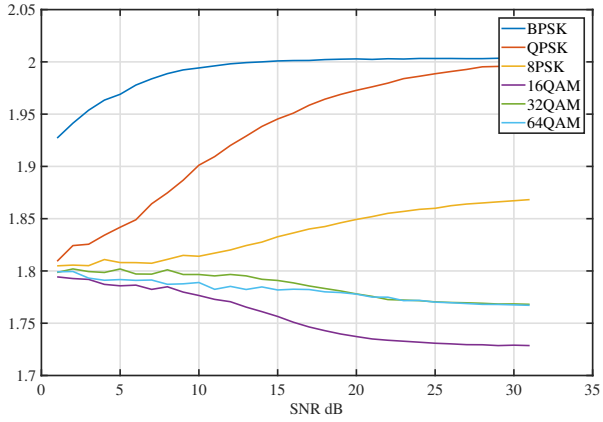

(b) Kurtosis $\theta(t)$

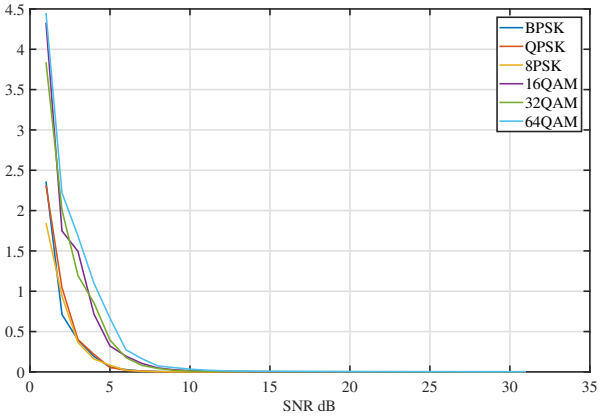

(c) Moment-order 12 A_n

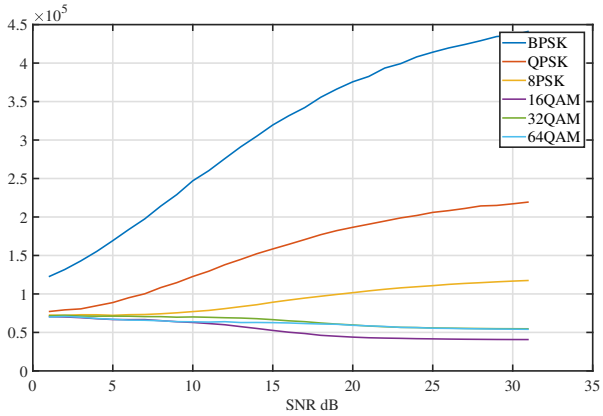

(d) Moment-order 12 $\theta(t)$

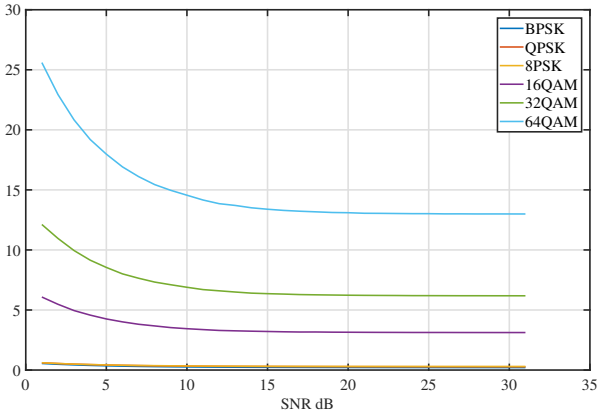

(e) β

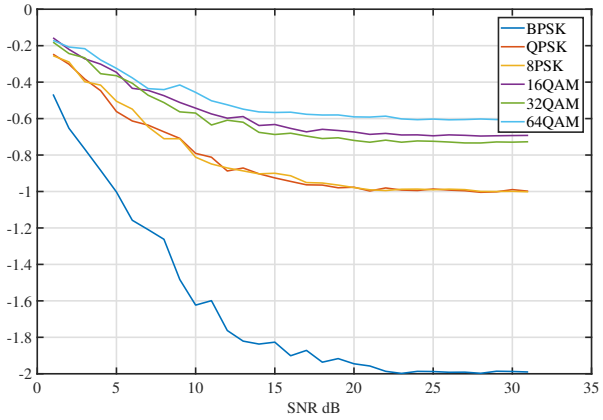

(f) C_{42} of the received signal

Figure 5.5: HOS features vs SNR (continued)

In Figure 5.5(a) the kurtosis of the instantaneous phase can be used to discriminate BPSK, QPSK and 8-PSK from the other modulations at low SNR.

Table 5.10: Feature set used for classification

	Features
1	σ^2 of the instantaneous phase
2	κ of the instantaneous phase
3	M_{12} of the instantaneous phase
4	β
5	Normalised C_{42}

Furthermore, the 12th-order moment of the instantaneous phase, β and normalised C_{42} (Figure 5.5(d) - (f)) can be used to identify 16-QAM, 32-QAM and 64-QAM from the rest. The selected features showed a good amount of separation between each other. Therefore the use of a SVM is a suitable choice. Table 5.10 summarises the proposed feature set used for the proposed classifier.

5.5.3 Classifier Performance

From the results obtained in the previous experiment (experiment in Section 5.5.2), the final feature set are shown in Table 5.10, which is chosen as input for the SVM classifier. A linear SVM is selected for classification (SVM with a linear kernel function). A total of 12 000 training samples are used as input to the classifier. 6000 samples are used for training, while the other 6000 samples are held out for verification and validation of the classification algorithm. The SVM is implemented in MATLAB using the Classification Learner Toolbox.

The performance of the classifier is tested for two use cases:

1. SNR known to the classifier (SNR estimation included as part of the feature set).
2. SNR unknown to the classifier (SNR estimation excluded from the feature set).

SNR Estimate Included

Figures 5.6(a) - (e) show scatter-plots for the features versus SNR. These plots try to identify predictors that separate the modulation classes well by plotting the predictors against each other, to create a multi-dimensional view of the features. This helps to identify the features which contribute to class separation, and to allow for training of the SVM with only those features. The plots only show that an increased SNR improves the ability to separate features, and therefore an SNR feature estimation could be used for classification.

The plots presented show how the inclusion of an SNR estimate improves the separation between the modulation classes. Figure 5.6(a) show that moment-order 12 is able to separate the PSK signals from the QAM signals. At low SNR (SNR $\leq$ 8 dB) this feature is able to tell BPSK from the rest, and at SNR $\geq$ 10 dB, QPSK can be separated from the rest. Figure 5.6(e) show that the kurtosis versus SNR of the instantaneous phase do not contribute to identifying the modulations.

The signal power key β in Figure 5.6(c) has the ability to tell 16-QAM, 32-QAM and 64-QAM from each other at any SNR value. β also has the ability to separate M-PSK signals from M-QAM signals.

SNR Estimate Excluded

Figures 5.7(a) - (d) show scatter-plots for the features plotted against each other. Figure 5.7(a) and (b) show how the feature values group together to form separation between the modulation classes. Figure 5.7(b) shows that BPSK and QPSK can be separated from 8-PSK and the QAM modulation classes. The plots show the feature values over an SNR range of 0 dB - 20 dB.

Figure 5.8 shows the fourth-order cumulant versus β for only the PSK modulations. Because the values for β is so large for QAM signals compared to PSK, Figure 5.7(d) does not show how separation is accomplished for the PSK modulation group.

Figure 5.8 shows that C_{42} versus β can separate BPSK from QPSK/8-PSK. From evaluating all the possible combinations of these features, it is still difficult to find a good enough separation between QPSK and 8-PSK modulations. However, this is where estimating an SNR value helps to distinguish QPSK from 8-PSK.

Probability of Correct Classification

The performance of the trained classifier is tested on two data sets. The procedure described in Chapter 3 to generate a message signal, to modulate the signal, and to transmit through an AWGN channel is followed.

For testing the performance of the classifier, the same parameters in Table 5.9 are used. A feature table is extracted for each modulation class, one set will include the SNR label, and the other will not. Figure 5.9 shows the results obtained from testing the classifier performance.

From Figure 5.9(a) it is clear that including an SNR estimate results in an overall performance classification accuracy increase. The classification accuracy for 8-PSK modulations increases from 55% to 67% at an SNR of 1 dB, while the classification accuracy for QPSK modulation increases from 83% to 85% at 4 dB.

Overall, the classification accuracy for the other modulations remains the same, and including the SNR value in the feature set does not contribute to any classification accuracy improvement. Figure 5.9 confirms the result shown in Figures 5.6 - 5.7 which show that the features are able to separate BPSK from QPSK/8-PSK and (16, 32, 64)-QAM modulation classes, and that the features have trouble separating QPSK from 8-PSK at low SNR. The probability of correct classification for the other modulation schemes (those not clearly seen in Figures 5.6 - 5.7) were 100%.

5.6 Conclusion

This chapter presented an FB classification approach in an AWGN channel. Statistical features derived from the instantaneous amplitude and phase of the received signal were used to classify M-PSK and M-QAM signals. Two experimental procedure were discussed to motivate the selection of an appropriate sample and frame size. The features were evaluated over a range of SNR values. The final features used to classify the M-PSK and M-QAM signals are presented in Table 5.10. A SVM was used to classify the modulations based on the extracted features. The performance of the SVM was evaluated for two use-cases: with and without SNR estimation.

The result showed that including an SNR estimate in the feature set improves performance. The results also showed that without the SNR estimation good classification performance could be achieved. The next chapter will continue to evaluate the performance of the FB classifier in a multipath fading channel.

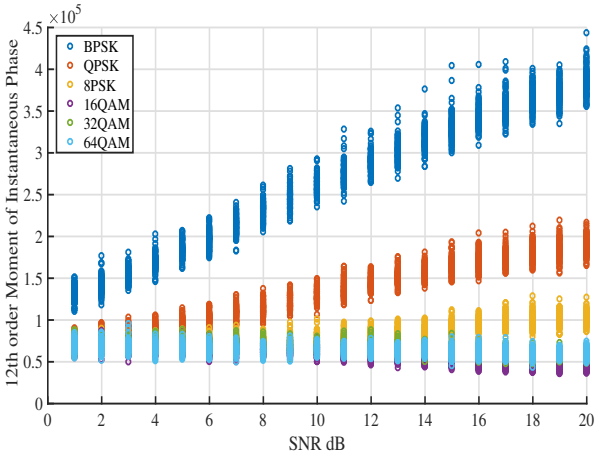

(a) Moment-order 12 $\theta(t)$ vs SNR

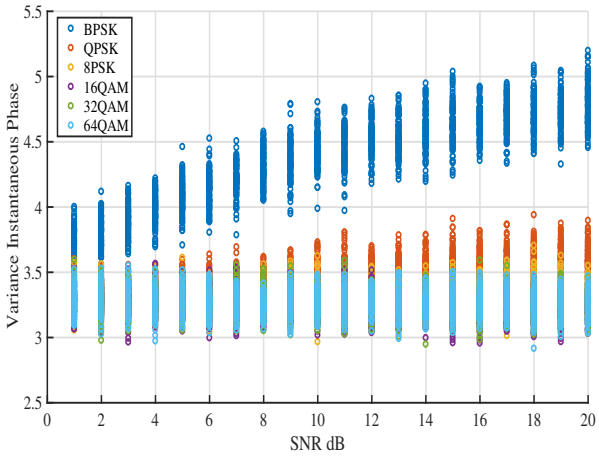

(b) Variance $\theta(t)$ vs SNR

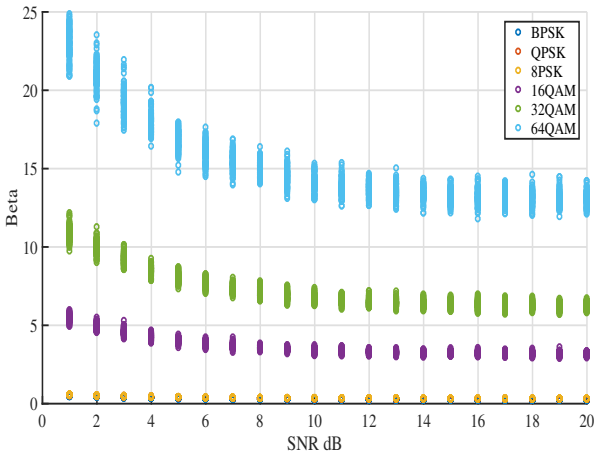

(c) β vs SNR

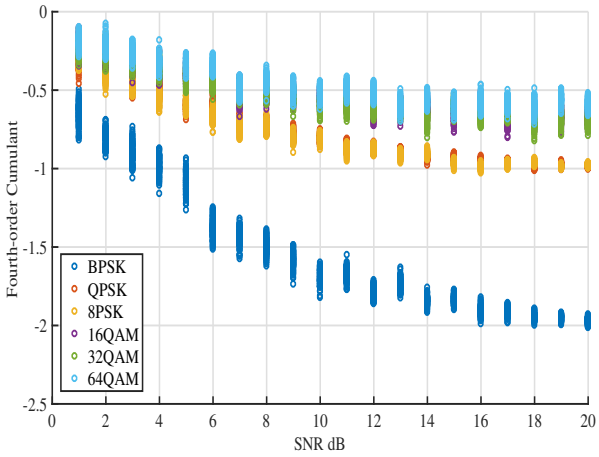

(d) C_{42} vs SNR

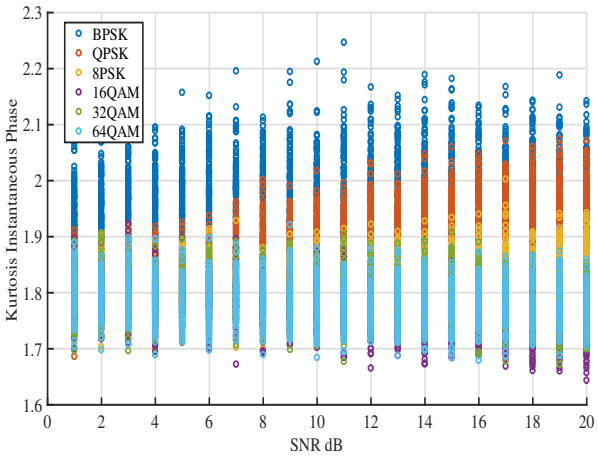

(e) Kurtosis $\theta(t)$ vs SNR

Figure 5.6: Scatterplot: Training feature set for SVM (SNR estimation included)

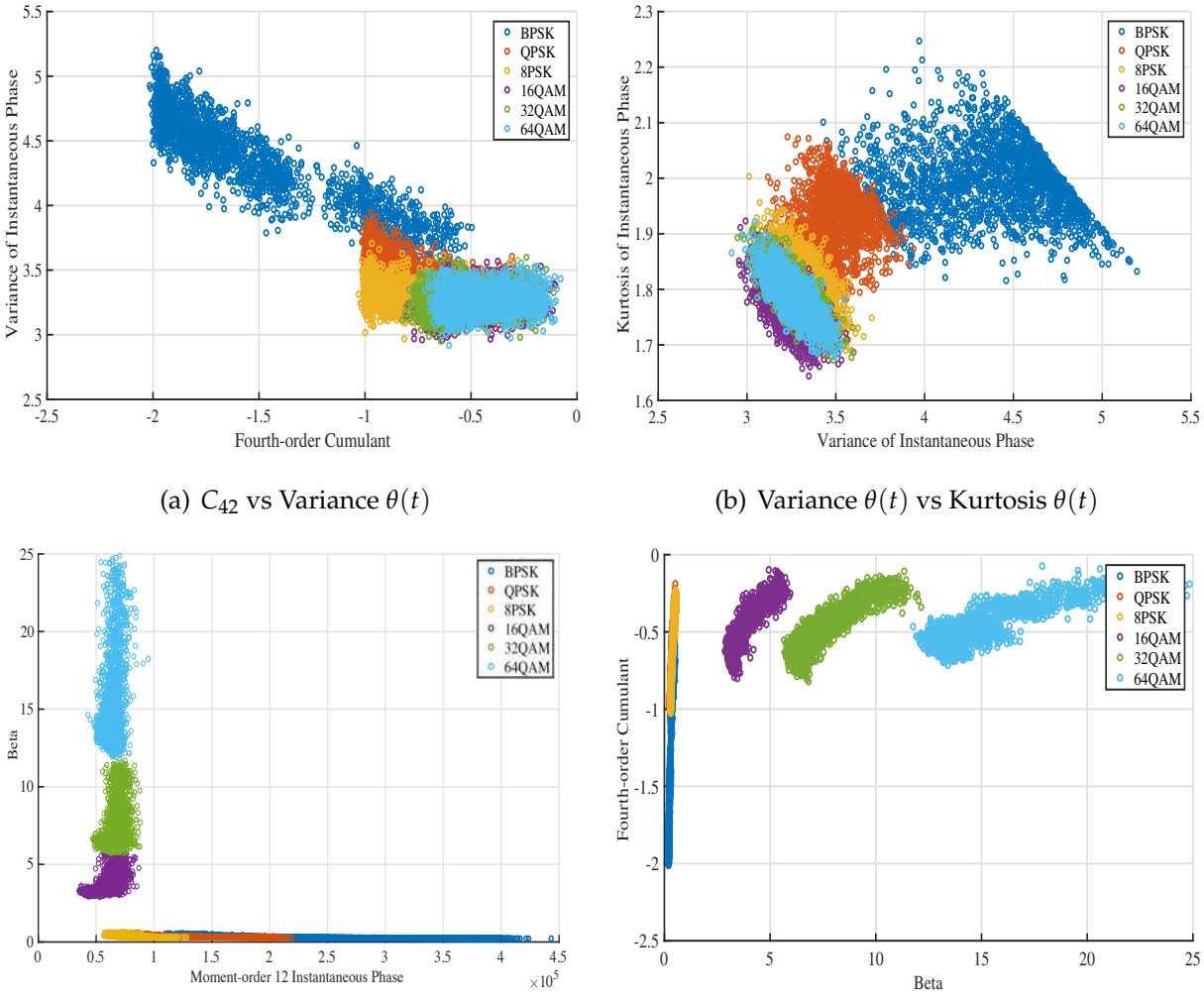

(a) C_{42} vs Variance $\theta(t)$

(b) Variance $\theta(t)$ vs Kurtosis $\theta(t)$

(c) Moment-order 12 $\theta(t)$ vs β

(d) β vs C_{42}

Figure 5.7: Scatterplot: Training feature set for SVM (SNR estimation excluded)

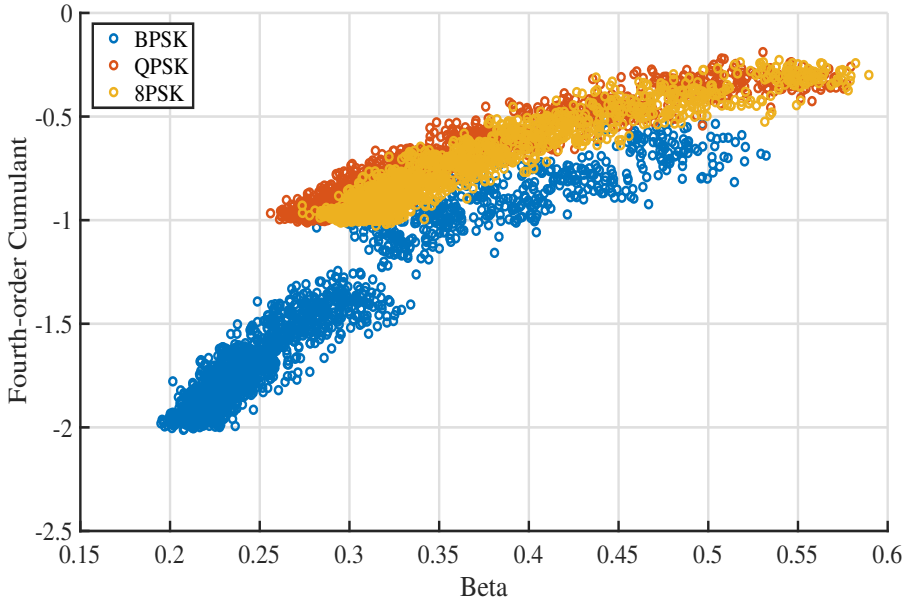

Figure 5.8: C_{42} vs β for PSK modulations

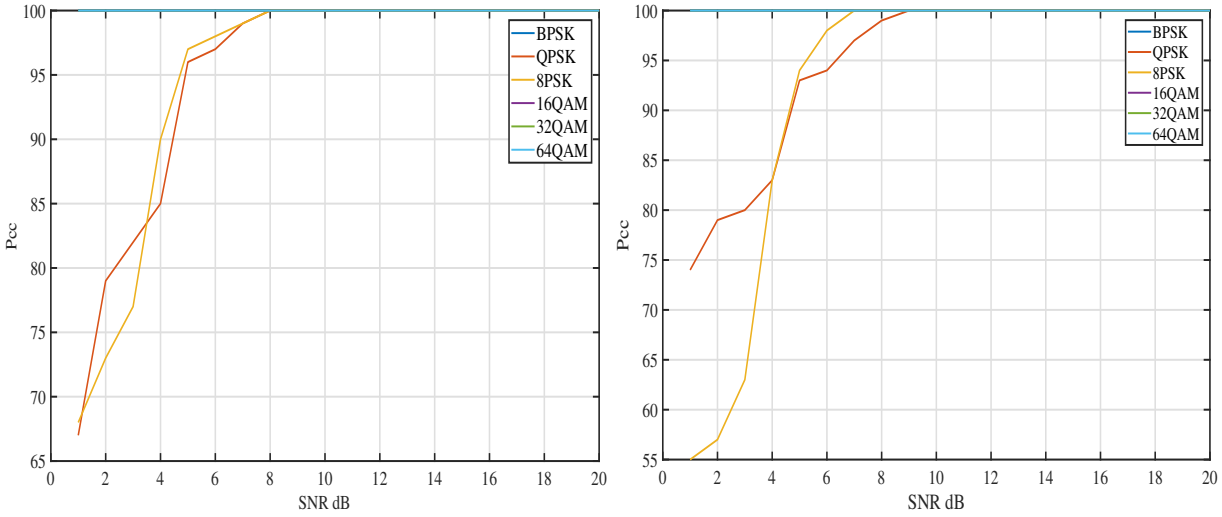

(a) SNR estimate included in feature set

(b) SNR estimate excluded from feature set

Figure 5.9: Probability of correct classification vs SNR

Chapter 6

Feature-based AMC in a Multipath Fading Channel

This chapter presents the methodology followed to evaluate the performance of the statistical feature-based AMC system in the presence of a multipath fading channel. The feature set proposed in Chapter 5 is used for classifying modulations in a multipath channel. Mitigate inter-symbol interference (ISI) through channel equalisation and carrier synchronisation is discussed. The performance of the classifier is evaluated for two use cases: stationary transmitter and receiver, and for a moving receiver.

6.1 Introduction

Higher-order cumulants have been proposed as main features for classification of modulations in a multipath fading channel [28], [36], [37], and [38]. Cumulants can characterise the shape of the distribution, which make them simple and effective to use.

Transmitting a signal through a multipath channel causes ISI. ISI is a form of distor-

tion that causes symbols to overlap and become indistinguishable from the transmitted symbols. A multipath scattering environment causes the receiver to see delayed versions of the transmitted symbols, which cause interference with other symbol transmissions. Figure 6.1 illustrates how reflections from objects result in multiple copies of the same signal to arrive at the receiver.

The ISI degrades the performance of the classifier. One of either two approaches can be followed to alleviate the influence of multipath effect: channel equalisation and channel estimation. An equaliser attempts to mitigate ISI and improve the receiver performance. In a narrowband signal, a one-tap equaliser can compensate for a frequency-flat fading channel, and for wideband signals, an equaliser with multiple taps helps compensate for a frequency-selective fading channel [2].

Three general equalizers have been proposed [2]:

1. Linear equalizers (symbol-spaced and fractionally spaced),
2. Decision-feedback equalizers,
3. and Maximum-Likelihood Sequence Estimation (MLSE).

Furthermore, linear and decision-feedback equalisers are adaptive equalisers that make use of adaptive algorithms. Some of the adaptive algorithms include:

1. Least Mean Square (LMS),
2. Signed LMS,
3. Normalized LMS,
4. Variable-step-size LMS,
5. Recursive least squares (RLS),
6. and Constant modulus algorithm (CMA).

The CMA is a linear equaliser and makes use of the constant modulus algorithm to equalise a linearly modulated baseband signal through a dispersive channel [43]. The

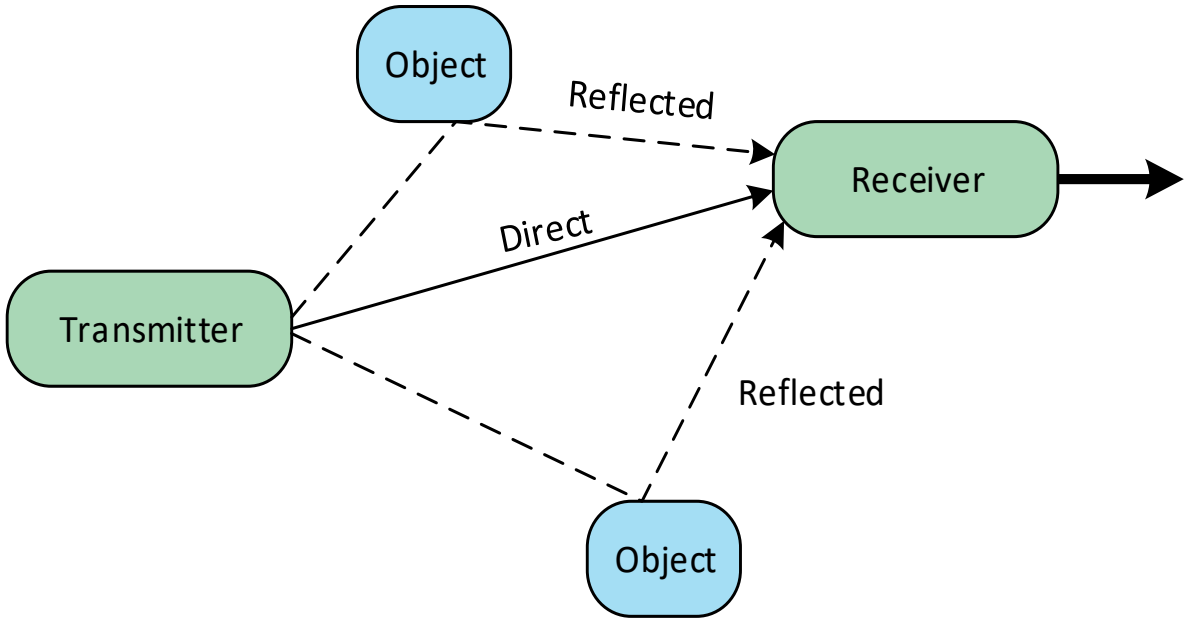

Figure 6.1: Direct and reflected paths between a stationary transmitter and moving receiver.

CMA can achieve good performance for M-PSK signals since M-PSK signal's constellation has a character of a constant modulus. M-QAM signals for modulation order M greater than 16, the CMA fails [43]. If the modulation group (PSK or QAM) is known, a CMA equaliser can be designed.

To structure a fitting equaliser requires apriori information about the channel, such as the number of taps, the adaptive algorithm's step size and the signal constellation. Generally speaking, the modulation type needs to be known to design a proper equaliser. AMC tries to identify the unknown modulation type, which is the issue.

AMC tries to identify the modulation type of a signal, and currently, no need exists to demodulate. Therefore, if a reduction of ISI can be achieved, the result would be satisfactory. Carrier synchronisation is another fading channel compensation approach to mitigate ISI. Carrier synchronisation compensates for carrier frequency and phase offsets induced by a fading channel. The carrier-synchroniser uses a Phase-Locked-Loop (PLL)-based algorithm. The output of the carrier synchroniser is a frequency-shifted version of the input signal.

The received signal symbols suffering from multipath fading can be represented by:

$$y(n) = \sum_{k=0}^{L-1} h(k)x(n-k) + g(n), \tag{6.1}$$

where $x(n)$ is the initial transmitted modulated symbols, $h(k), k = 0, ..., L-1$ are the fading channel coefficients, and L is the multipath fading channel length. $g(n)$ is the AWGN with a zero mean and a variance of σ^2.

In [28], [36], [37], and [38] the authors chose to follow a channel estimation approach to make the features more robust. The authors proposed a solution to estimate the transmitted symbol's fourth-order cumulants form the received signals symbols. The authors proposed finding a coefficient relevant to the channel coefficients. This parameter scales the received symbol's fourth-order cumulants by an approximation to recover an estimated fourth-order cumulant of the transmitted symbols. Estimating this channel coefficient parameter is discussed in more detail in [36].

To mitigate ISI, a carrier synchronisation approach is followed in this chapter. The feature set proposed in Chapter 5 is extracted from the compensated symbols. The performance of the classifier is evaluated to see to what extent classification of signals in a multipath fading channel can be achieved.

6.2 Methodology

In Chapter 2 the procedure for simulating a multipath channel is discussed. The multipath channel is presented by a TDL model, which is characterised by a discrete number of impulses. The channel is realised by an finite impulse response (FIR) filter, with a particular impulse response. In Chapter 3 two fading channel models are exhibited: the ITU-R M.1225 models and the COST 207 channel model.

3GPP suggested the COST 207 TU model for simulating GSM/EDGE signals [49], and according to Rohde-Schwarz [61], the COST 207 model is sufficient to simulate fading

conditions for DVB-T. The 6-tap TU model is the proposed channel model for analyses. The TU model is characterised by 6-taps, with its relative delay and power profile. The power amplitudes are characterised by a Rayleigh distribution, which varies according to its respective Doppler spectrum.

The UHF frequency band supports a host of different communication services, and each operating at different frequencies, with different channel bandwidths. Table 6.1 shows a summary of typical digital signals in the UHF band (courtesy of GEW Technologies):

Table 6.1: Examples of common digital signals in the UHF band.

Signal	**Frequency**	**Typical Bandwidth**
TETRA	420.4625 MHz	25 kHz
GSM	954.2025 MHz	200 kHz
UMTS	2112.5 MHz	5 MHz
DVB-T	530 MHz	8 MHz
AIS	161.975 MHz and 162.025 MHz	25 kHz
Wi-Fi	2462 MHz	20 MHz

The performance of the classifier is assessed for two use-cases: a stationary transmitter and receiver, and secondly for a stationary transmitter and moving receiver. The test set-up will assume to have no LOS path between the transmitter and receiver. The use of a pulse-shaping filter is ignored. The classifier will rely on carrier synchronisation to compensate for ISI. The channel is evaluated in the absence of AWGN.

The implementation procedure explained in Chapter 3 is followed likewise. Table 6.2 summarises the test parameters for the multipath channel. The same set of modulations are classified. A SVM is trained with a training set which consists of 12 000 samples (2000 per modulation).

6.2.1 Stationary Transmitter and Receiver

For the first test, a stationary transmitter and receiver are evaluated. For a stationary set-up, the maximum Doppler shift is 0 Hz, according to equation (3.35). The ampli-

Table 6.2: Experimental Parameters

Parameter	Symbol	Value
Modulations	M	BPSK, QPSK, 8PSK, 16QAM, 32QAM, 64QAM
Number of signal symbols	N	1000 symbols
Symbol rate	S	9600 baud
Bit rate	B	$S \times log_2 M$
Oversample rate	N_s	4
Training dataset Size		12 000 entries (2000 per modulation)
Mobile speed	v	Varied per iteration
Carrier frequency	f_c	Varied per iteration
Speed of light in free space	c	3×10^8 m/s
Max Doppler shift	f_d	$v \times f_c / c$

tude variation of the received signal components will correspond to a Rayleigh distribution. For the purpose of the simulation, varying the carrier frequency will have no impact on the channel conditions.

Firstly, Digital Terrestrial Television (DTT) channel 42 at 642.0 MHz is selected, with a mobile speed of 0 m/s. The experimental parameters in Table 6.2 are used, with $f_c = 642.0$ MHz and $v = 0$ m/s.

6.2.2 Moving Receiver

The second test will vary the speed of the receiver for different digital services. The digital services include DTT and TETRA. DTT covers a range of frequencies in the UHF. TETRA signals are single-carrier with QPSK modulation employed. This makes TETRA signals attractive to use for evaluation purposes. Table 6.3 shows the maximum Doppler shift for five randomly selected DTT channels, at five randomly selected mobile speeds (v between 30 km/h and 120 km/h). A random number generator is used to generate the four mobile speeds and for selecting the four DTT channels.

Table 6.3: Moving receiver experimental parameters.

DTT Channel	Carrier Frequency	Mobile Speed	Maximum Doppler Shift
21	474 MHz	66 km/h	28 Hz
35	586 MHz	112 km/h	60 Hz
48	690 MHz	35 km/h	22 Hz
50	706 MHz	87 km/h	57 Hz

6.3 Simulation Results

The feature set proposed in Table 5.10 is extracted from the carrier synchronised version of the received signal. The features are plotted against each other to identify better which features contribute to separating the modulation classes from each other. The plots indicate the feature spread, and it shows how an increase in Doppler shift results in more ISI. The performance of the classifier is presented in a confusion matrix corresponding to each Doppler shift.

6.3.1 Feature Evaluation

Stationary Transmitter and Receiver

Figure 6.2(a) - (d) show the scatterplots for the features plotted against each other. The multipath channel introduces many impairments into the channel and causes severe ISI. The feature values are scattered broadly. Figure 6.2(a) show that the variance of the instantaneous phase creates separation between BPSK, QPSK and the rest. Figure 6.2(c) shows that the kurtosis of the instantaneous phase is able to separate BPSK from all the other modulations.

β showed (Figure 6.2(d)) to be able to separate the QAM modulation class from the PSK modulation class. In Section 6.1 CMA has been identified as a possible equalisation algorithm to reduce ISI for modulations with a constant modulus (PSK modulations). β is a good indication whether PSK or QAM signals are viewed. The fourth-order cumulant value is distorted and deviates drastically from the theoretical values. Chan-

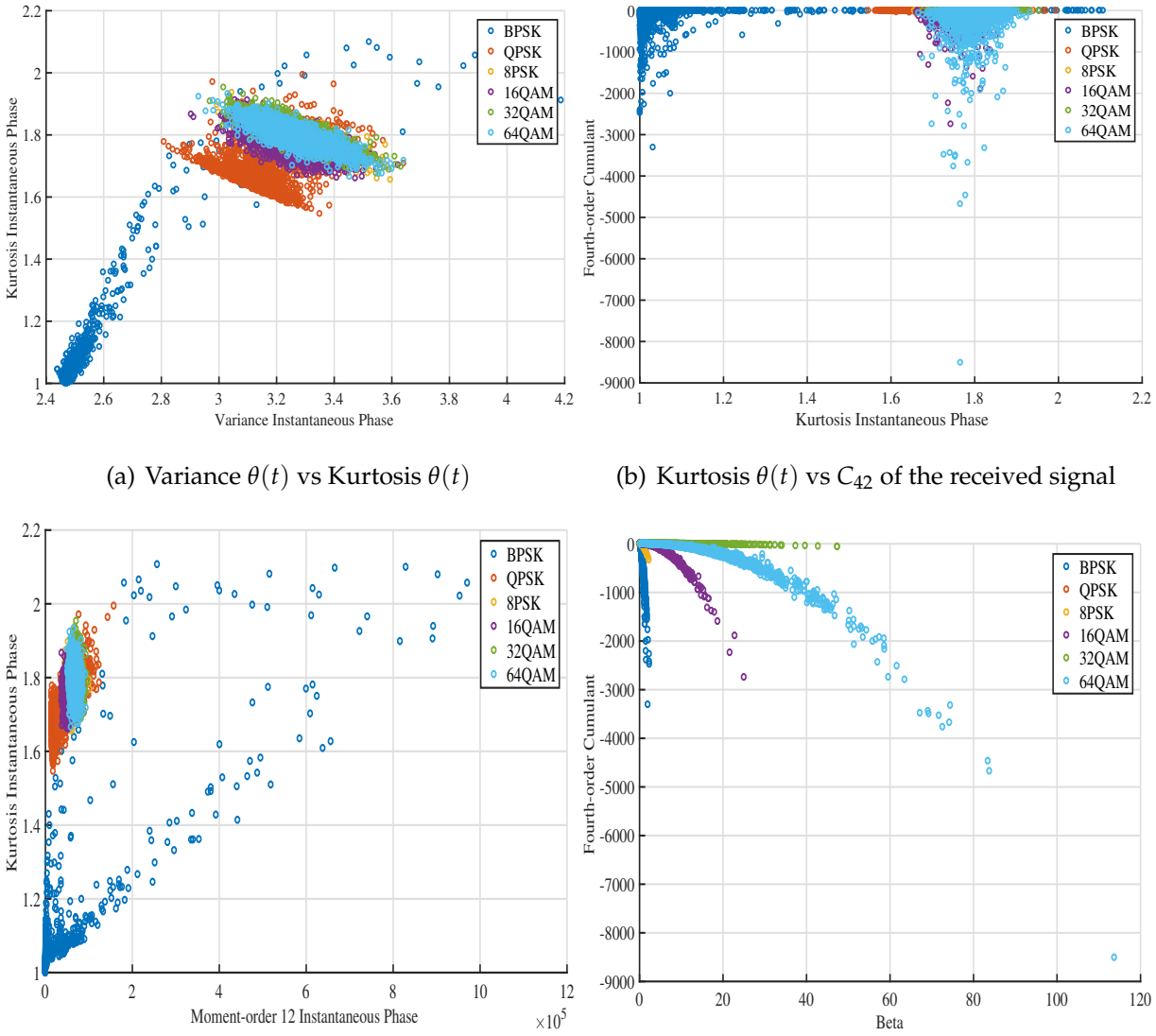

(a) Variance $\theta(t)$ vs Kurtosis $\theta(t)$

(b) Kurtosis $\theta(t)$ vs C_{42} of the received signal

(c) Moment-order 12 $\theta(t)$ vs Kurtosis $\theta(t)$

(d) β vs C_{42} of the received signal

Figure 6.2: Scatterplot: Training feature set for fading channel (0 Hz).

nel coefficient estimation [36] tries to mitigate the effect of multipath on the cumulant value.

Moving Receiver

Figure 6.3(a) - (b) show the scatterplots for the variance of the instantaneous phase versus the kurtosis of the instantaneous phase and the kurtosis of the instantaneous

phase versus the fourth-order cumulant of the received signal . Compared to Figure 6.2(a) and (b) the features are spread over a larger range of values.

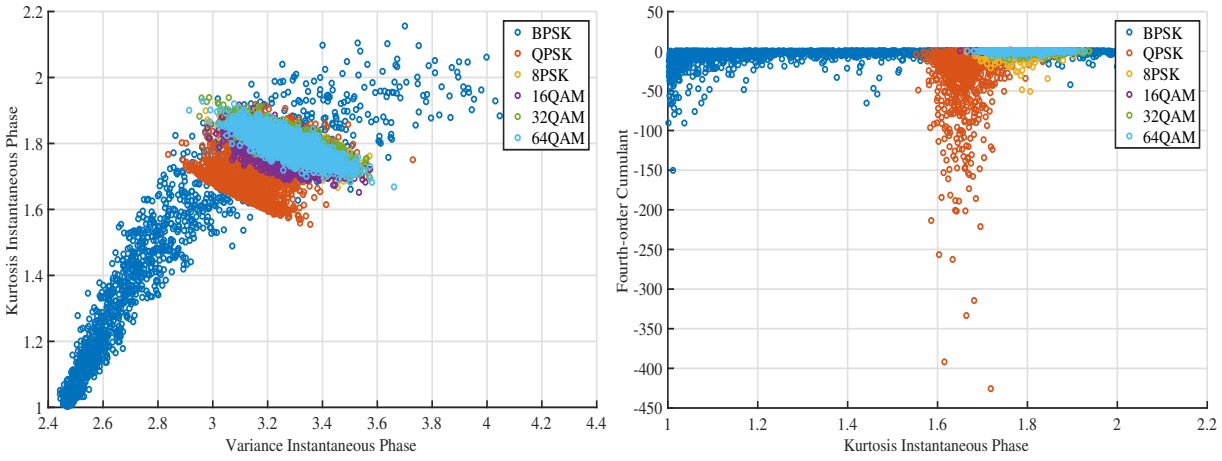

(a) Variance $\theta(t)$ vs Kurtosis $\theta(t)$ (b) Kurtosis $\theta(t)$ vs C_{42} of the received signal

Figure 6.3: Scatterplot: Training feature set for fading channel (22 Hz).

The stationary receiver use-case is a good reference to use for comparison. As the maximum Doppler shift increases, the coherence time of the channel will reduce, and the channel will remain constant for a smaller period, which results in more ISI.

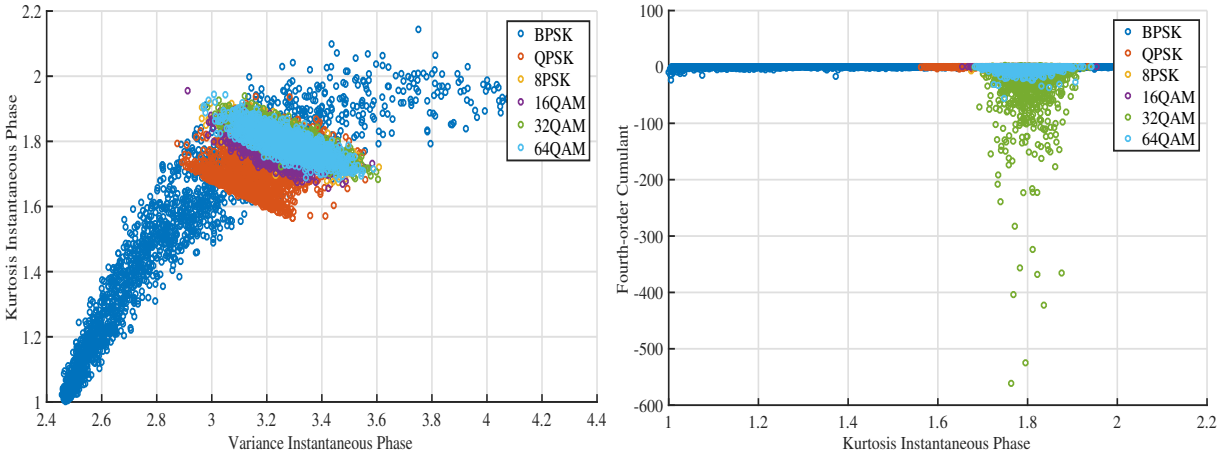

(a) Variance $\theta(t)$ vs Kurtosis $\theta(t)$ (b) Kurtosis $\theta(t)$ vs C_{42} of the received signal

Figure 6.4: Scatterplot: Training feature set for fading channel (28 Hz).

Figure 6.4 - 6.6 illustrates the same scatterplots for the same two features. The results

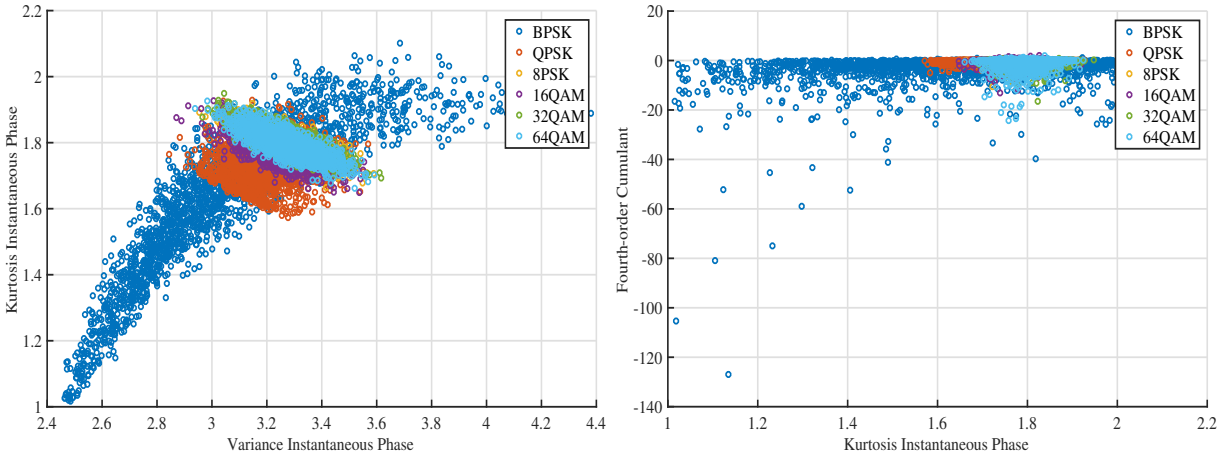

(a) Variance $\theta(t)$ vs Kurtosis $\theta(t)$ (b) Kurtosis $\theta(t)$ vs C_{42} of the received signal

Figure 6.5: Scatterplot: Training feature set for fading channel (57 Hz).

demonstrate how an increase in Doppler shift increases ISI which cause continuous degradation of the classifier's performance.

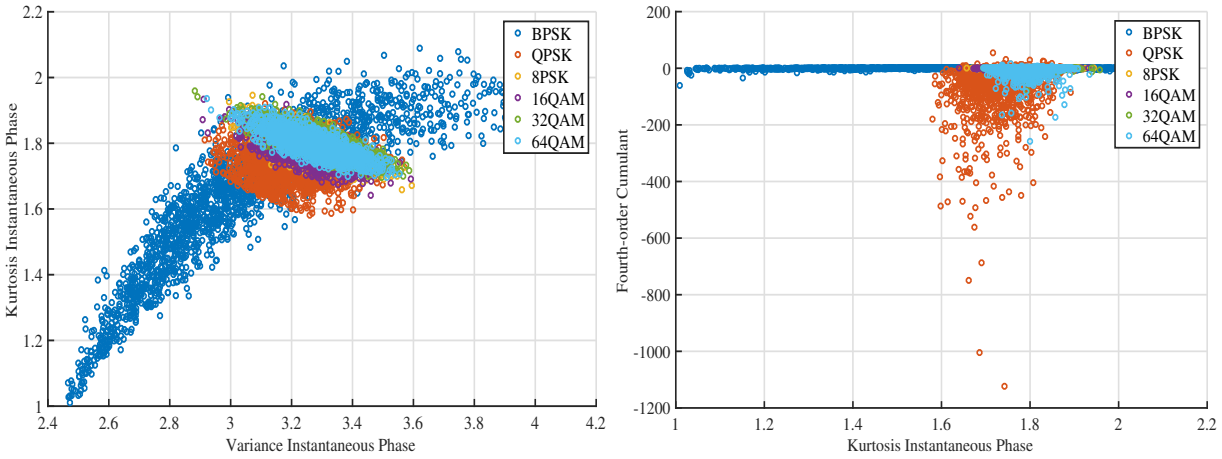

(a) Variance $\theta(t)$ vs Kurtosis $\theta(t)$ (b) Kurtosis $\theta(t)$ vs C_{42} of the received signal

Figure 6.6: Scatterplot: Training feature set for fading channel (60 Hz).

6.3.2 Classifier Performance

Stationary Transmitter and Receiver

The classifier performance is presented in the form of a confusion matrix in Table 6.4 for the stationary transmitter and receiver use-case. From the confusion matrix it is

Table 6.4: Performance of SVM at 0 Hz Doppler shift

Doppler shift	Modulation	BPSK	QPSK	8-PSK	16-QAM	32-QAM	64-QAM
0 Hz	BPSK	99%	-	-	-	-	-
	QPSK	-	90%	9%	≤ 1	-	-
	8PSK	-	1%	99%	≤ 1	-	-
	16QAM	-	1%	6%	89%	≤ 1	4%
	32QAM	-	≤ 1	1%	8%	90%	≤ 1
	64QAM	-	≤ 1	≤ 1	4%	21%	75%

clear that the SVM is capable of distinguishing BPSK modulated signals from the rest with a 99% accuracy. This is to be expected since Figure 6.2(a) and (b) showed that the features clustered nicely together for BPSK.

Figure 6.2(a) showed that the relationship between the variance and the kurtosis of the instantaneous phase distinguishes QPSK from the other modulations. Table 6.4 shows that QPSK signals are correctly classified with a 90% accuracy. Figure 6.2(d) illustrates β's capability to distinguish the PSK modulations from the QAM signals. The classifier accuracy for 16-QAM and 32-QAM is 89% and 90% respectively. For 64-QAM the classifier had difficulty distinguishing it with a 75% classification accuracy.

The confusion matrix does not tell the whole story. Any multipath scattering environment causes ISI, therefore as the constellation size increases, the more overlapping of symbols will take place, and discriminating between QAM modulations becomes increasingly more difficult, as the constellation diagram for the different order of QAM modulations become indistinguishable from each other.

Moving Receiver

The classifier performance is presented in the form of a confusion matrix in Table 6.5 for the different Doppler shifts. Table 6.5 shows the results for 22 Hz, 28 Hz, 57 Hz and 60 Hz respectively. From the different Doppler shifts, it was to be expected that

Table 6.5: Performance of SVM at multiple Doppler shifts

Doppler shift	Modulation	BPSK	QPSK	8-PSK	16-QAM	32-QAM	64-QAM
22 Hz	BPSK	90%	5%	5%	-	-	-
	QPSK	-	86%	14%	≤ 1	-	≤ 1
	8PSK	-	3%	97%	-	-	-
	16QAM	-	≤ 1	4%	80%	16%	≤ 1
	32QAM	-	-	1%	18%	79%	2%
	64QAM	-	-	-	8%	12%	80%
28 Hz	BPSK	87%	7%	6%	-	≤ 1	-
	QPSK	≤ 1	86%	13%	≤ 1	≤ 1	-
	8PSK	≤ 1	3%	97%	≤ 1	-	-
	16QAM	-	3%	1%	86%	2%	8%
	32QAM	-	1%	≤ 1	15%	82%	2%
	64QAM	-	-	-	15%	2%	83%
57 Hz	BPSK	88%	5%	7%	≤ 1	≤ 1	-
	QPSK	1%	73%	26%	≤ 1	-	-
	8PSK	≤ 1	7%	92%	≤ 1	-	-
	16QAM	-	≤ 1	2%	81%	14%	2%
	32QAM	-	-	≤ 1	16%	68%	16%
	64QAM	-	-	≤ 1	8%	29%	63%
60 Hz	BPSK	80%	2%	17%	≤ 1	-	-
	QPSK	2%	90%	5%	2%	1%	≤ 1
	8PSK	1%	≤ 1	98%	1%	-	-
	16QAM	-	-	2%	79%	14%	4%
	32QAM	-	-	≤ 1	18%	63%	19%
	64QAM	-	-	≤ 1	10%	30%	60%

the performance of the SVM would degrade as the Doppler shift increases. This is especially true for (16, 32, 64)-QAM modulations. The classification accuracy for these modulations decreased from 80% to 79%, 79% to 63% and 80% to 60% for 16-, 32-, and 64-QAM respectively.

6.4 Conclusion

This chapter presented an evaluation of the proposed classifier in a multipath fading channel. The performance was evaluated for a stationary transmitter and receiver and then for a moving receiver. The next chapter will focus on the final concluding remarks and proposed recommendations for future work.

Chapter 7

Conclusions and Recommendations

In this chapter, the research work conducted is reflected on. The research goal and objectives are reviewed, and a summary of the work presented is provided. Recommendations for further improvement and areas which require more research are discussed.

7.1 Research Overview

Chapter 1 introduced radio spectrum as a natural resource which needs to be managed. Around the world spectrum regulatory bodies are tasked with managing and assigning spectrum to users. The spectrum is assigned to incumbents based on an auctioning approach. This auctioning approach for managing spectrum leads to under-utilised spectrum, which causes an artificial spectrum scarcity which is called white space.

CR has been proposed as a prime enabler for spectrum reuse in DSA. CR tries to overcome the problem of spectrum scarcity by assigning spectrum to a SU. Spectrum sensing is a crucial element and should be performed first before allowing SU access. AMC has been proposed as an alternative spectrum sensing technique. The ITU-R

proposed a recommendation for identifying digital signals based on a signal's internal and external properties. The internal properties of a signal can only be used when the signal's I/Q data is available.

Chapter 2 presented an overview of some basic data- and telecommunication concepts. Firstly digital-to-analog conversion, digital modulation, signal space models and communication channel models were presented. These concepts were important to understand, as they laid the foundation for understanding AMC.

Chapter 3 introduced the two classification approaches mostly used in AMC: a LB approach and a FB approach. The FB approach received more attention in previous years due to its simplicity regarding implementation, and performance in classification accuracy when paired with a good feature set. Furthermore, Chapter 3 laid the foundation on which a statistical FB classifier were developed. Chapter 3 presented related work on FB classifiers and motivated the selection of the modulation classes and selecting an appropriate feature set. A discussion on machine learning algorithms was presented. The general system model for FB classification was presented and discussed in detail. Chapter 4 continued to the verification and validation of the proposed system model and the implementation thereof.

Chapter 5 presented the methodology for evaluating the statistical feature set in an AWGN channel. After feature evaluation, the final feature set which is used for classification was presented. The performance of a SVM-based classier was evaluated for two use-cases (with and without an SNR estimate). Moreover, Chapter 6 evaluated the performance of the proposed classier in a multipath fading channel. Chapter 6 continued towards testing the performance of the classifier in a stationary transmitter/receiver fading channel.

7.2 Revisiting the Research Question and Objectives

In Section 1.4 it was stated that the research aims to provide a simple approach towards automatically identifying and classifying digital modulations as part of spectrum sensing. The research objectives from Section 1.5 included:

- selecting the type of classification approach (LB or FB),
- comparing the performance of the classifier in different communication channels,
- and testing the performance of the classifier on recorded I/Q data.

The following sections will show how each of these objectives was addressed in the dissertation.

7.2.1 Selecting the Classification Approach

A FB classification approach, which is also known as a pattern-recognition approach, was selected in the dissertation. Chapter 3 presented the motivation for following a FB classification approach instead on a LB approach. The FB approach is easier to implement and not as computationally intensive as the LB approach.

Following a FB classification approach involved investigating two important aspects: the feature extraction process and selecting the classification algorithm. Throughout the literature and related work on this topic, five types of feature classes were identified. From our discussion presented in this chapter, an instantaneous time-domain and HOS feature based approach were selected. From the related work, this presented to be a simple and computationally inexpensive approach. A linear SVM, which is a supervised machine learning approach, showed to be a good selection for the proposed classification algorithm. A SVM has proven to be superior in performance when it comes to a real world problem, and a SVM avoids the problem of overfitting the data points.

From the NFP provided by ICASA, the UHF frequency band was identified to as the frequency band which hosts most of the civilian digital communication services in the country. This included digital television, cellular, navigation, wireless LAN, Bluetooth, trunked radio and satellite broadcasting. Most of these services make use of an M-PSK or M-QAM modulation, either as a single carrier service or as part of the sub-carriers in a multi-carrier modulation such as OFDM. The final modulations included in the modulation set were (2, 4, 8)-PSK and (16, 32, 64)-QAM.

7.2.2 Performance Evaluation in an AWGN and Fading Channel

Chapter 5 presented an extensive investigation to determine an appropriate sample size and frame length to help keep the computational complexity and computational time reasonable. The number of samples proposed was based on calculating the theoretical noise-free normalised fourth-order cumulant of the received signal samples. A sample size between $n = 1000$ and $n = 10000$ was proposed. The frame length of 100 was determined by comparing the time it takes to extract the features from the received samples for a given frame and sample size combination.

Six features were evaluated to find the best feature set which can distinguish between M-PSK and M-QAM modulations. From the instantaneous amplitude and phase, the mean (μ), variance (σ^2), skewness (s), kurtosis (κ), higher order-moments (σ^m), and cumulants (C_{pq}) were evaluated. The signal power key β was also evaluated. The final feature set included the σ^2 of the instantaneous phase, κ of the instantaneous phase, M_{12} of the instantaneous phase, normalised C_{42}, and β. A SVM was trained, and the classification performance was evaluated for two use-cases. It was found that including an SNR estimate as part of the feature set results in a classification accuracy improvement for QPSK and 8-PSK signals only. The classification accuracy for the QPSK modulated signal improved from 83% to 85% at 4 dB. For the 8-PSK modulated signal including an SNR estimate improved the classification accuracy for low SNR from 55% to 67% at 1 dB. For higher SNRs (above 8 dB) the classification accuracy was 100%.

Chapter 6 presented an evaluation of the proposed classifier in a multipath fading channel. The COST 207 channel was implemented for two use-cases: a stationary transmitter and receiver and secondly for a moving receiver (varying the Doppler shift). Four randomly selected DTT channels were selected and four randomly selected carrier frequencies (22 Hz, 28 Hz, 57 Hz and 60 Hz Doppler shift).

An overall classification accuracy of 90% was reported for the stationary case. The overall classification accuracy for the different Doppler shifts were 85 %, 86%, 77.5% and 78%, respectively.

7.2.3 Performance Evaluation using Recorded I/Q Data

Finally, the performance of the classifier is evaluated using raw recorded I/Q data of a TETRA signal at 421 MHz (see future work section 7.3.1). The TETRA 1 standard uses a $\pi/4$-DQPSK modulation. Therefore the expected modulation class is known.

The proposed classifier classified the TETRA signal as a being an 8-PSK modulation. Even though the classification result is incorrect, the classifier was able to tell that a PSK modulation was detected. Further implementation of equalisers to compensate for multipath fading will improve the result as mentioned in section 7.3.1.

7.3 Recommendations for Future Work

The work presented in this dissertation laid a good foundation for future studies on modulation classification. The focus of this research was on using the internal signal characteristics to classify digital signals. Furthermore, the assumption was made that the digital signals have been separated from the analog signals in the UHF frequency band. Many analog services are still operational in the UHF band. Using a signal's external characteristics, such as the carrier frequency, signal bandwidth and spectral shape would aid in discriminating between analog and digital signals in the frequency

band under consideration.

Further improvements can include carrier frequency and bandwidth estimates which can be obtained from an estimated power spectral density [19], baud rate estimation via a tracking loop [19], and constellation independent algorithms can be used to equalise the effect of the pulse shaping filter [19].

Single-carrier modulations were investigated in this study. The next logical step is to incorporate a method for identifying multi-carrier waveforms such as OFDM. The implementation of pulse-shaping filters in the transmitter and receiver chain will help to develop a more robust classifier for real-world implementation. Another recommendation for future work is to find a simple blind equalisation approach to mitigate the effect of multipath fading encountered by the transmitted signal.

Moreover, the performance and robustness of the proposed classifier need to be tested when an *Unknown* parameter is introduced into the set of modulation classes. Currently, the classifier will try to fit the monitored signal into either a PSK or QAM modulation group. When the SNR starts to fall below 5 dB the modulations, especially for QAM modulations, the different modulation orders cannot be uniquely identified. When an unknown class is included as part of the classifier prediction outputs, it will produce a better result. The performance of the classifier needs to be tested in a controlled lab environment generating test signals and modulating them before using real world raw I/Q data.

7.3.1 Evaluating Recorded I/Q data

This section evaluates the performance of the classifier using recorded I/Q data. The recorded I/Q data is provided by GEW Technologies. GEW Technologies provide fixed and mobile RF monitoring and direction finding systems. The Sky-i7000 provides a radio monitoring solution for a frequency range of 9 kHz to 3.6 GHz, with a 20 MHz instantaneous bandwidth. The Sky-i7000 was used to record data in the Constantia area, Cape Town.

TErrestrial Trunked RAdio (TETRA) is a digital trunked mobile radio standard which is developed to meet the needs of traditional Professional Mobile Radio (PMR) [62] organisations such as public safety, transportation, government and military. TETRA supports different carrier frequencies from 380 - 420 MHz in multiples of 25 kHz. The commonly adopted standard is specified in [63]. According to [62], four multilevel modulation schemes have been introduced in the new TETRA 2 architecture. The modulation schemes include $\pi/8$-D8PSK, 4-QAM, 16-QAM and 64-QAM to boost data throughput. The TETRA 1 standard used a $\pi/4$-DQPSK modulation scheme. The channel using QAM modulations are provided with multiple sub-carriers to achieve robust performance in frequency-selective fading channels.

TETRA 1, which is the widely adopted standard, is as single-carrier service with a $\pi/4$-shifted DQPSK modulation with a root-raised cosine modulation filter and a roll-off factor of 0.35 [63]. The $\pi/4$-DQPSK modulation is a QPSK modulated signal with a $\pi/4$ phase-offset. For the above-mentioned reason (TETRA being a single carrier signal), makes it a suitable candidate signal to use for evaluating the performance of the proposed classifier.

The Sky-i7000 uses the PXGF streaming and file format for streaming and storing the I/Q samples. The PXGF streaming and file format provides a framework for streaming and storage of sampled data along with metadata. The PXGF format is loosely based on the Microsoft RIFF file format, which is based on the concept of chunks.

7.3.2 Recorded TETRA Signal

Table 7.1 shows the recording parameters for the TETRA signal:

Table 7.1: PXGF TETRA recording metadata

Parameter	**Value**
Carrier frequency	421.41 MHz
Sample rate	32 kHz
Recorded bandwidth	20 kHz

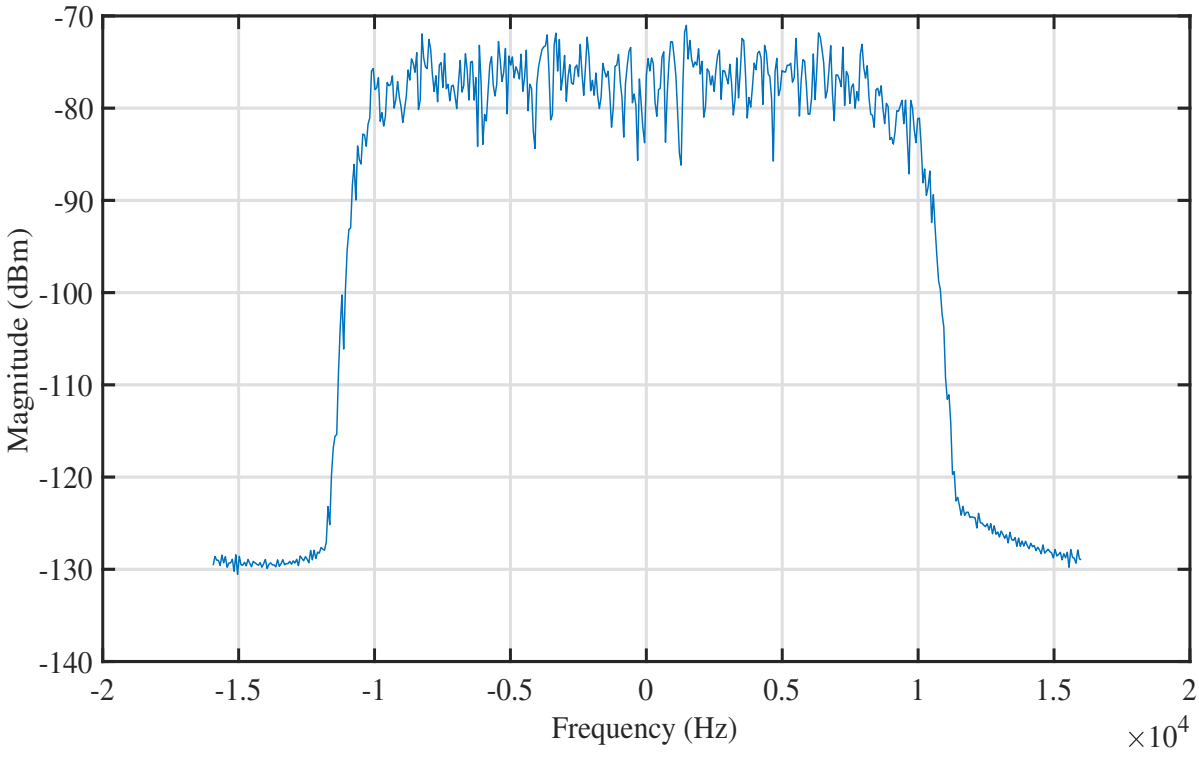

Figure 7.1: PSD plot from the received PXGF samples.

Figure 7.2(a) - (b) show a screen-shot from the Sky-i7000. The Sky-i7000 is tuned to 421.41 MHz and shows the spectrum of the observed signal. A bandwidth of 20 kHz is shown in red. From Figure 7.2(b) it is clear that the signals in view is in the TETRA band. Figure 7.2(b) show four TETRA signals inside a 100 KHz bandwidth (4 $\times$ 25 KHz).

Figure 7.1 is the zero-centered power spectral density plot constructed in MATLAB from the raw recorded I/Q data (without compensating for the antenna losses). The recorded data are raw complex samples received from the ADC. These values need to be scaled appropriately to get the full-scale values. The recording is for a time of 3 seconds, at a sample rate of 32 kHz. This results in a total of 96 000 raw I/Q samples. The 96 000 samples are divided into 100 frames.

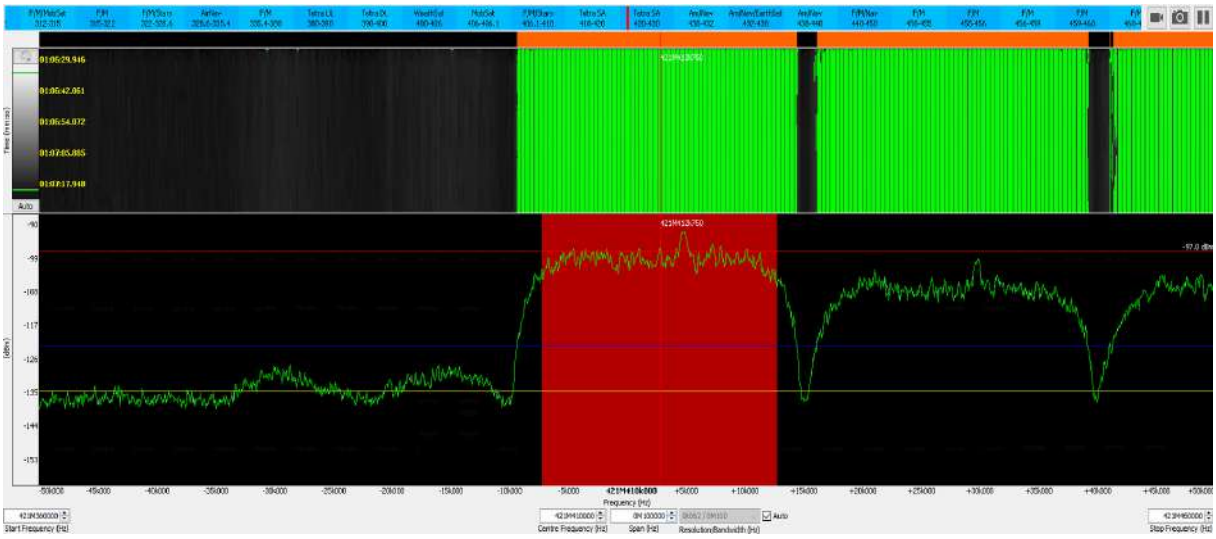

(a) TETRA signal at 421.41 MHz

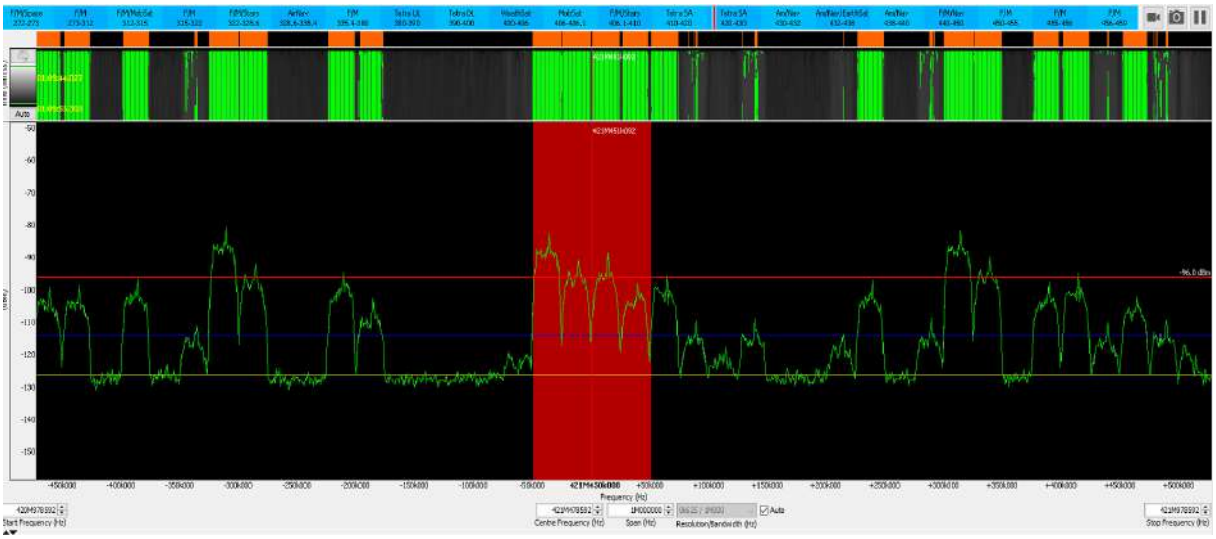

(b) TETRA band showing four TETRA signals.

Figure 7.2: TETRA signal from the Sky-i7000.

7.3.3 TETRA Classification

In this section, the performance of the classifier is evaluated using the recorded TETRA signal. For the purpose of evaluating the classifier, a stationary transmitter and receiver is assumed. The monitoring site has a fixed monitoring receiver. The received signal is compensated for carrier frequency offset (carrier synchronisation).

The recorded signal is recorded in a harsh environment where the effect of multipath propagation is unavoidable, therefore a channel equaliser is needed to compensate for the fading effects. From the TETRA standard mentioned in [63], a pulse-shaping filter is also used for transmission. The proposed multipath classifier does not compensate for any of these effects. However, the classifier is tested to see how it would perform given the recorded samples.

Figure 7.3 shows the constellation diagram for the recorded signal. Through visual inspection, the constellation diagram shows properties of a PSK signal. The effect of the multipath channel is seen. The received samples are scattered throughout the constellation diagram.

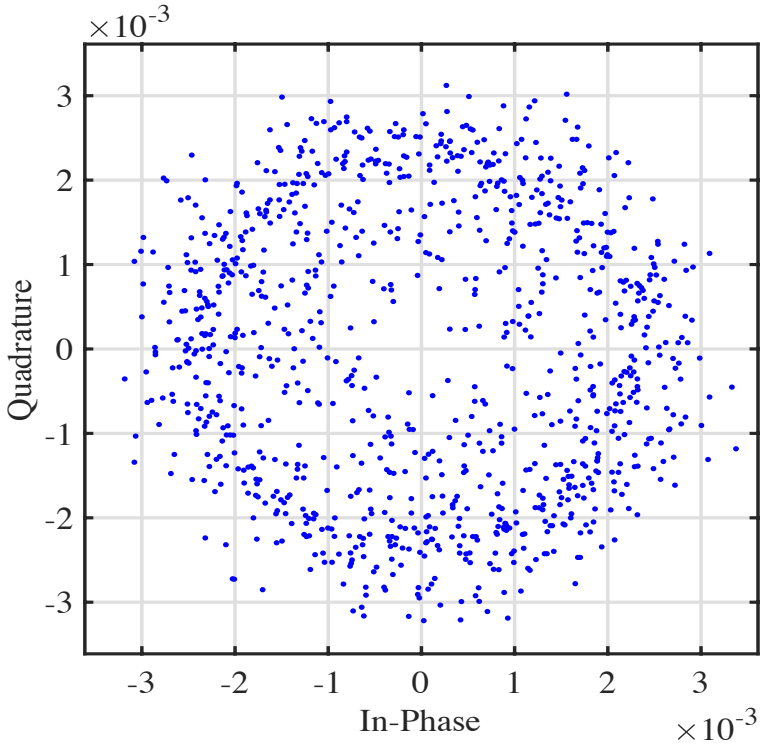

Figure 7.3: Constellation diagram for the recorded signal (one frame).

Figure 7.4 show the output obtained for the modulation classifier for the stationary transmitter and receiver use-case. The classifier analysed 100 frames. From the 100 frames, the classifier classified 99 of the frames as an 8-PSK modulated signal, and one of the frames to be a QPSK signal. From [63] is known that the TETRA 1 stan-

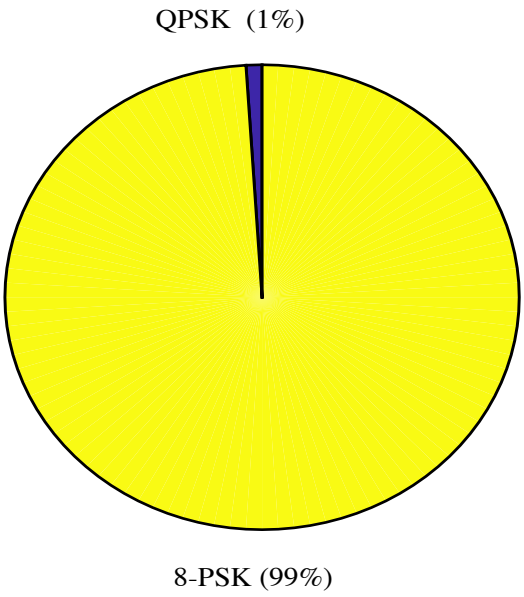

Figure 7.4: Modulation classifier output for the recorded signal.

dard makes use of an $\pi/4$-DQPSK modulation. Even though the classifier could not correctly classify the signal as QPSK, it was possible to place the signal in the PSK modulation group, which is a good result.

From Section 6.3.1 β has shown its ability to separate PSK modulations from QAM modulations. Since a PSK modulation is also defined as a constant modulus modulation, an appropriate equaliser can be implemented to mitigate the effect of multipath fading.

7.4 Conclusion

The research done in this dissertation showed that following a simple FB classification approach to classify M-PSK and M-QAM signals in the UHF frequency band in an AWGN and fading channel proved to have successful classification accuracy.

The work also showed that using HOS extracted from the instantaneous amplitude and phase of the received signal can be used as features to classify the digital modula-

tions. The inclusion of the signal power key β showed to have played a critical role in separating PSK modulated signals from QAM signals. Including carrier synchronisation without channel equalisation does not contribute on its own to mitigate the effect of multipath propagation.

The robustness of the classifier can be improved through the inclusion of equalisers, pulse-shaping filters and multipath channel coefficient estimation, especially for real-world testing and implementation.

Bibliography

[1] B. A. Forouzan, *Data Communications and Networking*. McGraw-Hill, 2013, vol. 1.

[2] A. Goldsmith, *Wireless Communications*. New York: Cambridge University Press, 2005.

[3] Y. K. Cho Kim, *MIMO-OFDM Wireless Communications with MATLAB*.

[4] R. Jain, "Channel Models: A Tutorial, WiMAX Forum AATG," *WiMAX Forum*, pp. 1–21, 2007.

[5] "Final radio frequency spectrum regulations," in *Government Gazette*, Rebuplic of South Africa, 28 June 2013, no. 36336, notice 576.

[6] "Final radio frequency spectrum regulations," in *Government Gazette*, Rebuplic of South Africa, 30 Mar 2015, no. 38641, notice 279.

[7] L. E. Frenzel, *Electronic communication systems*. McGraw-Hill, 2008.

[8] E. Z. Tragos, S. Zeadally, A. G. Fragkiadakis, and V. A. Siris, "Spectrum assignment in cognitive radio networks: A comprehensive survey," *IEEE Communications Surveys and Tutorials*, vol. 15, no. 3, pp. 1108–1135, 2013.

[9] Z. Li, Q. Liao, and A. Striegel, "Toward a socially optimal wireless spectrum management," *2010 5th IEEE Workshop on Networking Technologies for Software Defined Radio Networks, SDR 2010*, pp. 7–12, 2010.

[10] A. M. Wyglinski, M. Nekovee, and T. Hou, *Cognitive Radio Communications and Networks Principles and Practice*. Elsevier Inc., 2010.

[11] Z. Alom, T. K. Godder, and S. Member, "A Survey of Spectrum Sensing Techniques in Cognitive Radio Network," *Proceedings of 2015 3rd International Conference on Advances in Electrical Engineering*, pp. 161–164, 2015.

[12] Z. Zhu and A. K. Nandi, *Automatic Modulation Classification Principles, Algorithms and Applications*, first edit ed. London: Wiley, 2015, vol. 1.

[13] O. Dobre, A. Abdi, Y. Bar-Ness, and W. Su, "Survey of automatic modulation classification techniques: classical approaches and new trends," *IET Communications*, vol. 1, no. 2, pp. 137–156, 2007.

[14] *Technical identification of digital signals*, ITU-R Recommendation SM.1600-2.

[15] M. M. Prakasam, P., "Digital Modulation Identification Model Using Wavelet Transform and Statistical Parameters," *Journal of Computer Systems, Networks, and Communications*, vol. 2008, pp. 1–8, 2008.

[16] H. Hu, J. Song, and Y. Wang, "Signal Classification Based on Spectral Correlation Analysis and SVM in Cognitive Radio," *22nd International Conference on Advanced Information Networking and Applications 2008*, pp. 883–887, 2008.

[17] A.Prochazka, J.Uhlir, P. Rayner, and N. Kingsbury, *Signal Analysis and Prediction*. Springer Science+Business Media, 1998.

[18] A. Hazza, M. Shoaib, S. A. Alshebeili, and A. Fahad, "An overview of feature-based methods for digital modulation classification," *2013 1st International Conference on Communications, Signal Processing, and their Applications (ICCSPA)*, vol. 1, no. 08, pp. 1–6, 2013.

[19] A. Swami and B. M. Sadler, "Hierarchical digital modulation classification using cumulants," *IEEE Transactions on Communications*, vol. 48, no. 3, pp. 416–429, 2000.

[20] M. W. Aslam, S. Member, Z. Zhu, and S. Member, "Combination of Genetic Programming and KNN," *IEEE Transactions on Wireless Communications*, vol. 11, no. 8, pp. 2742–2750, 2012.

[21] B. Picinbono, "On Instantaneous Amplitude and Phase of Signals," *Signal Processing, IEEE Transactions*, vol. 45, no. 3, pp. 552–560, 1997.

[22] W. L. Tranter, K. S. Shanmugan, T. S. Rappaport, and K. L. Kosbar, *Principles of Communication Systems Simulation with Wireless Applications*. Prentice Hall, 2004.

[23] *Guidelines for evaluation of radio transmission technology*, ITU-R Recommendation IMT-2000.

[24] "COST 207 Digital land mobile radio communications," Tech. Rep., 1988.

[25] Rohde & Schwarz, "Fading Channel Simulation in DVB," pp. 1–13.

[26] M. Aslam, Z. Zhu, and A. Nandi, "Automatic digital modulation classification using Genetic Programming with K-Nearest Neighbor," *Military Communications Conference, 2010 - Milcom 2010*, pp. 1731–1736, 2010.

[27] J. J. Popoola, "Effect of training algorithms on performance of a developed automatic modulation classification using artificial neural network," *IEEE Africon*, 2013.

[28] P. Shih and D. C. Chang, "An automatic modulation classification technique using high-order statistics for multipath fading channels," *ITS Telecommunications (ITST), 2011 11th International Conference on transceiver design*, pp. 691–695, 2011.

[29] H. Alharbi, S. Mobien, S. Alshebeili, and F. Alturki, "Automatic modulation classification of digital modulations in presence of HF noise," *EURASIP Journal on Advances in Signal Processing*, vol. 2012, no. 1, p. 1, 2012.

[30] J. J. Popoola and R. V. Olst, "Automatic Classification of Combined Analog and Digital Modulation Schemes using Feedforward Neural Network," *IEEE Africon*, pp. 13–15, 2011.

[31] X. W. Yaqin Z, Guanghui R, "Automatic digital modulation recognition using artificial neural networks," *IEEE*, pp. 257–260, 2003.

[32] E. E. Azzouz and A. K. Nandi, "Automatic identification of digital modulation types," *Signal Processing*, vol. 47, no. 1, pp. 55–69, 1995.

[33] A. D. Pambudi, S. Tjondronegoro, and H. Wijanto, "Statistical properties proposed for blind classification OFDM modulation scheme," *Proceeding - ICARES 2014: 2014 IEEE International Conference on Aerospace Electronics and Remote Sensing Technology*, pp. 89–93, 2014.

[34] H. Gang, L. Jiandong, and L. Donghua, "Study of modulation recognition based on HOCs and SVM," *Vehicular Technology Conference, 2004. VTC 2004-Spring. 2004 IEEE 59th*, vol. 2, no. 60372048, pp. 898 – 902 Vol.2, 2004.

[35] A. Ebrahimzadeh and S. E. Mousavi, "Classification of communications signals using an advanced technique," *Applied Soft Computing Journal*, vol. 11, no. 1, pp. 428–435, 2011.

[36] P. Liu and P.-L. Shui, "A new cumulant estimator in multipath fading channels for digital modulation classification," *IET Communications*, vol. 8, no. 16, pp. 2814–2824, 2014. [Online]. Available: http://digital-library.theiet.org/content/journals/10.1049/iet-com.2014.0175

[37] V. D. Orlic and M. L. Dukic, "Automatic modulation classification algorithm using higher-order cumulants under real-world channel conditions," *IEEE Communications Letters*, vol. 13, no. 12, pp. 917–919, 2009.

[38] H. C. Wu, M. Saquib, and Z. Yun, "Novel automatic modulation classification using cumulant features for communications via multipath channels," *IEEE Transactions on Wireless Communications*, vol. 7, no. 8, pp. 3098–3105, 2008.

[39] F. C. B. F. Muller, C. Cardoso, and A. Klautau, "A front end for discriminative learning in automatic modulation classification," *IEEE Communications Letters*, vol. 15, no. 4, pp. 443–445, 2011.

[40] M. Richterova, "Signal Modulation Recognizer Based on Method of Artificial Neural Networks," *Progress In Electromagnetics Research Symposium*, no. 2, pp. 1–4, 2005.

[41] J. J. Popoola, "Sensing and Detection of a Primary Radio Signal in a Cognitive Radio Environment using Modulation Identification Technique," 2012.

[42] D.-C. Chang and P.-K. Shih, "Cumulants-based modulation classification technique in multipath fading channels," *IET Communications*, vol. 9, no. 6, pp. 828–835, 2015. [Online]. Available: http://digital-library.theiet.org/content/journals/10.1049/iet-com.2014.0773

[43] L. Yang, Z. Ji, X. Xu, X. Dai, and P. Xu, "Modulation classification in multipath fading environments," *Proceedings of 4th IEEE Internatilonal Symposium on Wireless Communication Systems 2007, ISWCS*, pp. 171–174, 2007.

[44] A. E. Zadeh, "Automatic recognition of radio signals using a hybrid intelligent technique," *Expert Systems with Applications*, vol. 37, no. 8, pp. 5803–5812, 2010. [Online]. Available: http://dx.doi.org/10.1016/j.eswa.2010.02.027

[45] Nasdaq, "Excess Kurtosis," 2017. [Online]. Available: www.nasdaq.com/investing/glossary/e/excess-kurtosis

[46] S. Xi and H.-c. Wu, "Robust Automatic Modulation Classification Using Cumulant Features in the Presence of Fading Channels," *Wireless Communications and Networking Conference, 2006*, vol. 00, no. c, pp. 2094–2099, 2006.

[47] ETSI, "ETSI EN 302 755 Digital Video Broadcasting," pp. 1–189, 2011.

[48] "3rd Generation Partnership Project; Technical Specification Group GSM/EDGE Radio Access Network; Radio transmission and reception," 3GPP, Report, 2016.

[49] "3GPP The Mobile Broadband Standard," 2016. [Online]. Available: http://www.3gpp.org/technologies/keywords-acronyms/98-lte

[50] "Spread spectrum and code modulation of gps carrier," 2017. [Online]. Available: https://www.e-education.psu.edu/geog862/node/1753

[51] M. Bkassiny, Y. Li, and S. K. Jayaweera, "A survey on machine-learning techniques in cognitive radios," *IEEE Communications Surveys and Tutorials*, vol. 15, no. 3, pp. 1136–1159, 2013.

[52] "Machine learning: A review of classification and combining techniques," *Artificial Intelligence Review*, vol. 26, no. 3, pp. 159–190, 2006.

[53] N. Seliya, T. M. Khoshgoftaar, and J. Van Hulse, "A study on the relationships of classifier performance metrics," *Proceedings - International Conference on Tools with Artificial Intelligence, ICTAI*, pp. 59–66, 2009.

[54] Y. Jiao, "Performance measures in evaluating machine learning based bioinformatics predictors for classifications," *Quantitative Biology*, vol. 4, no. 4, pp. 320–330, 2016. [Online]. Available: https://findit.dtu.dk/en/catalog/2349331144

[55] "Mathworks MATLAB R2018a Documentation - Control random number generation," 2018. [Online]. Available: https://www.mathworks.com/help/matlab/ref/rng.html?searchHighlight=Mersenne%20Twister&s_tid=doc_srchtitle

[56] R. G. Sargent, "Proceedings of the 2010 Winter Simulation Conference B. Johansson, S. Jain, J. Montoya-Torres, J. Hugan, and E. Yücesan, eds." *Simulation*, no. 2001, pp. 135–150, 2010. [Online]. Available: http://www.informs-sim.org/wsc10papers/014.pdf

[57] J. P. C. Kleijnen, "Sensitivity analysis and optimization in simulation: design of experiments and case studies," *Simulation Conference Proceedings, 1995. Winter*, no. i, pp. 133–140, 1995.

[58] R. Johnson, "MATLAB Programming Style Guidelines," Tech. Rep. October, 2002. [Online]. Available: http://www.datatool.com/downloads/MatlabStyle2%20book.pdf

[59] H. Mathis, "On the Kurtosis of Digitally Modulated Signals with Timing Offsets," pp. 86–89, 2001.

[60] B. Kim, J. Kim, H. Chae, D. Yoon, and J. W. Choi, "Deep Neural Network-based Automatic Modulation Classification Technique," pp. 579–582, 2016.

[61] Rohde & Schwarz, "Fading Channel Simulation in DVB," pp. 1–13.

[62] “TR 102 300-7 - V1.2.1 - Terrestrial Trunked Radio (TETRA); Voice plus Data (V+D): Designers’ guide; Part 7: TETRA High-Speed Data (HSD); TETRA Enhanced Data Service (TEDS),” ETSI, Report, 2016.

[63] “Terrestrial Trunked Radio (TETRA); VoiceplusData(V+D); Part 2: Air Interface (AI),” ETSI, 2001.

Appendix A

Research Publications

A.1 SATNAC 2016 Work-in-progress Paper

A work-in-progress paper presented on *Statistical Feature Extraction for Automatic Modulation Classification* which appeared in the proceedings of Southern Africa Telecommunication Networks and Applications Conference (SATNAC) for 2016.

A.2 SATNAC 2017 Paper

Peer reviewed article presented on *Statistical Feature Evaluation for Automatic Modulation Classification* which appeared in the proceedings of SATNAC for 2017.

Statistical Feature Extraction for Automatic Modulation Classification

Herman Blackie, Melvin Ferreira
TeleNet Research Group
School of Electrical, Electronic and Computer Engineering
North-West University, Potchefstroom Campus, South Africa
Email: 23377852@student.nwu.ac.za, melvin.ferreira@nwu.ac.za

***Abstract*—This paper presents a statistical feature extraction based approach to Automatic Modulation Classification (AMC). First order statistical features are extracted from two digitally modulated signals to confirm whether these features can be used to distinguish between the signals. Furthermore, the paper presents an outline of our work which is done towards classifying modulated signals, after which the performance of current classification techniques are tested on measured In-phase and Quadrature (I/Q) data.**

***Index Terms*—Automatic Modulation Classification, feature-based classification, statistical features**

I. Introduction

With the current increase in bandwidth and subsequent spectrum usage, modulation schemes employed in telecommunication systems have become more complex. To accommodate more bandwidth, the modulation schemes must make use of the available spectrum more efficiently. This increase in modulation scheme complexity has changed the way modulated waveforms can be reliably and accurately detected and classified. AMC is the intermediate step between signal detection and information recovery. An Automatic Modulation Classifier is a system that can identify the modulation type of a received signal. Once the modulation scheme of the received signal has been identified, the appropriate demodulator can be selected.

AMC plays an important role in various civilian and military applications [1], [2], [3], [4] such as signal confirmation, interference identification, surveillance, monitoring, spectrum management, electronic warfare signal intelligence, counter channel jamming, and threat analysis. Blind classification in AMC plays an important role in Software Define Radio (SDR) and Cognitive Radio (CR). In an ideal vision of a CR, the future system must be able to sense signals present in the spectrum and classify the signals automatically for efficient usage of spectral resources.

Therefore, the bigger challenge lies in using current classifiers or new combinations of classification techniques to classify modulated signals using practical I/Q data. The focus of this paper is to extract first order statistical features to see whether it is possible to distinguish between BPSK and QPSK modulated signals as an initial result.

The remainder of this paper is organized as follows. Section II provides the reader background followed by Section III which provides related work in AMC followed by the proposed research methodology in Section IV. Section V will present our initial results in distinguishing between different modulations. Lastly, the initial result is discussed with future work in Section VI and VII respectively.

II. Background

AMC can be divided into two groups [4], [3]; a decision-theoretic approach and pattern recognition approach. Decision-theoretic approach is known as Likelihood-based (LB) classifiers and pattern recognition approach is known as Feature-based (FB) classifiers. LB classifiers are more accurate than FB classifiers, however LB classifiers are computationally complex [4]. On the other hand, FB classifiers are easier to implement with near-optimal performance when designed properly [5].

The pattern recognition approach is composed of two subsystems. The first subsystem is for feature extraction, and secondly a pattern recognizer to process the features. The extracted feature set must be able to represent the signal information present in the modulated signal. The extracted features are then compared to a threshold or used as input to train an Artificial Neural Network (ANN) to classify the modulations [5] according to a decision rule.

According to [4], there are three FB algorithms used to distinguish between modulations. This includes instantaneous amplitude, phase and frequency-based algorithms, wavelet transform-based algorithms and signal statistics-based algorithms. In [6], a compressive sampling-based algorithm is introduced. In [5], [7], [8], feature extraction comprises of two basic steps. The received signal is captured and then converted to the appropriate domain through transforms such as wavelet (WT)-, discrete Fourier (DFT)-, discrete cosine (DCT)- and discrete sine-transforms (DST) [9].

The features are extracted from the relevant domain to distinguish between the modulation classes. These features are then either from a higher order statistical nature (cumulants, moments, mean, variance, skewness, kurtosis index) or first order (instantaneous amplitude, phase and frequency) [4].

III. Related Work

Wong et. al. [10] introduced AMC using ANN to classify modulations using a feature set of higher-order statistics (HOS). In [10] is mentioned that HOS are not affected by Additive White Gaussian Noise (AWGN). HOS provide a good way to obtain features to illustrate the two-dimensional probability density function (PDF), i.e. the constellation diagram. Wong [10] recorded a 99% successful classification at Signal-to-Noise Ratio (SNR) as low as 0 dB. Pambudi

et. al. [11] used five statistical properties to classify OFDM modulated signals in a NLOS (Non-Line-Of-Sight) scheme, with six multipath components. In [11], an FFT is performed on the received signal. The output of the FFT process is extracted to get the statistical properties such as, mean, variance, skewness, kurtosis index and moment order for three possible different modulation schemes (64-QAM, 16-QAM and QPSK). The mean, skewness and kurtosis index are the first, third and fourth order moment of the received OFDM signal magnitude. Popoola et. al. [12] derived statistical features from the instantaneous amplitude, phase, and frequency of the simulated modulated signal and used as input to an ANN classifier. In literature surveyed from [1] – [12] the communication channel and transmission of modulated signals over the channel is simulated. Therefore, a proposed area for further research is to use measured I/Q data to test the performance of classifiers.

IV. Proposed Methodology

As mentioned in Section I, current classifiers or a new combination of classification techniques will be used to classify different modulated signals. An intensive literature study is done to gain an understanding of current classification techniques. For a first iteration a simple simulation model is created and the model complexity will gradually be increased. The features are extracted and used as input for the classier. An artificial intelligence approach such as ANN may be considered to classify the modulations. After evaluating the performance of the classifier using simulated I/Q data, recorded I/Q data will be used as input for the classier to test the performance of the classier against real data.

V. Initial Results and Discussion

As an initial approach, first order statistics are used to distinguish between BPSK and QPSK. The simulation is developed in *MATLAB* and simulates a AWGN communication channel. A random bit stream is generated and modulated using BPSK and QPSK. From the constellation diagram of BPSK and QPSK, their complex valued samples (I/Q streams) are separated into two vectors; the magnitude components ρ and the phase components θ. If each sample can be expressed as $z = a + jb$, and z represents a sample value, then $\rho = \sqrt{a^2 + b^2}$ and $\theta = tan^{-1}(b/a)$, where a is the in-phase (I) component and b is the quadrature component (Q) of the signal. Fig. 1 shows the distribution (histogram) plot of the ρ and θ components.

VI. Conclusion and Future Work

From Fig.1 it can be concluded that BPSK and QPSK modulated signals show no unique differences in their magnitude distributions as expected. From the phase distribution, a clear distinction can be made between BPSK and QPSK. BPSK shows two groupings at 0 rad and π rad, whereas QPSK shows four groupings at $\pm\pi/4$ and $\pm 3/4\pi$ rad. Therefore, the histogram of the phase distribution of the modulated signals can be used to distinguish between BPSK and QPSK.

For future work, more modulation schemes will be added to the simulation model. Different noise models will be added to the channel model to simulate a wireless channel of increasing complexity. This will include fading channels and multipath effects and not just Gaussian noise. The feature set will be expanded to include more features, after which the automation of the classification process will be employed. This approach postulates to be easier to implement with a decrease in computational complexity.

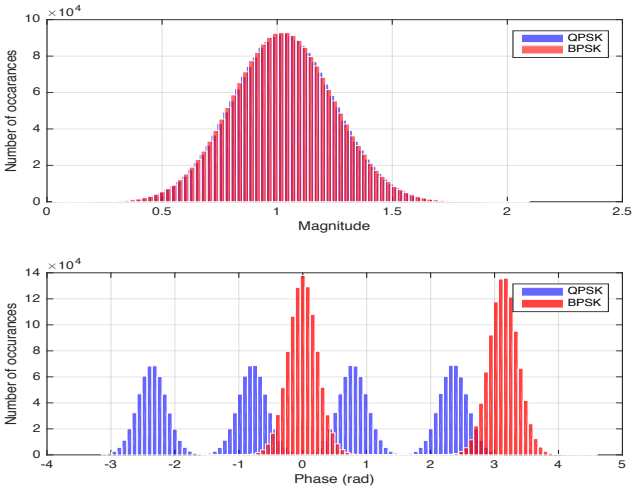

Fig. 1. Magnitude and phase distribution of a BPSK and QPSK signal at an SNR of 10 dB.

References

[1] E. E. Azzouz and A. K. Nandi, "Automatic identification of digital modulation types," *Signal Processing*, vol. 47, no. 1, pp. 55–69, 1995.

[2] N. Madhavan, A. P. Vinod, A. S. Madhukumar, and A. K. Krishna, "Spectrum sensing and modulation classification for cognitive radios using cumulants based on fractional lower order statistics," *AEU - International Journal of Electronics and Communications*, vol. 67, no. 6, pp. 479–490, 2013.

[3] Z. Zhu and A. K. Nandi, *Automatic Modulation Classification Principles, Algorithms and Applications*, first edit ed. London: Wiley, 2015, vol. 1.

[4] O. Dobre, A. Abdi, Y. Bar-Ness, and W. Su, "Survey of automatic modulation classification techniques: classical approaches and new trends," *IET Communications*, vol. 1, no. 2, pp. 137–156, 2007.

[5] J. J. Popoola, "Effect of training algorithms on performance of a developed automatic modulation classification using artificial neural network," 2013.

[6] Z. Sun, S. Wang, and X. Chen, "Feature-Based Digital Modulation Recognition Using Compressive Sampling," *Mobile Information Systems*, vol. 2016, pp. 1–10, 2016.

[7] P. Prakasam and M. Madheswaran, "Digital Modulation Identification Model Using Wavelet Transform and Statistical Parameters," *Journal of Computer Systems, Networks, and Communications*, vol. 2008, pp. 1–8, 2008.

[8] A. Nandi and E. Azzouz, "Modulation recognition using artificial neural networks," *Signal Processing*, vol. 56, no. 2, pp. 165–175, 1997.

[9] R. M. Al-makhlasawy, M. M. Abd, and H. A. El-khobby, "Automatic Modulation Recognition in OFDM Systems using Cepstral Analysis and a Fuzzy Logic Interface," pp. 56–62, 2012.

[10] M. L. D. Wong and A. K. Nandi, "Automatic digital modulation recognition using artificial neural network and genetic algorithm," *Signal Processing*, vol. 84, no. 2, pp. 351–365, 2004.

[11] A. D. Pambudi, S. Tjondronegoro, and H. Wijanto, "Statistical properties proposed for blind classification OFDM modulation scheme," *Proceeding - ICARES 2014: 2014 IEEE International Conference on Aerospace Electronics and Remote Sensing Technology*, pp. 89–93, 2014.

[12] J. J. Popoola and R. V. Olst, "Automatic classification of combined analog and digital modulation schemes using feedforward neural network," *IEEE Africon*, no. September, pp. 13–15, 2011.

Herman Blackie is a student pursuing an M.Eng in Computer Engineering at the North-West University. He received his B.Eng in 2015 from the North-West University. His research interests include spectrum monitoring and sensing.

Statistical Feature Evaluation for Automatic Modulation Classification

Herman Blackie, Melvin Ferreira
School of Electrical, Electronic and Computer Engineering
[1]23377852@student.g.nwu.ac.za
[2]melvin.ferreira@nwu.ac.za
North-West University, Potchefstroom Campus, South Africa

***Abstract*—This paper presents an investigative study towards a simple approach of classifying M-ary PSK and M-ary QAM signals, in an Additive White Gaussian Noise (AWGN) channel. Our ultimate aim is to evaluate the possibility of implementing a modulation classifier on commodity hardware (such as a single-board computer), to perform feature extraction or classification on the hardware. The feature set must therefore be simple to derive, and must not be computationally complex. A set of statistical features are evaluated which are derived from the received signal's instantaneous amplitude and phase. The results obtained are compared to each other to see which of the features are able to distinguish the modulations from each other in a noisy environment. A Support Vector Machine (SVM) is trained to classify modulations with the proposed feature set. Experimental results indicate that our approach has a high percentage of correct classification at low Signal-to-Noise Ratio (SNR).**

***Index Terms*—Automatic Modulation Classification, M-PSK, M-QAM, higher-order statistics, feature based classification**

I. Introduction

An Automatic Modulation Classification (AMC) system detects the unknown modulation type of a received signal with the purpose to demodulate the signal and retrieve its information content. AMC plays an important role in military and civilian applications such as signal confirmation, interference identification, surveillance, monitoring, spectrum management, counter channel jamming and signal intelligence [1], [2]. Future Software Defined Radio (SDR) and Cognitive Radio (CR) systems must be able to sense the spectrum for signals present in the pursuit of Dynamic Spectrum Access (DSA). This interest in increasing spectrum access and improving spectrum efficiency, combined with SDR and new realisations that machine learning can be applied [1] to radios, have created interesting possibilities. Two general classes of AMC algorithms exist: Likelihood-based (LB) and Feature-based (FB) classifiers.

Many features have been proposed in classifying modulations, ranging from instantaneous amplitude, phase and frequency, Fourier and Wavelet transform features, higher-order statistics, cyclic cumulants, constellation shape recovery, probability density function based methods and unsupervised clustering [3], [4].

In this paper, an investigative study is presented to find a simple approach to classifying M-ary PSK and M-ary QAM signals by using statistical properties as features in an AWGN channel. The mean value, variance, skewness, kurtosis, moment-order and higher-order cumulants of the received signal's instantaneous amplitude and phase are evaluated, and the most appropriate set of statistical properties are used to classify the modulations. The ultimate goal is to implement a modulation classifier onto cheap commodity hardware, which does not necessary have access to high processing power, and without the need to perform complex domain transforms.

The remainder of the paper is organised as follows. In Section II a brief background on AMC, machine learning classifiers and communication channels are presented. Section III provides related work, followed by our system model in Section IV. Section V gives our experimental methodology, Section VI discusses the results, and finally Section VII concludes the paper.

II. Background

A. Automatic Modulation Classification Approaches

In an ideal AMC system, a tradeoff must be made between classification accuracy, robustness against unpredictable channel conditions, computational efficiency and versatility in terms of modulation types [1]. When developing a AMC system, two steps are involved [1], [5]: pre-processing of the received signal and the selection of classification algorithm. Two main classification approaches have been studied in this regard [1], [2], [3], [4], [6]; a decision-theoretic approach and a pattern recognition approach. Decision theoretic approach is known as LB classifiers [7] and pattern recognition approach is known as [8] FB classifiers.

LB classifiers are by far the most popular approach, which is motivated by the optimality of its classification accuracy, when channel conditions are perfectly characterised. LB classifiers treat the classification problem as a hypothesis testing problem. The likelihood function of the received signal is compared to a predetermined threshold for decision making. The requirement of a threshold adds another layer of performance improvement, but more tentative efforts must be made to select the thresholds. Even though LB classifiers are a more suitable solution, it suffers from computational complexity and is difficult to implement as complete knowledge of the recevied signal's probability density function must be known to derive the likelihood function of the signal. Some of the LB classifiers studied in literature [1], [3] include machine learning (ML), Average likelihood ratio test (ALRT), Generalized likelihood ratio test (GLRT), and Hybrid likelihood ratio test (HLRT).

The FB classification approach is much easier to implement and is not as computationally complex as the LB approach. The selection of suitable features and classification algorithm is the challenge. FB classifiers can be divided into two subsystems; the feature extraction subsystem and the classifier subsystem, shown conceptually in Fig. 1. Several features are extracted from the received signal and a decision is made based on the values of those features. The features

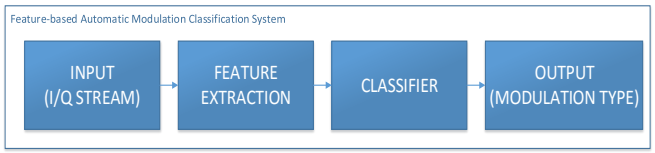

Fig. 1. Conceptual feature-based classification approach

extracted must be able to represent the difference between signal classes. The features are either instantaneous amplitude, frequency and phase, Fourier and Wavelet transform based or higher-order statistic (moments and cumulants) based. Similarly, Hazza et al. [4] showed that many combinations of classification algorithms and features have been used to solve the classification problem.

B. Machine Learning Classifiers

Various machine learning techniques have been employed to simplify the decision-making process and to reduce the dimension of the feature set, while at the same time maintaining a classification algorithm which is computationally efficient.

1) Artificial Neural Networks: Neural networks solve what is known as a supervised regression and classification problems. The model takes input and output data to find the connection between them. Neural networks are a computational approach which tries to mimic the way a biological brain solves problems. It is characterised by its pattern of connections between neurons [9].

2) Support Vector Machines: The concept of a support vector machine revolves around the idea of a "margin" either side of a hyperplane that separates data classes [9]. The goal is to maximise the margin by creating the largest possible distance between the separating hyperplane and the instances on either side. A higher-dimensional space, also known as the feature space can be used to define a hyperplane in higher dimensions to separate classes which cannot be separated otherwise. Linear and non-linear algorithms exist to define the hyperplane.

3) k-Nearest Neighbour: The k-Nearest Neighbour (KNN) classification approach is based on the principle that the instances within a dataset will generally exist in close proximity to other instances with the same properties [9]. The training dataset is vectors in a multidimensional feature space, with its class label. An unclassified instance can be labeled by observing the class of its nearest neighbors. *k* is a user-defined constant, and the unlabelled instance is classified by assigning the label which is most frequent among the k training samples. KNN are sensitive to the choice of the similarity function used to compare instances. Many algorithms exist which calculates the best possible value for *k*.

In [1] Zhu et al stated that SVM only needs the training data when establishing the separating hyperplane. The training signal is not involved in any further calculation after training, therefore the testing stage is relatively inexpensive, compared with KNN, with regards to computations, which makes it suitable for implementing on commodity hardware.

C. Communication Channels

Two of the commonly used communication channel models used to evauluate AMC are the AWGN channel and the Rayleigh- and Rician multipath fading channels. AWGN is added noise that might be intrinsic to the information systems [10], [11]. This type of noise is caused by external sources such as atmospheric conditions, extraterrestrial sources (solar, cosmic), and internal noise at the receiver. Internal noise includes thermal noise, reflections caused by transmission line impedance mismatching, etc. The term white refers to the idea that the noise has uniform power across the frequency band (constant spectral density) and a Gaussian distribution of amplitude.

Rayleigh- and Rician channels [11] falls within the class of small-scale fading (rapid variations of the signal levels due to the constructive and destructive interference of multiple signal paths due to shadowing, reflection, refractions). Fading in the broad sense causes variations of the signal amplitude over time and frequency. In general, any wireless channel is subject to line-of-sight (LOS) and non line-of-sight (NLOS) propagation. The probability density function (PDF) of a signal received in a LOS environment follows a Rician distribution, while that in a NLOS environment follows a Rayleigh distribution [11].

The strongest scattering component usually corresponds to the LOS component (specular component). All the other components are NLOS components.

In (1) the PDF of a Rician channel is expressed, where $\widetilde{p}(\theta)$ denotes the PDF of angle of arrival (AoA) for the scattering components and θ_0 denotes the AoA for the specular component [11] .

$$p(\theta) = \frac{1}{K+1}\widetilde{p}(\theta) + \frac{K}{K+1}\delta(\theta - \theta_0) \tag{1}$$

K is defined as the Rician factor, which denotes the strength of the LOS component.

$$K = \frac{c^2}{2\sigma^2} \tag{2}$$

where c^2 is the power of the LOS component and $2\sigma^2$ is the power of the scattering component. A Rician channel approaches an AWGN channel as $K >> 0dB$ and a Rayleigh channel as $K < 0dB$.

III. Related Work

Table I gives a summary of related feature based classifiers with higher-order signal statistics as features.

In [12] Ebrahimzadeh et al. achieved a classification accuracy of 83.23%, 88.23%, 93.62%, 96.14%, and 97.82% at -3, 0, 3, 6 and 9 dB SNR respectively, through a particle swarm optimisation algorithm, to enhance the classification performance of a radial-basis function neural network. In [6] Shih et al. used a decision tree classification approach, which achieved a classification accuracy of 95% for a SNR lower than 10 dB, and 100% for a SNR over 15 dB.

Aslam et al. [5] introduced a Genetic Programming (GP) and KNN classification approach. A classification accuracy of 81% at a SNR of 5 dB with a sample size of 1024 using a KNN classifier was advised. Combining KNN with GP a

TABLE I
A SUMMARY OF RELATED WORK

Author(s)	Features	Modulations	Channel
Ebrahimzadeh [12] et al.	HOS (moments, cumulants up to order eight)	ASK2, ASK4, [2, 4, 8]-PSK [8, 16, 32, 64, 128]-QAM	AWGN
Shih et al. [6]	Fourth-order cumulants	BPSK, QPSK, 8PSK, 16QAM, 64-QAM	AWGN, Rayleigh
Aslam et al. [5]	Fourth- and sixth order cumulants	BPSK, QPSK, 16QAM, 64QAM	AWGN
Pambudi et al. [13]	Mean, variance, skewness, kurtosis, HOS	QPSK, 16QAM, 64QAM, OFDM	Rayleigh
Prakasam et al. [14]	Wavelet transform, mean, variance	M-ary PSK, M-ary QAM, GMSK, M-ary FSK	AWGN

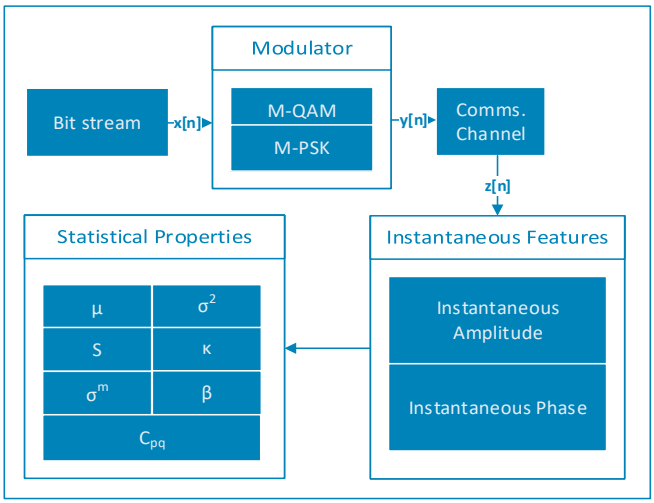

Fig. 2. M-PSK and M-QAM generation and statistical feature extraction

performance increase of 7% were achieved. At a SNR of 15 dB an accuracy of 97% with 1024 samples were achieved.

Pambudi et al. [13] concluded that the variance, skewness, and kurtosis were able to distinguish QPSK subcarriers in an OFDM system from 16QAM and 64QAM. Higher-order moment 10, 14, 18 and 20 were able to distinguish 16QAM from 64QAM.

Prakasam et al. [14] used a Wavelet transform and statistical parameters A SNR lower bound of 5 dB produced a classification accuracy of 96.8%. A decision tree approach was followed. More related work is found in [3] and [4] gives a survey of AMC techniques, approaches and trends, and an overview of the different feature based methods respectively.

Our approach simplifies the feature extraction process by combining first, second, third and fourth-order moments (which is simple to compute) with higher-order moments and cumulants to characterise M-ary PSK and M-ary QAM signals. The smallest number of features are chosen, which are able to distinguish between the modulation in low SNR.

IV. SYSTEM MODEL

A mathematical expression of the signal model and features are presented. Fig. 2 shows a high-level implementation of the feature extraction block shown conceptually in Fig. 1.

In Fig 2 [13] the generation of M-ary PSK and M-ary QAM signals are shown, with the implementation of the statistical feature extraction. The input bit stream $x[n]$ is modulated by PSK and QAM, which results in complex symbols. The transmitted signal $y[n]$ is corrupted by AWGN channel, producing the received signal $z[n]$.

Baseband modulation produces the complex envelope $y[n]$ of the message signal $x[n]$, and $y[n]$ is a complex-valued signal that is related to the output of a passband modulator,

$$Y_1(t)cos(2\pi f_c t + \theta) - Y_2(t)sin(2\pi f_c t + \theta), \quad (3)$$

where f_c is the carrier frequency, θ is the carrier signal's initial phase. The baseband signal is equal to the real part of

$$[(Y_1(t) + jY_2(t))e^{j\theta}]exp(j2\pi f_c t) \quad (4)$$

which is

$$[(Y_1(t) + jY_2(t))e^{j\theta}], \quad (5)$$

and the complex vector $y[n]$ is a sampling vector of the complex signal.

If $s(t)$ is an analytical signal (complex valued signal) in the polar form of

$$s(t) = a(t)e^{j\theta(t)}, \quad (6)$$

$a(t)$ is the instantaneous amplitude of the signal and $\theta(t)$ is the instantaneous phase. The instantaneous amplitude is normalised (A_n) to eliminate the effect of bit energy for modulations with a higher power content such as M-ary QAM signals.

The received signal $z[n]$ is processed to extract the instantaneous amplitude and phase from the signal. The instantaneous amplitude and phase are used to extract the statistical features such as the mean (μ), variance (σ^2), skewness (s), kurtosis (κ), higher order-moments (σ^m), signal power key (β) and cumulants (C_{pq}).

These features allows characterisation of each modulations' respective PDF. Each modulation can be classified based on their respective distributions. When the signal shows Gaussian characteristics, it can be fully described using the first and second order moments (mean and variance). A non-Gaussian signal needs higher-order statistics to fully characterise it. Each feature is expressed mathematically as follows:

The first feature is mean of the received signal components, also know as the first order moment, denoted as

$$\mu(x) = \frac{1}{N}\sum_{i=0}^{N-1} x_i \quad (7)$$

where N is the total number of samples and x_i is the sample value at i. The second feature is the variance of the received signal components, which is the second order moment.

$$\sigma^2(x) = \frac{1}{N}\sum_{n=0}^{N-1}(x_i - \mu)^2 \quad (8)$$

The third feature is the called the skewness, which is the third order moment, and expressed mathematically as

$$s(x) = \frac{1}{\sigma^3}\frac{\sum_{n=0}^{N-1}(x_i-\mu)^3}{N}. \quad (9)$$

The fourth feature is the kurtosis or the fourth-order moment of the received signal's components,

$$\kappa(x) = \frac{1}{\sigma^4}\frac{\sum_{n=0}^{N-1}(x_i-\mu)^4}{N}. \quad (10)$$

The fifth feature extracted is the higher order-moment

$$\sigma^m(x) = \frac{1}{N}\sum_{n=0}^{N-1}(x_i-\mu)^m \quad (11)$$

where m is the moment order. Another usefull feature is the cumulants of a random variable. The advantage of cumulants over moments is its benefit to recognize Gaussian and non-Gaussian signals [15]. When signals are non-Gaussian the first two moments do not define their PDF and therefore higher-order statistics (order greater than two) can reveal other information about the signal that second-order statistics cannot. Ideally the entire PDF is needed to characterise a non-Gaussian signal. Cumulants of order three or higher of Gaussian noise vanishes completely. The bispectrum of a non-Gaussian signal will filter out the Gaussian noise part and consequently will represent only third-order and higher cumulants of the signal. Bispectrum is a statistic used to search for non-linear interactions, also known as the Fourier transform of the third-order cumulant generating function.

According to [15], the cumulative distribution function (CDF) of a random variable x, denoted by $F(x)$. The central moment about the mean of order v of x is

$$\mu_v = \int_{-\infty}^{\infty}(x-m)^v dF, \quad (12)$$

where $v = 1, 2, 3, 4, ...$ and m is the mean of x. Next one can introduce the characteristic function

$$\phi(t) = \int_{-\infty}^{\infty} exp(jtx)dF = \sum_{v=0}^{\infty}\mu_v(jt)^v/v!, \ \forall\mathbb{R}\in t \quad (13)$$

where $j=\sqrt{-1}$, $exp(x)$ is the exponential function, and μ_v is the moment of order v about the origin. The coefficients of $(jt)^v/v!$ is the power series Taylor expansion of the characteristic function $\phi(t)$, which is the moments of a random variable [15]. The moments are a set of descriptive constants of a distribution. Under certain conditions, moments are not capable of fully describing a distribution, where cumulants have the ability to do so. Cumulants make up another set of constants.

In [15] cumulants are expressed as,

$$\phi(t) = \int_{-\infty}^{\infty} exp(jtx)dF = exp\left\{\sum_{v=1}^{\infty}C_v(jt)^v/v!\right\}$$

where C_v is the cumulants of x. C_v is the coefficients of $(jt)^v/v!$ in the power series Taylor expansion of the natural logarithm of the characteristic function $\phi(t)$, or $\ln\phi(t)$. The moments of a complex random variable (auto-moment [12]) is given as

$$M_{pq} = E[s^{p-q}(s^*)^q] \quad (15)$$

and the cumulans are expressed in the general form of

$$Cum[s_1,...,s_n] = \sum_{\forall v}(-1)^{q-1}!E\left\{\prod_{j\in v_1}s_j\right\}..!E\left\{\prod_{j\in v_q}s_j\right\} \quad (16)$$

where p is the moment order and s^* is the complex conjugate of s, and $s = a+jb$ with a zero-mean discrete signal sequence.

According to [5] the higher fourth-order cumulants can be expressed in one of three possible ways,

$$\begin{aligned} C_{40} &= cum(y(n),y(n),y(n),y(n)) \\ &= M_{40} - 3M_{20}^2 \\ C_{41} &= cum(y(n),y(n),y(n),y(n)^*) \\ &= M_{40} - 3M_{20}M_{21} \\ C_{42} &= cum(y(n),y(n),y(n)^*,y(n)^*) \\ &= M_{42} - |M_{20}|^2 - 2M_{21}^2 \end{aligned} \quad (17)$$

Our sixth feature is the ratio between the absolute value of the ratio of C_{40} and C_{42}. This feature was introduced by [6] to distinguish between 8PSK and QPSK modulated signals. Another useful feature is the signal power key, β. This feature is used to differentiate between a signal with complex and real signal components.

$$\beta = \frac{\sum_{n=0}^{N} r_Q[n]^2}{\sum_{n=0}^{N} r_I[n]^2} \quad (18)$$

where $r_Q[n]$ and $r_I[n]$ are the quadrature and in-phase components of the signal respectively [2].

V. Methodology

Two simulation experiments are conducted in this section. The first experiment evaluates the statistical features to determine the smallest number of features needed to distinguish the modulation schemes. The second experiment evaluates the performance of a SVM, in an AWGN channel, in classifying the modulations based on the final feature set determined in the first experiment. Our feature extraction and classification model is implemented in MATLAB. For the first experiment, for each modulation scheme, the mean, variance, skewness, kurtosis, 12^{th}-order moment of the instantaneous amplitude and phase are extracted and compared at SNR levels of 0 dB to 15 dB. Two fourth-order cumulants of the received signal and the signal power key is also evaluated. In Fig. 3-5 the results achieved are presented.

The SNR levels range from 0 dB to 15 dB (1 dB increments). The modulations considered include BPSK, QPSK, 8PSK, 16QAM, 32QAM, and 64QAM, which is chosen based on the most commonly used technologies and their respective modulation schemes employed in the UHF frequency band (300 MHz - 5 GHz) as set out in the National Frequency Plan (NFP) by the Independent Communications Authority of South Africa (ICASA) as stated in [16]. For our second

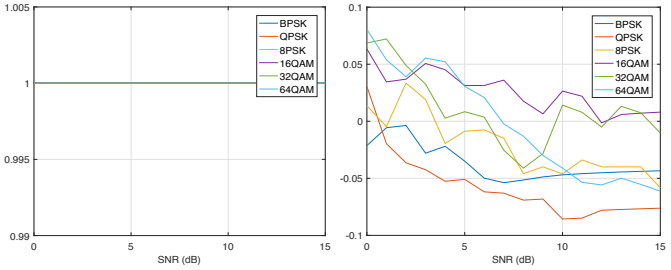

(a) Mean A_n (b) Mean $\theta(t)$

Fig. 3. First and second order statistical features

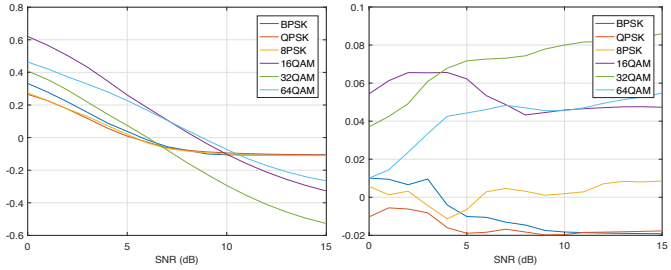

(a) Skewness A_n (b) Skewness $\theta(t)$

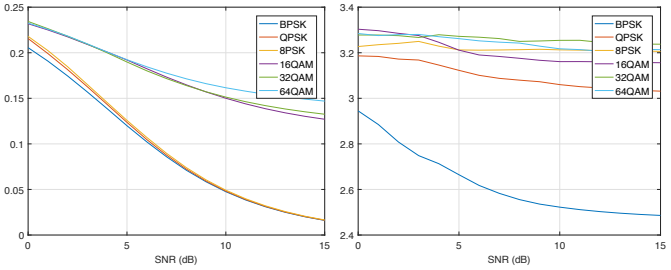

(c) Variance A_n (d) Variance $\theta(t)$

Fig. 4. Third and fourth order statistical features

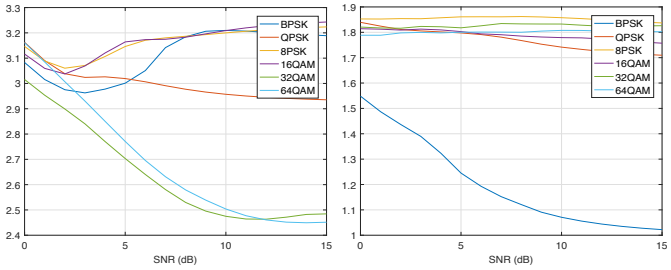

(c) Kurtosis A_n (d) Kurtosis $\theta(t)$

experiment, the SVM has been chosen as our initial classifier to evaluate the performance of these features in classifying the modulations in AWGN noise. The SVM is chosen on the basis of its ability to separate the modulations from each other through a hyperplane when the selected features show a big enough separation between them. Experimental parameters are summarised in Table II. Refer to our system

TABLE II
EXPERIMENTAL PARAMETERS

Parameter	Value
Modulations	[BPSK,QPSK,8PSK, 16QAM,32QAM,64QAM]
Number of Signal Symbols	1024 symbols
Number of iterations	100
Training dataset Size	1000 entries (per modulation)
SNR	0:15 dB in 1 dB increments

model in Fig. 2, where a random symbol stream is generated at the beginning of each experimental iteration. The generated random symbols are based on a uniform pseudo-random number generator while keeping the seed value constant per modulation. This ensures that the performance of the classifier is message independent. The random symbol stream is modulated using M-ary PSK and M-ary QAM modulation. The baseband modulated signal is sent through the communication channel from where the features are extracted. With five input features and six possible outputs, a total of 6000 data elements were used to train the classifiers. The training data were randomly sorted and loaded. Fifty percent of the generated data were used for training, 25% were used for validation and the last 25% for testing.

VI. RESULTS

A. Feature Evaluation

From the results obtained, it is clear that the mean of the normalised instantaneous amplitude and phase in Fig. 3a and 3b does not contribute anything in discriminating the modulations. The variance of the normalised instantaneous amplitude (Fig. 3c) makes a clear distinction between M-ary PSK and M-ary QAM signals. The variance of the instantaneous phase in Fig. 3d discriminates BPSK and QPSK from the other modulations. In Fig. 4d the kurtosis of the instantaneous phase can be used to discriminate 8PSK from the other modulations. Furthermore, the 12th-order moment of the normalised instantaneous amplitude, β and $|\frac{C_{40}}{C_{42}}|$ (Fig. 5) can be used to identify 16QAM, 32QAM and 64QAM from the rest. The features chosen show a good amount of separation between them, therefore the use of a SVM is a suitable choice.

B. Performance of Classifier

Using the results obtained in VI-A, the following features (Table III) are chosen as input for a SVM classifier. The performance of the classifier is presented in Table IV in the form of a confusion matrix at different SNRs.

TABLE III
STATISTICAL FEATURES USED FOR CLASSIFICATION

	Features
1	σ^2 of the instantaneous phase
2	κ of the instantaneous phase
3	M_{12} of the normalised instantaneous amplitude
4	β
5	$\|C_{40}/C_{42}\|$

There can be seen that QPSK and 8PSK show an 85% (15% classified as 8PSK) and 88% (12% classified as QPSK) accuracy at 0 dB respectively, while the results for BPSK, 16QAM, 32QAM, and 64QAM are promising at 100% accuracy. For a SNR of 5 dB and above the performance of the classifier is 100%. Compared to related work, as discussed in section III, the performance of classifying these M-ary PSK and M-ary QAM modulation, given our set of features, compare well.

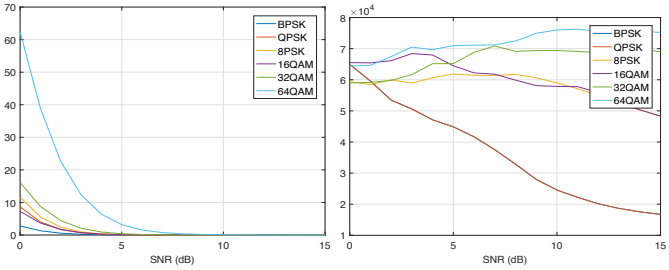

(a) Moment-order 12 A_n (b) Moment-order 12 $\theta(t)$

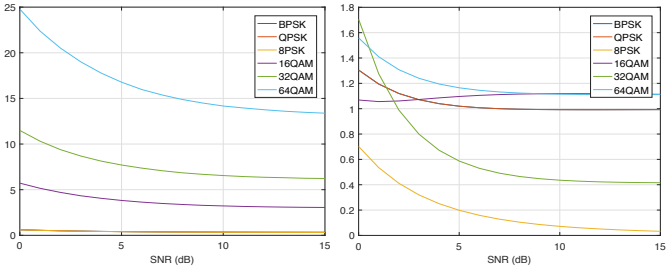

(c) β (d) $|C_{40}/C_{42}|$

Fig. 5. Higher-order statistical features

TABLE IV
PERFORMANCE OF SVM AT DIFFERENT SNRS

SNR	Modulation Type	BPSK	QPSK	8PSK	16QAM	32QAM	64QAM
0dB	BPSK	100%					
	QPSK		85%	15%			
	8PSK		12%	88%			
	16QAM				100%		
	32QAM					100%	
	64QAM						100%
5dB	BPSK	100%					
	QPSK		100%				
	8PSK			100%			
	16QAM				100%		
	32QAM					100%	
	64QAM						100%
10dB	BPSK	100%					
	QPSK		100%				
	8PSK			100%			
	16QAM				100%		
	32QAM					100%	
	64QAM						100%

In [6] BPSK, QPSK, 8PSK, 16QAM and 64QAM were classified with a performance accuracy of 95% at SNR lower than 10 dB.

VII. CONCLUSION

The aim of this paper was to discover which of the statistical properties derived from the instantaneous amplitude and phase of the received signal can be used to successfully classify M-ary PSK and M-ary QAM signals corrupted by an AWGN channel. The features were evaluated over a range of SNR values. The final features used to classify the M-ary PSK and M-ary QAM signals are presented in Table III. A SVM was used to classify the modulations with an overall classification accuracy of 95% at 0 dB and 100% classification accuracy at a SNR of 5 dB and above. Compared to the related work in [6] and [14] our approach achieved good accuracy.

VIII. FUTURE WORK

For future work, a Rician- and Rayleigh communication channel will be added to the simulation model to test the robustness of the features against multipath propagation. The performance of the classifier will be evaluated using I/Q streams from recorded signals. The feature set may adapt and expand to accommodate the changes in the communication channel to ensure good performance. More will done to determine which classification algorithm (SVM, Artificial Neural Network (ANN) and KNN) will be better suited for our problem, given these adapted channel conditions. The implementation of the feature extraction processes on hardware such as a Raspberry Pi 3 single-board computer will be investigated.

REFERENCES

[1] Z. Zhu and A. K. Nandi, *Automatic Modulation Classification Principles, Algorithms and Applications*, first edit ed. Wiley, 2015, vol. 1.
[2] J. J. Popoola, "Effect of training algorithms on performance of a developed automatic modulation classification using artificial neural network," 2013.
[3] O. Dobre, A. Abdi, Y. Bar-Ness, and W. Su, "Survey of automatic modulation classification techniques: classical approaches and new trends," *IET Communications*, vol. 1, no. 2, pp. 137–156, 2007.
[4] A. Hazza, M. Shoaib, S. A. Alshebeili, and A. Fahad, "An overview of feature-based methods for digital modulation classification," *2013 1st International Conference on Communications, Signal Processing, and their Applications (ICCSPA)*, vol. 1, no. 08, pp. 1–6, 2013.
[5] M. Aslam, Z. Z. Zhu, and A. Nandi, "Automatic digital modulation classification using Genetic Programming with K-Nearest Neighbor," *Military Communications Conference, 2010 - Milcom 2010*, pp. 1731–1736, 2010.
[6] P. Shih and D. C. Chang, "An automatic modulation classification technique using high-order statistics for multipath fading channels," *ITS Telecommunications (ITST), 2011 11th International Conference on*, pp. 691–695, 2011.
[7] H. Alharbi, S. Mobien, S. Alshebeili, and F. Alturki, "Automatic modulation classification of digital modulations in presence of HF noise," *EURASIP Journal on Advances in Signal Processing*, vol. 2012, no. 1, p. 1, 2012.
[8] J. J. Popoola and R. V. Olst, "Automatic classification of combined analog and digital modulation schemes using feedforward neural network," *Ieee Africon*, no. September, pp. 13–15, 2011.
[9] S. B. Kotsiantis, I. D. Zaharakis, and P. E. Pintelas, "Machine learning: A review of classification and combining techniques," *Artificial Intelligence Review*, vol. 26, no. 3, pp. 159–190, 2006.
[10] L. E. Frenzel, *Electronic communication systems*, 2008.
[11] Y. K. Cho Kim, *MIMO-OFDM Wireless Communications with MATLAB*.
[12] A. Ebrahimzadeh and S. E. Mousavi, "Classification of communications signals using an advanced technique," *Applied Soft Computing Journal*, vol. 11, no. 1, pp. 428–435, 2011.
[13] A. D. Pambudi, S. Tjondronegoro, and H. Wijanto, "Statistical properties proposed for blind classification OFDM modulation scheme," *Proceeding - ICARES 2014: 2014 IEEE International Conference on Aerospace Electronics and Remote Sensing Technology*, pp. 89–93, 2014.
[14] P. Prakasam and M. Madheswaran, "Digital Modulation Identification Model Using Wavelet Transform and Statistical Parameters," *Journal of Computer Systems, Networks, and Communications*, vol. 2008, pp. 1–8, 2008.
[15] A.Prochazka, J.Uhlir, P. Rayner, and N. Kingsbury, *Signal Analysis and Prediction*, 1998.
[16] "Final radio frequency spectrum regulations," in *Government Gazette*, Rebuplic of South Africa, 30 Mar 2015, no. 38641, notice 279.

ACKNOWLEDGEMENT

The authors would like to thank the reviewers for their constructive feedback, and for the TeleNet group at the North-West University for their financial support.

Herman Blackie is pursuing his M.Eng in Computer Engineering at the North-West University. He received his B.Eng degree in 2015. His research topics include spectrum sensing and modulation recognition.